DNA Molecular Modeling vol.1: Wk9

Contents of Volumes 1 and 2

Molecular models of DNA

Molecular models of DNA structures are representations of the molecular geometry and topology of Deoxyribonucleic acid (→ DNA) molecules using one of several means, such as: closely packed spheres (CPK models) made of plastic, metal wires for 'skeletal models', graphic computations and animations by computers, artistic rendering, and so on, with the aim of simplifying and presenting the essential, physical and chemical, properties of DNA molecular structures either *in vivo* or *in vitro*. Computer molecular models also allow animations and molecular dynamics simulations that are very important for understanding how DNA functions *in vivo*. Thus, an old standing dynamic problem is how DNA "self-replication" takes place in living cells that should involve transient uncoiling of supercoiled DNA fibers. Although DNA consists of relatively rigid, very large elongated biopolymer molecules called "fibers" or chains (that are made of repeating nucleotide units of four basic types, attached to deoxyribose and phosphate groups), its molecular structure *in vivo* undergoes dynamic configuration changes that involve dynamically attached water molecules and ions. Supercoiling, packing with histones in chromosome structures, and other such supramolecular aspects also involve *in vivo* DNA topology which is even more complex than DNA molecular geometry, thus turning molecular modeling of DNA into an especially challenging problem for both molecular biologists and biotechnologists. Like other large molecules and biopolymers, DNA often exists in multiple stable geometries (that is, it exhibits conformational isomerism) and configurational, quantum states which are close to each other in energy on the potential energy surface of the DNA molecule. Such geometries can also be computed, at least in principle, by employing *ab initio* quantum chemistry methods that have high accuracy for small molecules. Such quantum geometries define an important class of *ab initio* molecular models of DNA whose exploration has barely started.

In an interesting twist of roles, the DNA molecule itself was proposed to be utilized for quantum computing. Both DNA nanostructures as well as DNA 'computing' biochips have been built (see biochip image at right).

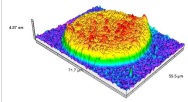

DNA computing biochip:3D

The more advanced, computer-based molecular models of DNA involve molecular dynamics simulations as well as quantum mechanical computations of vibro-rotations, delocalized molecular orbitals (MOs), electric dipole moments, hydrogen-bonding, and so on.

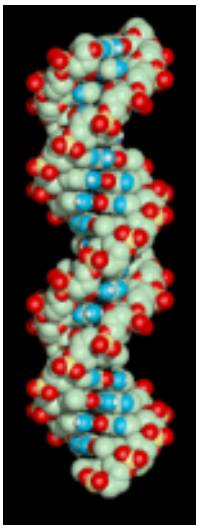

Spinning DNA generic model.

Importance

From the very early stages of structural studies of DNA by X-ray diffraction and biochemical means, molecular models such as the Watson-Crick double-helix model were successfully employed to solve the 'puzzle' of DNA structure, and also find how the latter relates to its key functions in living cells. The first high quality X-ray diffraction patterns of A-DNA were reported by Rosalind Franklin and Raymond Gosling in 1953[1] . The first calculations of the Fourier transform of an atomic helix were reported one year earlier by Cochran, Crick and Vand [2] , and were followed in 1953 by the computation of the Fourier transform of a coiled-coil by Crick[3] . The first reports of a double-helix molecular model of B-DNA structure were made by Watson and Crick in 1953[4] [5] . Last-but-not-least, Maurice F. Wilkins, A. Stokes and H.R. Wilson, reported the first X-ray patterns of *in vivo* B-DNA in partially oriented salmon sperm heads [6] . The development of the first correct double-helix molecular model of DNA by Crick and Watson may not have been possible without the biochemical evidence for the nucleotide base-pairing ([A---T]; [C---G]), or Chargaff's rules[7] [8] [9] [10] [11] [12] .

Examples of DNA molecular models

Animated molecular models allow one to visually explore the three-dimensional (3D) structure of DNA. The first DNA model is a space-filling, or CPK, model of the DNA double-helix whereas the third is an animated wire, or skeletal type, molecular model of DNA. The last two DNA molecular models in this series depict quadruplex DNA [13] that may be involved in certain cancers[14] [15] . The last figure on this panel is a molecular model of hydrogen bonds between water molecules in ice that are similar to those found in DNA.

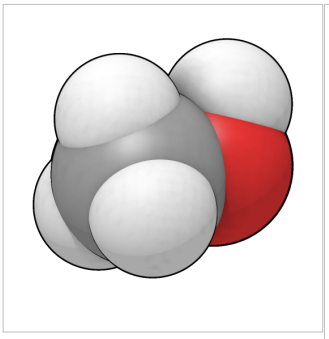

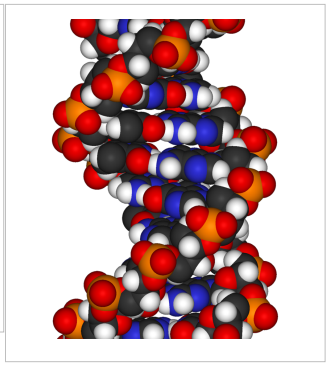

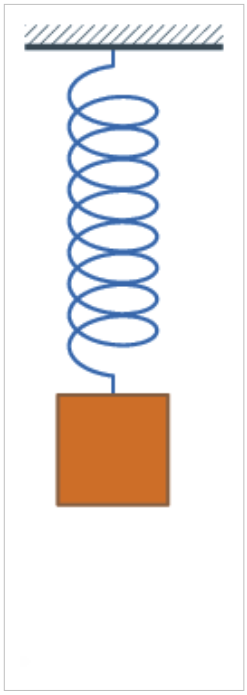

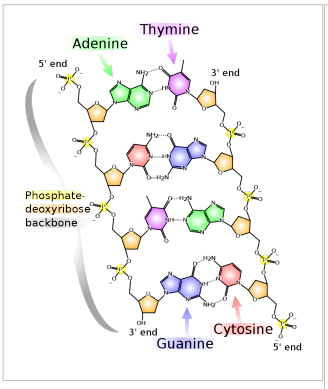
Thymine
Adenine
5' end
3' end
Phosphate-
deoxyribose
backbone
3' end
Guanine
Cytosine
5' end

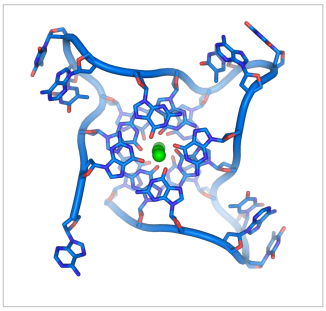

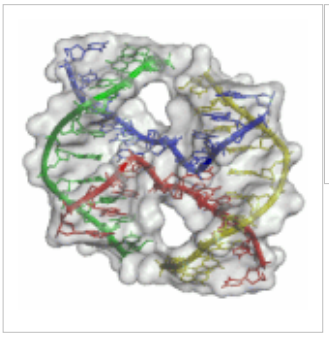

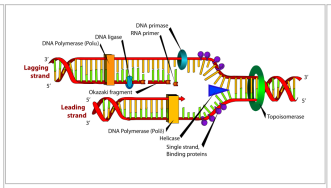
DNA primase
RNA primer
DNA ligase
DNA Polymerase (Pol I)
Lagging strand
Okazaki fragment
Leading strand
Topoisomerase
DNA Polymerase (Pol I)
Helicase
Single strand. Binding proteins

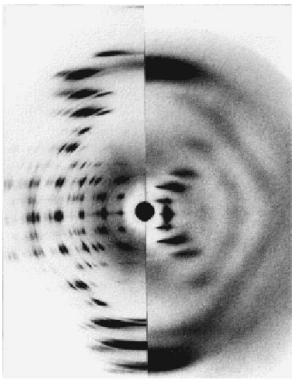

A-DNA B-DNA

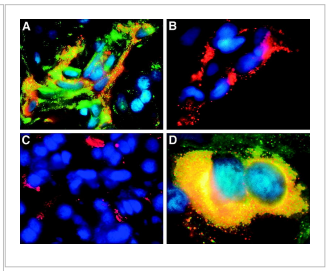
A
B
C
D

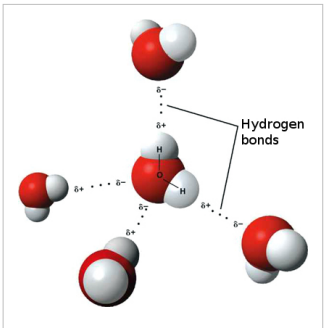

- Spacefilling models or CPK models - a molecule is represented by overlapping spheres representing the atoms.

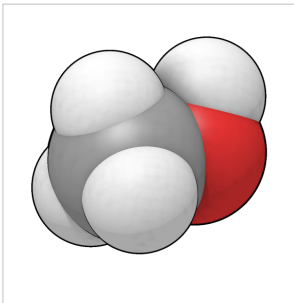

Images for DNA Structure Determination from X-Ray Patterns

The following images illustrate both the principles and the main steps involved in generating structural information from X-ray diffraction studies of oriented DNA fibers with the help of molecular models of DNA that are combined with crystallographic and mathematical analysis of the X-ray patterns. From left to right the gallery of images shows:

- *First row*:
- 1. Constructive X-ray interference, or diffraction, following Bragg's Law of X-ray "*reflection by the crystal planes*";
- 2. A comparison of A-DNA (crystalline) and highly hydrated B-DNA (paracrystalline) X-ray diffraction, and respectively, X-ray scattering patterns (courtesy of Dr. Herbert R. Wilson, FRS- see refs. list);
- 3. Purified DNA precipitated in a water jug;
- 4. The major steps involved in DNA structure determination by X-ray crystallography showing the important role played by molecular models of DNA structure in this iterative, structure--determination process;
- *Second row*:
- 5. Photo of a modern X-ray diffractometer employed for recording X-ray patterns of DNA with major components: X-ray source, goniometer, sample holder, X-ray detector and/or plate holder;
- 6. Illustrated animation of an X-ray goniometer;
- 7. X-ray detector at the SLAC synchrotron facility;
- 8. Neutron scattering facility at ISIS in UK;
- *Third and fourth rows*: *Molecular models of DNA structure at various scales*; figure #11 is an actual electron micrograph of a DNA fiber bundle, presumably of a single

bacterial chromosome loop.

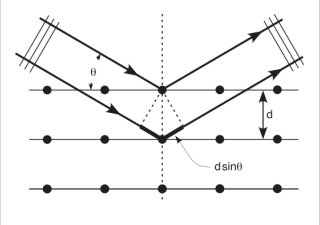

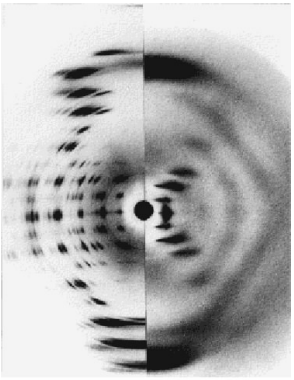

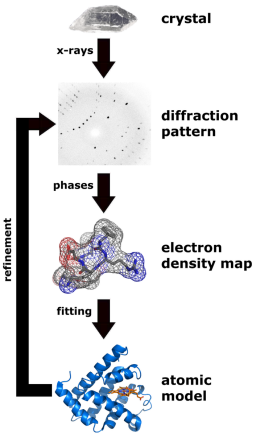

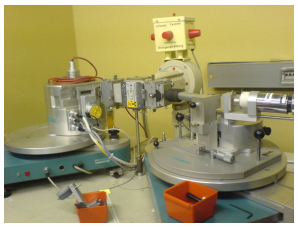

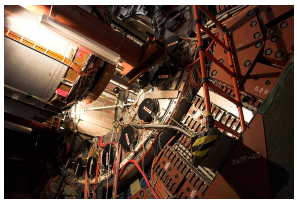

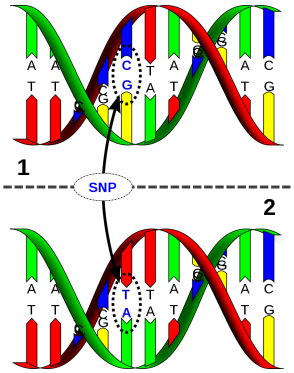

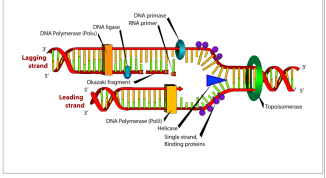

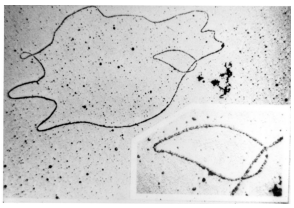

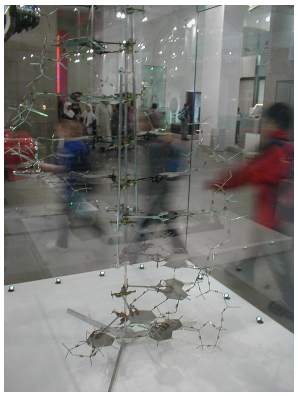

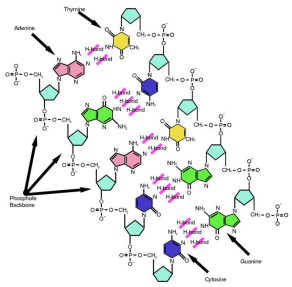

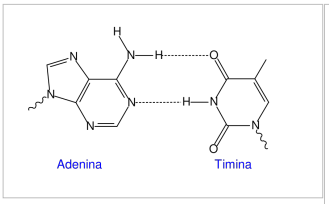

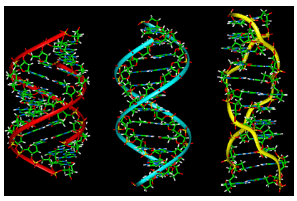

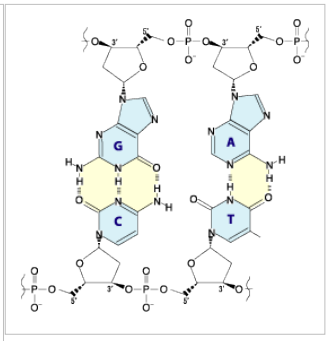

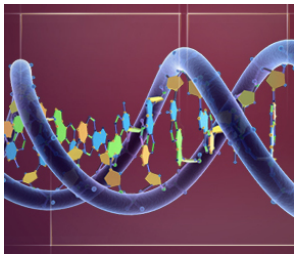

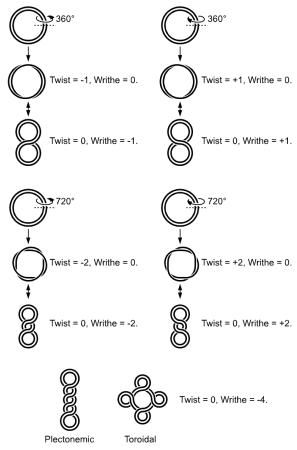

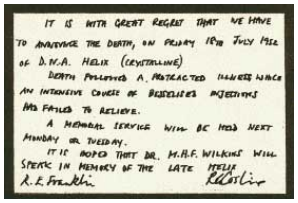

Paracrystalline lattice models of B-DNA structures

A paracrystalline lattice, or paracrystal, is a molecular or atomic lattice with significant amounts (e.g., larger than a few percent) of partial disordering of molecular arranegements. Limiting cases of the paracrystal model are nanostructures, such as glasses, liquids, etc., that may possess only local ordering and no global order. Liquid crystals also have paracrystalline rather than crystalline structures.

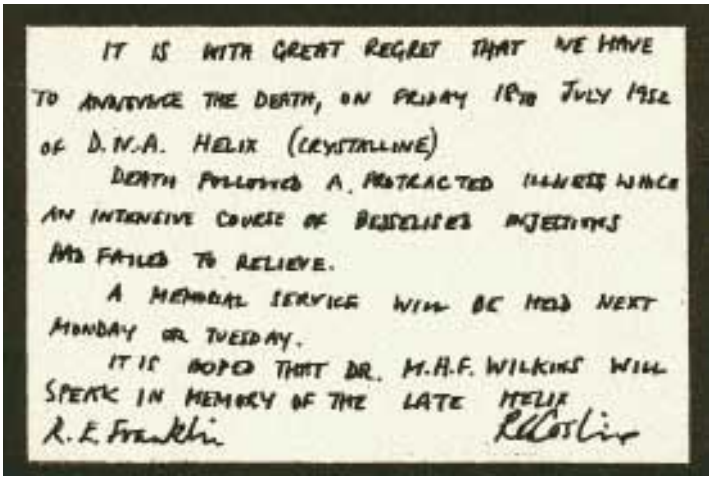

DNA Helix controversy in 1952

Highly hydrated B-DNA occurs naturally in living cells in such a paracrystalline state, which is a dynamic one in spite of the relatively rigid DNA double-helix stabilized by parallel hydrogen bonds between the nucleotide base-pairs in the two complementary, helical DNA chains (see figures). For simplicity most DNA molecular models ommit both water and ions dynamically bound to B-DNA, and are thus less useful for understanding the dynamic behaviors of B-DNA *in vivo*. The physical and mathematical analysis of X-ray[16] [17] and spectroscopic data for paracrystalline B-DNA is therefore much more complicated than that of crystalline, A-DNA X-ray diffraction patterns. The paracrystal model is also important for DNA technological applications such as → DNA nanotechnology. Novel techniques that combine X-ray diffraction of DNA with X-ray microscopy in hydrated living cells are now also being developed (see, for example, "Application of X-ray microscopy in the analysis of living hydrated cells" [18]).

Genomic and Biotechnology Applications of DNA molecular modeling

The following gallery of images illustrates various uses of DNA molecular modeling in Genomics and Biotechnology research applications from DNA repair to PCR and DNA nanostructures; each slide contains its own explanation and/or details. The first slide presents an overview of DNA applications, including DNA molecular models, with emphasis on Genomics and Biotechnology.

Gallery: DNA Molecular modeling applications

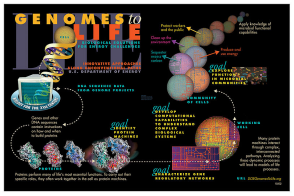

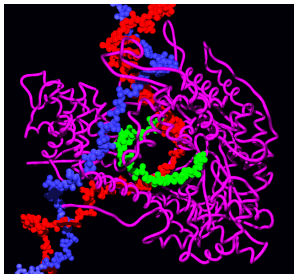
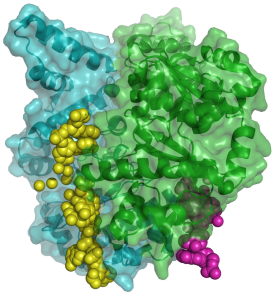

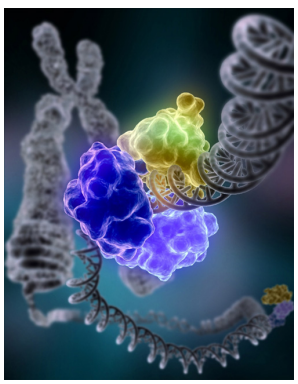
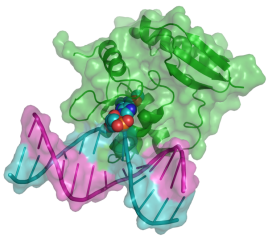
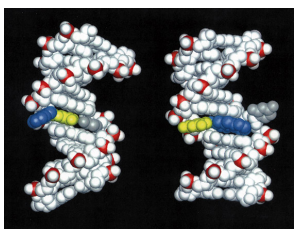
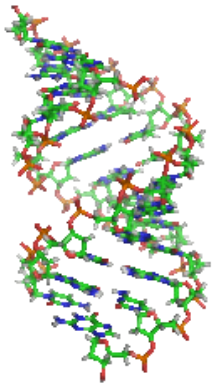

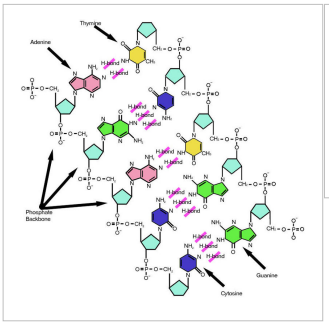
Thymine
Adenine
Phosphate Backbone
Guanine
Cytosine

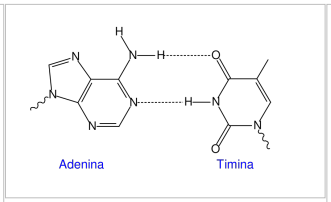
Adenina
Timina

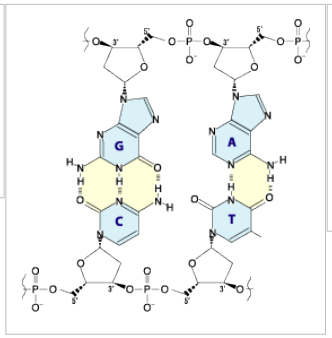
G
C
A
T

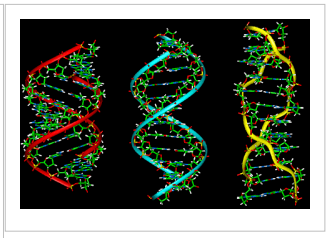

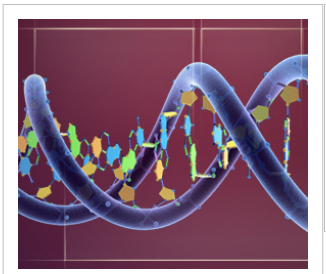

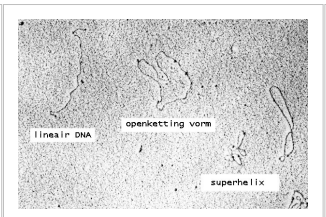
linear DNA
openkettling vorm
superhelix

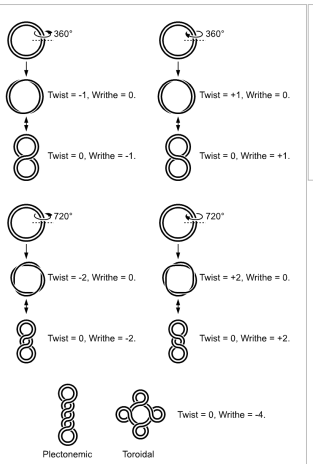
360°
Twist = -1, Writhe = 0.
Twist = 0, Writhe = -1.
360°
Twist = +1, Writhe = 0.
Twist = 0, Writhe = +1.
720°
Twist = -2, Writhe = 0.
Twist = 0, Writhe = -2.
720°
Twist = +2, Writhe = 0.
Twist = 0, Writhe = +2.
Twist = 0, Writhe = -4.
Plectonemic
Toroidal

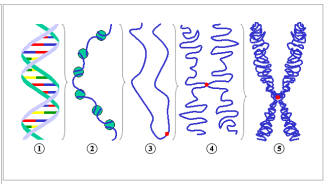
1
2
3
4
5

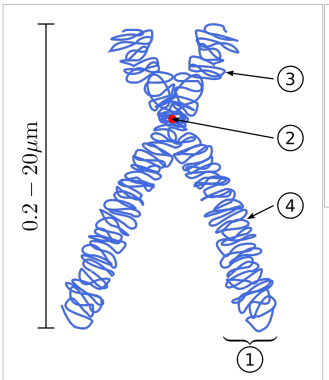
0.2 – 20μm
3
2
4
1

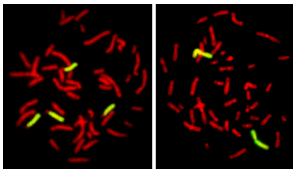

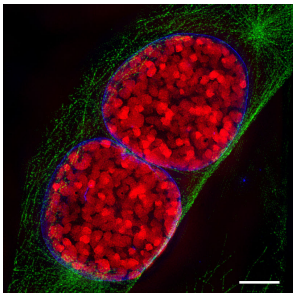

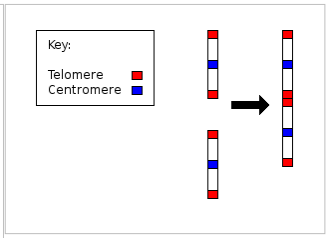
Key:
Telomere
Centromere

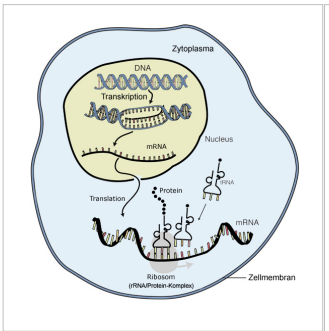
Zytoplasma
DNA
Transkription
Nucleus
mRNA
Translation
Protein
tRNA
mRNA
Ribosom
(rRNA/Protein-Komplex)
Zellmembran

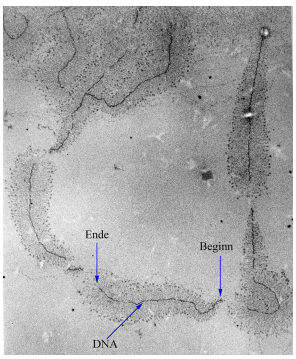
Ende
Beginn
DNA

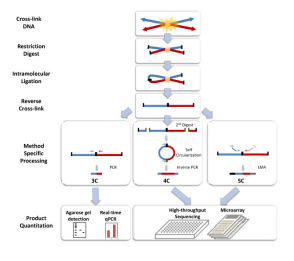
Cross-link DNA
Restriction Digest
Intramolecular Ligation
Reverse Cross-link
Method Specific Processing
3C
4C
5C
Product Quantitation
Agarose gel detection
Real-time qPCR
High-throughput Sequencing
Microarray

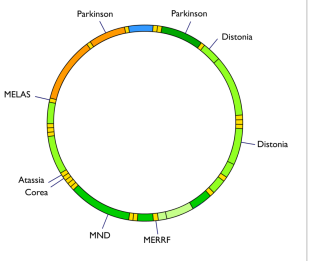
Parkinson
Parkinson
Distonia
MELAS
Distonia
Atassia
Corea
MND
MERRF

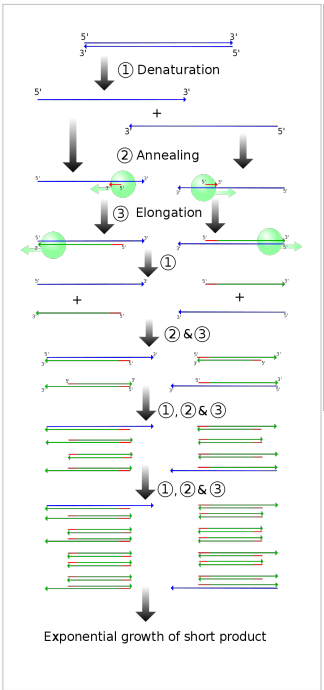

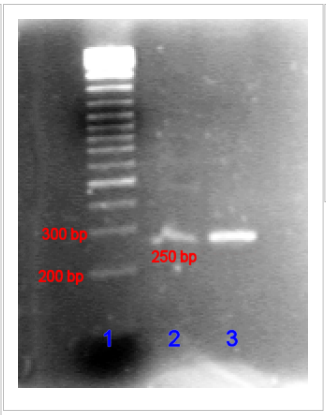

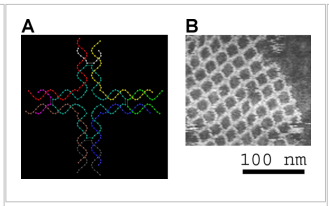

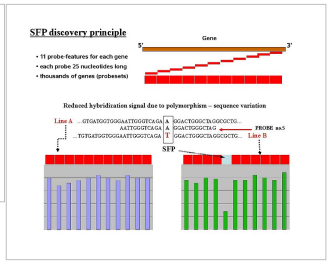

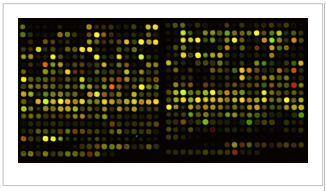

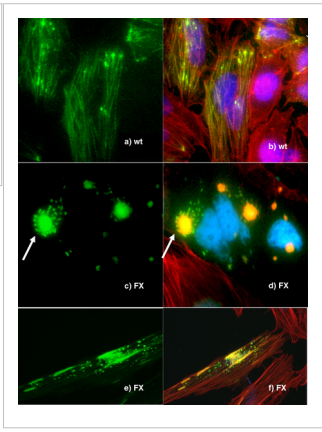

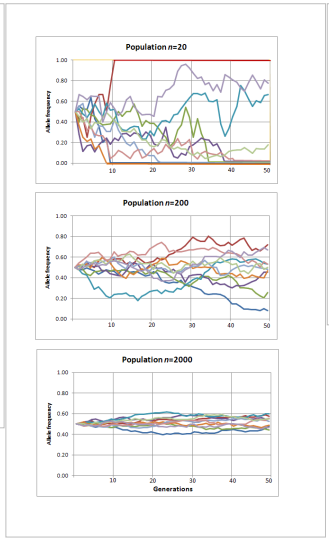

Databases for DNA molecular models and sequences

X-ray diffraction

- NDB ID: UD0017 Database [19]
- X-ray Atlas -database [20]
- PDB files of coordinates for nucleic acid structures from X-ray diffraction by NA (incl. DNA) crystals [21]
- Structure factors dowloadable files in CIF format [22]

Neutron scattering

- ISIS neutron source
- ISIS pulsed neutron source:A world centre for science with neutrons & muons at Harwell, near Oxford, UK. [23]

X-ray microscopy

- Application of X-ray microscopy in the analysis of living hydrated cells [24]

Electron microscopy

- DNA under electron microscope [25]

Atomic Force Microscopy (AFM)

Two-dimensional DNA junction arrays have been visualized by Atomic Force Microscopy (AFM)[26] . Other imaging resources for AFM/Scanning probe microscopy(SPM) can be freely accessed at:

- How SPM Works [27]
- SPM Image Gallery - AFM STM SEM MFM NSOM and more. [28]

Gallery of AFM Images

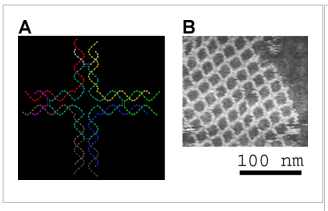

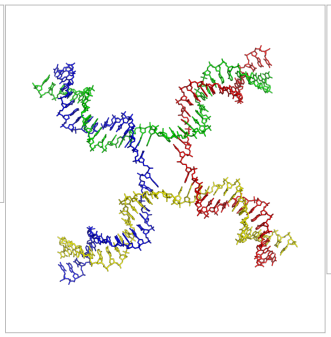

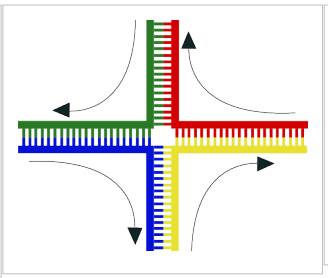

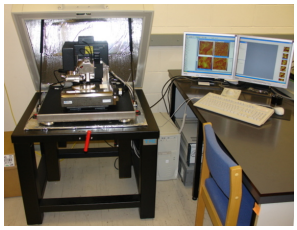

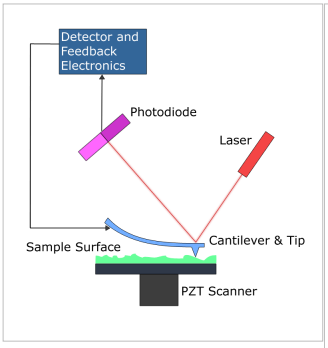

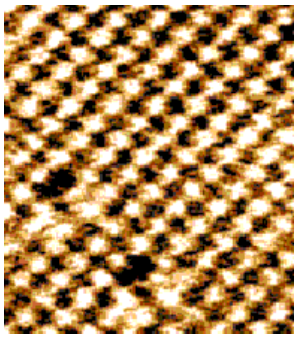

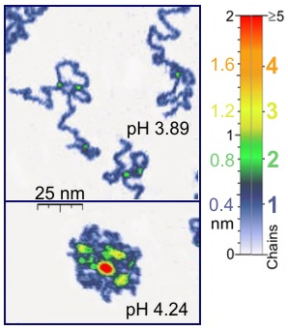

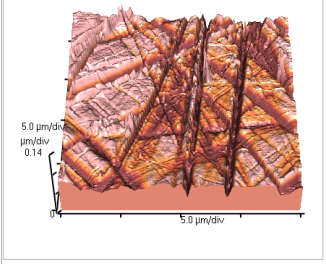

Mass spectrometry--Maldi informatics

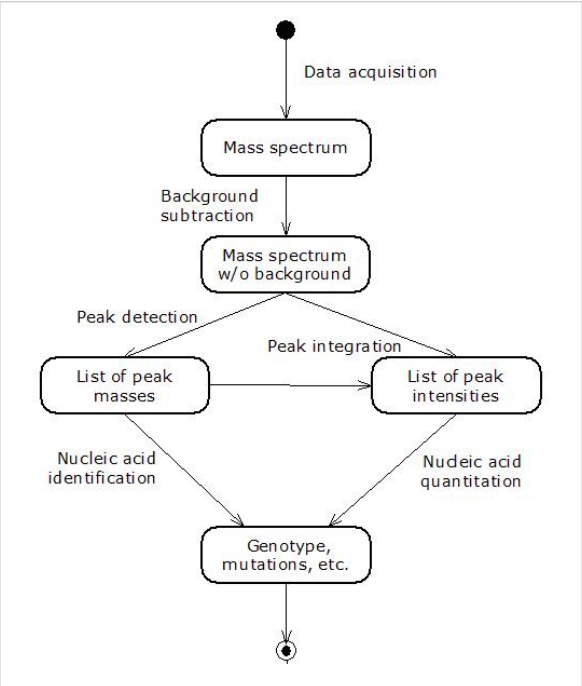

Spectroscopy

- Vibrational circular dichroism (VCD)
- → FT-NMR[29] [30]
  - NMR Atlas--database [31]
  - mmcif downloadable coordinate files of nucleic acids in solution from 2D-FT NMR data [32]
  - NMR constraints files for NAs in PDB format [33]
- NMR microscopy[34]
- Microwave spectroscopy
- FT-IR
- FT-NIR[35] [36] [37]
- Spectral, → Hyperspectral, and → Chemical imaging)[38] [39] [40] [41] [42] [43] [44] .
- Raman spectroscopy/microscopy[45] and → CARS[46] .
- → Fluorescence correlation spectroscopy[47] [48] [49] [50] [51] [52] [53] [54] , → Fluorescence cross-correlation spectroscopy and FRET[55] [56] [57] .
- → Confocal microscopy[58]

Gallery: CARS (Raman spectroscopy), Fluorescence confocal microscopy, and Hyperspectral imaging

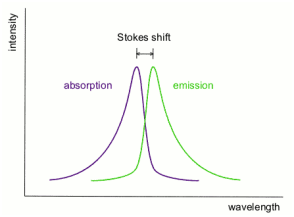

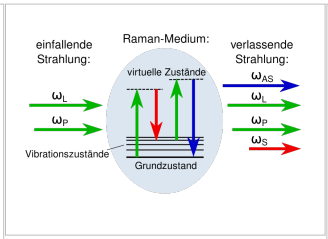

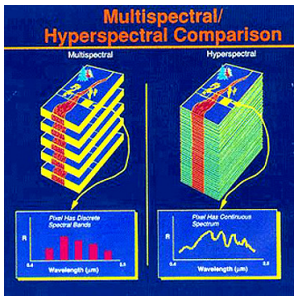

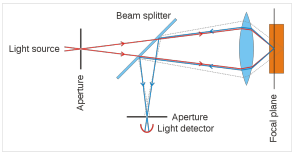

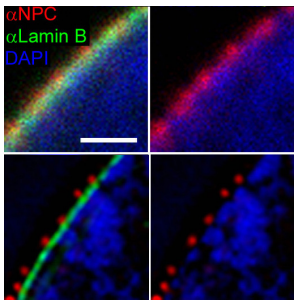

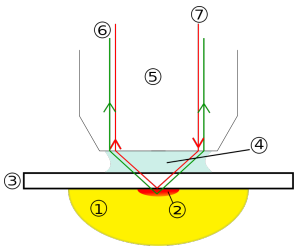

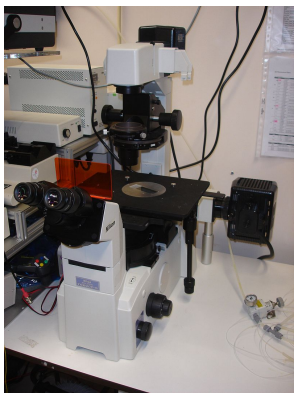

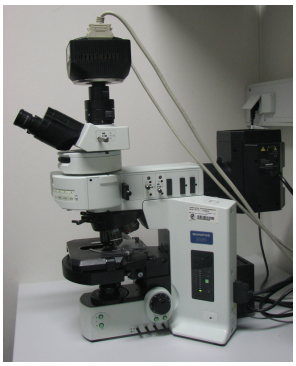

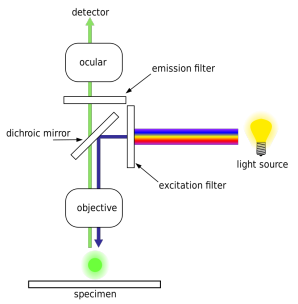

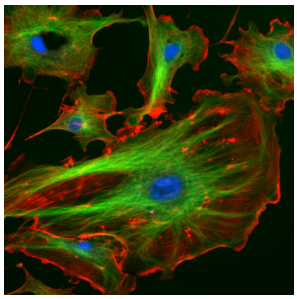

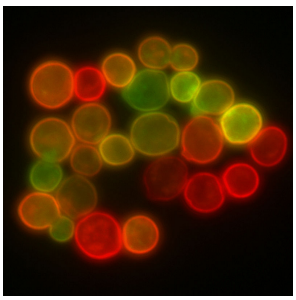

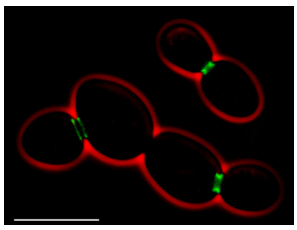

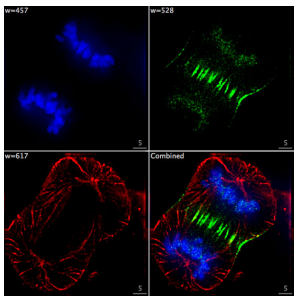

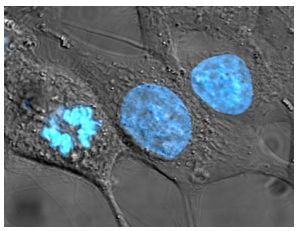

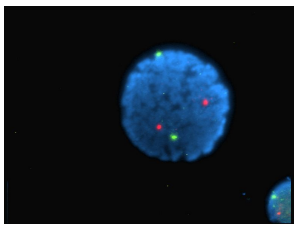
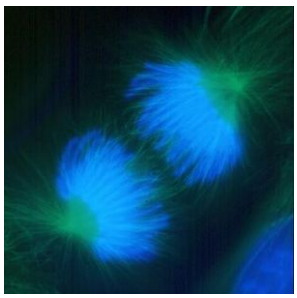
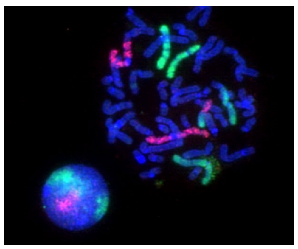
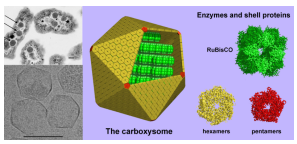

Genomic and structural databases

- CBS Genome Atlas Database [59] — contains examples of base skews.[60]
- The Z curve database of genomes — a 3-dimensional visualization and analysis tool of genomes [61][62] .
- DNA and other nucleic acids' molecular models: Coordinate files of nucleic acids molecular structure models in PDB and CIF formats [63]

Notes

[1] Franklin, R.E. and Gosling, R.G. recd.6 March 1953. Acta Cryst. (1953). 6, 673 The Structure of Sodium Thymonucleate Fibres I. The Influence of Water Content Acta Cryst. (1953). and 6, 678 The Structure of Sodium Thymonucleate Fibres II. The Cylindrically Symmetrical Patterson Function.

[2] Cochran, W., Crick, F.H.C. and Vand V. 1952. The Structure of Synthetic Polypeptides. 1. The Transform of Atoms on a Helix. Acta Cryst. 5(5):581-586.

[3] Crick, F.H.C. 1953a. The Fourier Transform of a Coiled-Coil., Acta Crystallographica 6(8-9):685-689.

[4] Watson, J.D; Crick F.H.C. 1953a. Molecular Structure of Nucleic Acids- A Structure for Deoxyribose Nucleic Acid., Nature 171(4356):737-738.

[5] Watson, J.D; Crick F.H.C. 1953b. The Structure of DNA., Cold Spring Harbor Symposia on Qunatitative Biology 18:123-131.

[6] Wilkins M.H.F., A.R. Stokes A.R. & Wilson, H.R. (1953). " Molecular Structure of Deoxypentose Nucleic Acids (http://www.nature.com/nature/dna50/wilkins.pdf)" (PDF). *Nature* **171**: 738–740. doi: 10.1038/171738a0 (http://dx.doi.org/10.1038/171738a0). PMID 13054693. .

[7] Elson D, Chargaff E (1952). "On the deoxyribonucleic acid content of sea urchin gametes". *Experientia* **8** (4): 143-145.

[8] Chargaff E, Lipshitz R, Green C (1952). "Composition of the deoxypentose nucleic acids of four genera of sea-urchin". *J Biol Chem* **195** (1): 155-160. PMID 14938364.

[9] Chargaff E, Lipshitz R, Green C, Hodes ME (1951). "The composition of the deoxyribonucleic acid of salmon sperm". *J Biol Chem* **192** (1): 223-230. PMID 14917668.

[10] Chargaff E (1951). "Some recent studies on the composition and structure of nucleic acids". *J Cell Physiol Suppl* **38** (Suppl).

[11] Magasanik B, Vischer E, Doniger R, Elson D, Chargaff E (1950). "The separation and estimation of ribonucleotides in minute quantities". *J Biol Chem* **186** (1): 37-50. PMID 14778802.

[12] Chargaff E (1950). "Chemical specificity of nucleic acids and mechanism of their enzymatic degradation". *Experientia* **6** (6): 201-209.

[13] http://ndbserver.rutgers.edu/atlas/xray/structures/U/ud0017/ud0017.html

[14] http://www.phy.cam.ac.uk/research/bss/molbiophysics.php

[15] http://planetphysics.org/encyclopedia/TheoreticalBiophysics.html

[16] Hosemann R., Bagchi R.N., *Direct analysis of diffraction by matter*, North-Holland Publs., Amsterdam – New York, 1962.

[17] Baianu, I.C. (1978). "X-ray scattering by partially disordered membrane systems.". *Acta Cryst.,* **A34** (5): 751–753. doi: 10.1107/S0567739478001540 (http://dx.doi.org/10.1107/S0567739478001540).

[18] http://www.ncbi.nlm.nih.gov/entrez/query.fcgi?cmd=Retrieve&db=pubmed&dopt=Abstract&list_uids=12379938

[19] http://ndbserver.rutgers.edu/atlas/xray/structures/U/ud0017/ud0017.html

[20] http://ndbserver.rutgers.edu/atlas/xray/index.html
[21] http://ndbserver.rutgers.edu/ftp/NDB/coordinates/na-biol/
[22] http://ndbserver.rutgers.edu/ftp/NDB/structure-factors/
[23] http://www.isis.rl.ac.uk/
[24] http://www.ncbi.nlm.nih.gov/entrez/query.fcgi?cmd=Retrieve&db=pubmed&dopt=Abstract&list_uids=12379938
[25] http://www.fidelitysystems.com/Unlinked_DNA.html
[26] Mao, Chengde; Sun, Weiqiong & Seeman, Nadrian C. (16 June 1999). "Designed Two-Dimensional DNA Holliday Junction Arrays Visualized by Atomic Force Microscopy". *Journal of the American Chemical Society* **121** (23): 5437–5443. doi: 10.1021/ja9900398 (http://dx.doi.org/10.1021/ja9900398). ISSN 0002-7863 (http://worldcat.org/issn/0002-7863).
[27] http://www.parkafm.com/New_html/resources/01general.php
[28] http://www.rhk-tech.com/results/showcase.php
[29] (http://www.jonathanpmiller.com/Karplus.html)- obtaining dihedral angles from ^{3}J coupling constants
[30] (http://www.spectroscopynow.com/FCKeditor/UserFiles/File/specNOW/HTML files/General_Karplus_Calculator.htm) Another Javascript-like NMR coupling constant to dihedral
[31] http://ndbserver.rutgers.edu/atlas/nmr/index.html
[32] http://ndbserver.rutgers.edu/ftp/NDB/coordinates/na-nmr-mmcif/
[33] http://ndbserver.rutgers.edu/ftp/NDB/nmr-restraints/
[34] Lee, S. C. et al., (2001). One Micrometer Resolution NMR Microscopy. *J. Magn. Res.*, **150**: 207-213.
[35] Near Infrared Microspectroscopy, Fluorescence Microspectroscopy,Infrared Chemical Imaging and High Resolution Nuclear Magnetic Resonance Analysis of Soybean Seeds, Somatic Embryos and Single Cells., Baianu, I.C. et al. 2004., In *Oil Extraction and Analysis.*, D. Luthria, Editor pp.241-273, AOCS Press., Champaign, IL.
[36] Single Cancer Cell Detection by Near Infrared Microspectroscopy, Infrared Chemical Imaging and Fluorescence Microspectroscopy.2004.I. C. Baianu, D. Costescu, N. E. Hofmann and S. S. Korban, q-bio/0407006 (July 2004) (http://arxiv.org/abs/q-bio/0407006)
[37] Raghavachari, R., Editor. 2001. *Near-Infrared Applications in Biotechnology*, Marcel-Dekker, New York, NY.
[38] http://www.imaging.net/chemical-imaging/ Chemical imaging
[39] http://www.malvern.com/LabEng/products/sdi/bibliography/sdi_bibliography.htm E. N. Lewis, E. Lee and L. H. Kidder, Combining Imaging and Spectroscopy: Solving Problems with Near-Infrared Chemical Imaging. Microscopy Today, Volume 12, No. 6, 11/2004.
[40] D.S. Mantus and G. H. Morrison. 1991. Chemical imaging in biology and medicine using ion microscopy., *Microchimica Acta*, **104**, (1-6) January 1991, doi: 10.1007/BF01245536
[41] Near Infrared Microspectroscopy, Fluorescence Microspectroscopy,Infrared Chemical Imaging and High Resolution Nuclear Magnetic Resonance Analysis of Soybean Seeds, Somatic Embryos and Single Cells., Baianu, I.C. et al. 2004., In *Oil Extraction and Analysis.*, D. Luthria, Editor pp.241-273, AOCS Press., Champaign, IL.
[42] Single Cancer Cell Detection by Near Infrared Microspectroscopy, Infrared Chemical Imaging and Fluorescence Microspectroscopy.2004.I. C. Baianu, D. Costescu, N. E. Hofmann and S. S. Korban, q-bio/0407006 (July 2004) (http://arxiv.org/abs/q-bio/0407006)
[43] J. Dubois, G. Sando, E. N. Lewis, Near-Infrared Chemical Imaging, A Valuable Tool for the Pharmaceutical Industry, G.I.T. Laboratory Journal Europe, No.1-2, 2007.
[44] Applications of Novel Techniques to Health Foods, Medical and Agricultural Biotechnology.(June 2004).,I. C. Baianu, P. R. Lozano, V. I. Prisecaru and H. C. Lin q-bio/0406047 (http://arxiv.org/abs/q-bio/0406047)
[45] Chemical Imaging Without Dyeing (http://witec.de/en/download/Raman/ImagingMicroscopy04.pdf)
[46] C.L. Evans and X.S. Xie.2008. Coherent Anti-Stokes Raman Scattering Microscopy: Chemical Imaging for Biology and Medicine., doi:10.1146/annurev.anchem.1.031207.112754 *Annual Review of Analytical Chemistry*, **1**: 883-909.
[47] Eigen, M., Rigler, M. Sorting single molecules: application to diagnostics and evolutionary biotechnology,(1994) *Proc. Natl. Acad. Sci. USA*, 91,5740-5747.
[48] Rigler, M. Fluorescence correlations, single molecule detection and large number screening. Applications in biotechnology,(1995) J. Biotechnol., 41,177-186.
[49] Rigler R. and Widengren J. (1990). Ultrasensitive detection of single molecules by fluorescence correlation spectroscopy, *BioScience* (Ed. Klinge & Owman) p.180.
[50] Single Cancer Cell Detection by Near Infrared Microspectroscopy, Infrared Chemical Imaging and Fluorescence Microspectroscopy.2004.I. C. Baianu, D. Costescu, N. E. Hofmann, S. S. Korban and et al., q-bio/0407006 (July 2004) (http://arxiv.org/abs/q-bio/0407006)

[51] Oehlenschläger F., Schwille P. and Eigen M. (1996). Detection of HIV-1 RNA by nucleic acid sequence-based amplification combined with fluorescence correlation spectroscopy, *Proc. Natl. Acad. Sci. USA* **93**:1281.
[52] Bagatolli, L.A., and Gratton, E. (2000). Two-photon fluorescence microscopy of coexisting lipid domains in giant unilamellar vesicles of binary phospholipid mixtures. Biophys J., 78:290-305.
[53] Schwille, P., Haupts, U., Maiti, S., and Webb. W.(1999). Molecular dynamics in living cells observed by fluorescence correlation spectroscopy with one- and two-photon excitation. Biophysical Journal, 77(10):2251-2265.
[54] Near Infrared Microspectroscopy, Fluorescence Microspectroscopy,Infrared Chemical Imaging and High Resolution Nuclear Magnetic Resonance Analysis of Soybean Seeds, Somatic Embryos and Single Cells., Baianu, I.C. et al. 2004., In *Oil Extraction and Analysis.*, D. Luthria, Editor pp.241-273, AOCS Press., Champaign, IL.
[55] FRET description (http://dwb.unl.edu/Teacher/NSF/C08/C08Links/pps99.cryst.bbk.ac.uk/projects/gmocz/fret.htm)
[56] doi:10.1016/S0959-440X(00)00190-1 (http://dx.doi.org/10.1016/S0959-440X(00)00190-1)Recent advances in FRET: distance determination in protein–DNA complexes. *Current Opinion in Structural Biology* **2001**, *11(2)*, 201-207
[57] http://www.fretimaging.org/mcnamaraintro.html FRET imaging introduction
[58] Eigen, M., and Rigler, R. (1994). Sorting single molecules: Applications to diagnostics and evolutionary biotechnology, Proc. Natl. Acad. Sci. USA 91:5740.
[59] http://www.cbs.dtu.dk/services/GenomeAtlas/
[60] Hallin PF, David Ussery D (2004). "CBS Genome Atlas Database: A dynamic storage for bioinformatic results and DNA sequence data". *Bioinformatics* **20**: 3682-3686.
[61] http://tubic.tju.edu.cn/zcurve/
[62] Zhang CT, Zhang R, Ou HY (2003). "The Z curve database: a graphic representation of genome sequences". Bioinformatics 19 (5): 593-599. doi:10.1093/bioinformatics/btg041
[63] http://ndbserver.rutgers.edu/ftp/NDB/models/

References

- *Applications of Novel Techniques to Health Foods, Medical and Agricultural Biotechnology.*(June 2004) I. C. Baianu, P. R. Lozano, V. I. Prisecaru and H. C. Lin., q-bio/0406047.
- F. Bessel, *Untersuchung des Theils der planetarischen Störungen*, Berlin Abhandlungen (1824), article 14.
- Sir Lawrence Bragg, FRS. *The Crystalline State, A General survey.* London: G. Bells and Sons, Ltd., vols. 1 and 2., 1966., 2024 pages.
- Cantor, C. R. and Schimmel, P.R. *Biophysical Chemistry, Parts I and II.*, San Franscisco: W.H. Freeman and Co. 1980. 1,800 pages.
- Eigen, M., and Rigler, R. (1994). Sorting single molecules: Applications to diagnostics and evolutionary biotechnology, *Proc. Natl. Acad. Sci. USA* **91**:5740.
- Raghavachari, R., Editor. 2001. *Near-Infrared Applications in Biotechnology*, Marcel-Dekker, New York, NY.
- Rigler R. and Widengren J. (1990). Ultrasensitive detection of single molecules by fluorescence correlation spectroscopy, *BioScience* (Ed. Klinge & Owman) p.180.
- Single Cancer Cell Detection by Near Infrared Microspectroscopy, Infrared Chemical Imaging and Fluorescence Microspectroscopy.2004. I. C. Baianu, D. Costescu, N. E. Hofmann, S. S. Korban and et al., q-bio/0407006 (July 2004).
- Voet, D. and J.G. Voet. *Biochemistry*, 2nd Edn., New York, Toronto, Singapore: John Wiley & Sons, Inc., 1995, ISBN: 0-471-58651-X., 1361 pages.
- Watson, G. N. *A Treatise on the Theory of Bessel Functions.*, (1995) Cambridge University Press. ISBN 0-521-48391-3.
- Watson, James D. and Francis H.C. Crick. A structure for Deoxyribose Nucleic Acid (http://www.nature.com/nature/dna50/watsoncrick.pdf) (PDF). *Nature* 171, 737–738,

25 April 1953.
- Watson, James D. *Molecular Biology of the Gene.* New York and Amsterdam: W.A. Benjamin, Inc. 1965., 494 pages.
- Wentworth, W.E. *Physical Chemistry. A short course.*, Malden (Mass.): Blackwell Science, Inc. 2000.
- Herbert R. Wilson, FRS. *Diffraction of X-rays by proteins, Nucleic Acids and Viruses.*, London: Edward Arnold (Publishers) Ltd. 1966.
- Kurt Wuthrich. *NMR of Proteins and Nucleic Acids.*, New York, Brisbane,Chicester, Toronto, Singapore: J. Wiley & Sons. 1986., 292 pages.
- Robinson, Bruche H.; Seeman, Nadrian C. (August 1987). "The Design of a Biochip: A Self-Assembling Molecular-Scale Memory Device". *Protein Engineering* **1** (4): 295–300. ISSN 0269-2139 (http://worldcat.org/issn/0269-2139). Link (http://peds.oxfordjournals.org/cgi/content/abstract/1/4/295)
- Rothemund, Paul W. K.; Ekani-Nkodo, Axel; Papadakis, Nick; Kumar, Ashish; Fygenson, Deborah Kuchnir & Winfree, Erik (22 December 2004). "Design and Characterization of Programmable DNA Nanotubes". *Journal of the American Chemical Society* **126** (50): 16344–16352. doi: 10.1021/ja044319l (http://dx.doi.org/10.1021/ja044319l). ISSN 0002-7863 (http://worldcat.org/issn/0002-7863).
- Keren, K.; Kinneret Keren, Rotem S. Berman, Evgeny Buchstab, Uri Sivan, Erez Braun (November 2003). " DNA-Templated Carbon Nanotube Field-Effect Transistor (http://www.sciencemag.org/cgi/content/abstract/sci;302/5649/1380)". *Science* **302** (6549): 1380–1382. doi: 10.1126/science.1091022 (http://dx.doi.org/10.1126/science.1091022). ISSN 1095-9203 (http://worldcat.org/issn/1095-9203). http://www.sciencemag.org/cgi/content/abstract/sci;302/5649/1380.
- Zheng, Jiwen; Constantinou, Pamela E.; Micheel, Christine; Alivisatos, A. Paul; Kiehl, Richard A. & Seeman Nadrian C. (2006). "2D Nanoparticle Arrays Show the Organizational Power of Robust DNA Motifs". *Nano Letters* **6**: 1502–1504. doi: 10.1021/nl060994c (http://dx.doi.org/10.1021/nl060994c). ISSN 1530-6984 (http://worldcat.org/issn/1530-6984).
- Cohen, Justin D.; Sadowski, John P.; Dervan, Peter B. (2007). "Addressing Single Molecules on DNA Nanostructures". *Angewandte Chemie* **46** (42): 7956–7959. doi: 10.1002/anie.200702767 (http://dx.doi.org/10.1002/anie.200702767). ISSN 0570-0833 (http://worldcat.org/issn/0570-0833).
- Mao, Chengde; Sun, Weiqiong & Seeman, Nadrian C. (16 June 1999). "Designed Two-Dimensional DNA Holliday Junction Arrays Visualized by Atomic Force Microscopy". *Journal of the American Chemical Society* **121** (23): 5437–5443. doi: 10.1021/ja9900398 (http://dx.doi.org/10.1021/ja9900398). ISSN 0002-7863 (http://worldcat.org/issn/0002-7863).
- Constantinou, Pamela E.; Wang, Tong; Kopatsch, Jens; Israel, Lisa B.; Zhang, Xiaoping; Ding, Baoquan; Sherman, William B.; Wang, Xing; Zheng, Jianping; Sha, Ruojie & Seeman, Nadrian C. (2006). "Double cohesion in structural DNA nanotechnology". *Organic and Biomolecular Chemistry* **4**: 3414–3419. doi: 10.1039/b605212f (http://dx.doi.org/10.1039/b605212f).

See also

- → DNA
- Molecular graphics
- DNA structure
- X-ray scattering
- Neutron scattering
- Crystallography
- Crystal lattices
- Paracrystalline lattices/Paracrystals
- → 2D-FT NMRI and Spectroscopy
- NMR Spectroscopy
- Microwave spectroscopy
- Two-dimensional IR spectroscopy
- Spectral imaging
- → Hyperspectral imaging
- → Chemical imaging
- NMR microscopy
- VCD or Vibrational circular dichroism
- FRET and FCS- Fluorescence correlation spectroscopy
- → Fluorescence cross-correlation spectroscopy (FCCS)
- Molecular structure
- Molecular geometry
- Molecular topology
- DNA topology
- Sirius visualization software
- Nanostructure
- → DNA nanotechnology
- Imaging
- Atomic force microscopy
- X-ray microscopy
- Liquid crystal
- Glasses
- QMC@Home
- Sir Lawrence Bragg, FRS
- Sir John Randall
- James Watson
- Francis Crick
- Maurice Wilkins
- Herbert Wilson, FRS
- Alex Stokes

External links

- DNA the Double Helix Game (http://nobelprize.org/educational_games/medicine/dna_double_helix/) From the official Nobel Prize web site
- MDDNA: Structural Bioinformatics of DNA (http://humphry.chem.wesleyan.edu:8080/MDDNA/)
- Double Helix 1953–2003 (http://www.ncbe.reading.ac.uk/DNA50/) National Centre for Biotechnology Education
- DNA under electron microscope (http://www.fidelitysystems.com/Unlinked_DNA.html)
- Ascalaph DNA (http://www.agilemolecule.com/Ascalaph/Ascalaph_DNA.html) — Commercial software for DNA modeling
- DNAlive: a web interface to compute DNA physical properties (http://mmb.pcb.ub.es/DNAlive). Also allows cross-linking of the results with the UCSC Genome browser and DNA dynamics.
- DiProDB: Dinucleotide Property Database (http://diprodb.fli-leibniz.de). The database is designed to collect and analyse thermodynamic, structural and other dinucleotide properties.
- Further details of mathematical and molecular analysis of DNA structure based on X-ray data (http://planetphysics.org/encyclopedia/BesselFunctionsApplicationsToDiffractionByHelicalStructures.html)
- Bessel functions corresponding to Fourier transforms of atomic or molecular helices. (http://planetphysics.org/?op=getobj&from=objects&name=BesselFunctionsAndTheirApplicationsToDiffractionByHelicalStructures)
- Application of X-ray microscopy in analysis of living hydrated cells (http://www.ncbi.nlm.nih.gov/entrez/query.fcgi?cmd=Retrieve&db=pubmed&dopt=Abstract&list_uids=12379938)
- Characterization in nanotechnology some pdfs (http://nanocharacterization.sitesled.com/)
- overview of STM/AFM/SNOM principles with educative videos (http://www.ntmdt.ru/SPM-Techniques/Principles/)
- SPM Image Gallery - AFM STM SEM MFM NSOM and More (http://www.rhk-tech.com/results/showcase.php)
- How SPM Works (http://www.parkafm.com/New_html/resources/01general.php)
- U.S. National DNA Day (http://www.genome.gov/10506367) — watch videos and participate in real-time discusssions with scientists.
- The Secret Life of DNA - DNA Music compositions (http://www.tjmitchell.com/stuart/dna.html)

DNA

Deoxyribonucleic acid (**DNA**) is a nucleic acid that contains the genetic instructions used in the development and functioning of all known living organisms and some viruses. The main role of DNA molecules is the long-term storage of information. DNA is often compared to a set of blueprints or a recipe, or a code, since it contains the instructions needed to construct other components of cells, such as proteins and RNA molecules. The DNA segments that carry this genetic information are called genes, but other DNA sequences have structural purposes, or are involved in regulating the use of this genetic information.

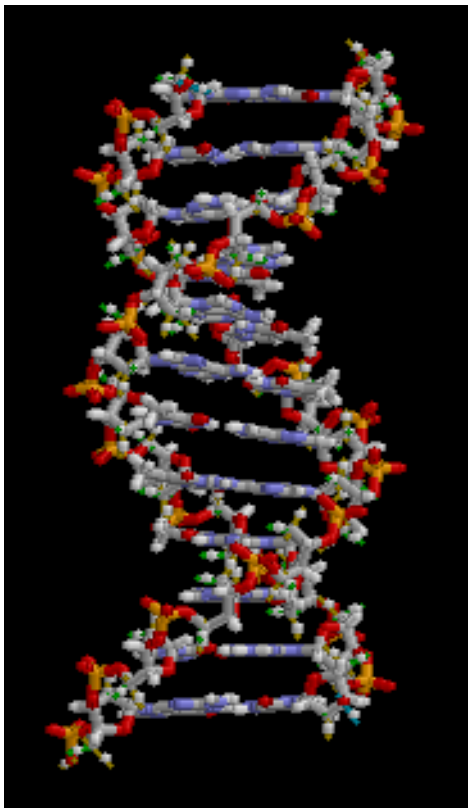

The structure of part of a DNA double helix

Chemically, DNA consists of two long polymers of simple units called nucleotides, with backbones made of sugars and phosphate groups joined by ester bonds. These two strands run in opposite directions to each other and are therefore anti-parallel. Attached to each sugar is one of four types of molecules called bases. It is the sequence of these four bases along the backbone that encodes information. This information is read using the genetic code, which specifies the sequence of the amino acids within proteins. The code is read by copying stretches of DNA into the related nucleic acid RNA, in a process called transcription.

Within cells, DNA is organized into structures called chromosomes. These chromosomes are duplicated before cells divide, in a process called DNA replication. Eukaryotic organisms (animals, plants, fungi, and protists) store most of their DNA inside the cell nucleus and some of their DNA in the mitochondria. Prokaryotes (bacteria and archaea) however, store their DNA in the cell's cytoplasm. Within the chromosomes, chromatin proteins such as histones compact and organize DNA. These compact structures guide the interactions between DNA and other proteins, helping control which parts of the DNA are transcribed.

Properties

DNA is a long polymer made from repeating units called nucleotides.[1] [2] [3] The DNA chain is 22 to 26 Ångströms wide (2.2 to 2.6 nanometres), and one nucleotide unit is 3.3 Å (0.33 nm) long.[4] Although each individual repeating unit is very small, DNA polymers can be very large molecules containing millions of nucleotides. For instance, the largest human chromosome, chromosome number 1, is approximately 220 million base pairs long.[5]

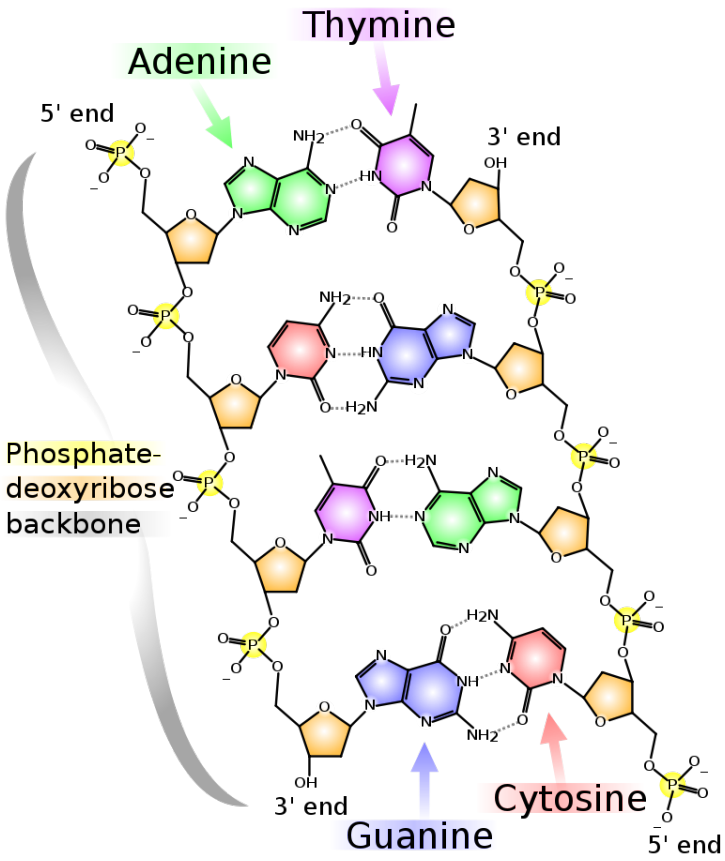

The chemical structure of DNA. Hydrogen bonds are shown as dotted lines.

In living organisms, DNA does not usually exist as a single molecule, but instead as a pair of molecules that are held tightly together.[6] [7] These two long strands entwine like vines, in the shape of a double helix. The nucleotide repeats contain both the segment of the backbone of the molecule, which holds the chain together, and a base, which interacts with the other DNA strand in the helix. In general, a base linked to a sugar is called a nucleoside and a base linked to a sugar and one or more phosphate groups is called a nucleotide. If multiple nucleotides are linked together, as in DNA, this polymer is called a polynucleotide.[8]

The backbone of the DNA strand is made from alternating phosphate and sugar residues.[9] The sugar in DNA is 2-deoxyribose, which is a pentose (five-carbon) sugar. The sugars are joined together by phosphate groups that form phosphodiester bonds between the third and fifth carbon atoms of adjacent sugar rings. These asymmetric bonds mean a strand of DNA has a direction. In a double helix the direction of the nucleotides in one strand is opposite to their direction in the other strand. This arrangement of DNA strands is called antiparallel. The asymmetric ends of DNA strands are referred to as the 5′ (*five prime*) and 3′ (*three prime*) ends, with the 5' end being that with a terminal phosphate group and the 3' end that with a terminal hydroxyl group. One of the major differences between DNA and RNA is the sugar, with 2-deoxyribose being replaced by the alternative pentose sugar ribose in RNA.[7]

The DNA double helix is stabilized by hydrogen bonds between the bases attached to the two strands. The four bases found in DNA are adenine (abbreviated A), cytosine (C), guanine (G) and thymine (T). These four bases are attached to the sugar/phosphate to form the complete nucleotide, as shown for adenosine monophosphate.

These bases are classified into two types; adenine and guanine are fused five- and six-membered heterocyclic compounds called purines, while cytosine and thymine are six-membered rings called pyrimidines.[7] A fifth pyrimidine base, called uracil (U), usually takes the place of thymine in RNA and differs from thymine by lacking a methyl group on its ring. Uracil is not usually found in DNA, occurring only as a breakdown product of cytosine.

Grooves

Twin helical strands form the DNA backbone. Another double helix may be found by tracing the spaces, or grooves, between the strands. These voids are adjacent to the base pairs and may provide a binding site. As the strands are not directly opposite each other, the grooves are unequally sized. One groove, the major groove, is 22 Å wide and the other, the minor groove, is 12 Å wide.[11] The narrowness of the minor groove means that the edges of the bases are more accessible in the major groove. As a result, proteins like transcription factors that can bind to specific sequences in double-stranded DNA usually make contacts to the sides of the bases exposed in the major groove.[12] This situation varies in unusual conformations of DNA within the cell *(see below)*, but the major and minor grooves are always named to reflect the differences in size that would be seen if the DNA is twisted back into the ordinary B form.

Structure of a section of DNA. The bases lie horizontally between the two spiraling strands.[10] Animated version at File:DNA orbit animated.gif - over 3 megabytes.

Base pairing

Each type of base on one strand forms a bond with just one type of base on the other strand. This is called complementary base pairing. Here, purines form hydrogen bonds to pyrimidines, with A bonding only to T, and C bonding only to G. This arrangement of two nucleotides binding together across the double helix is called a base pair. As hydrogen bonds are not covalent, they can be broken and rejoined relatively easily. The two strands of DNA in a double helix can therefore be pulled apart like a zipper, either by a mechanical force or high temperature.[13] As a result of this complementarity, all the information in the double-stranded sequence of a DNA helix is duplicated on each strand, which is vital in DNA replication. Indeed, this reversible and specific interaction between complementary base pairs is critical for all the functions of DNA in living organisms.[2]

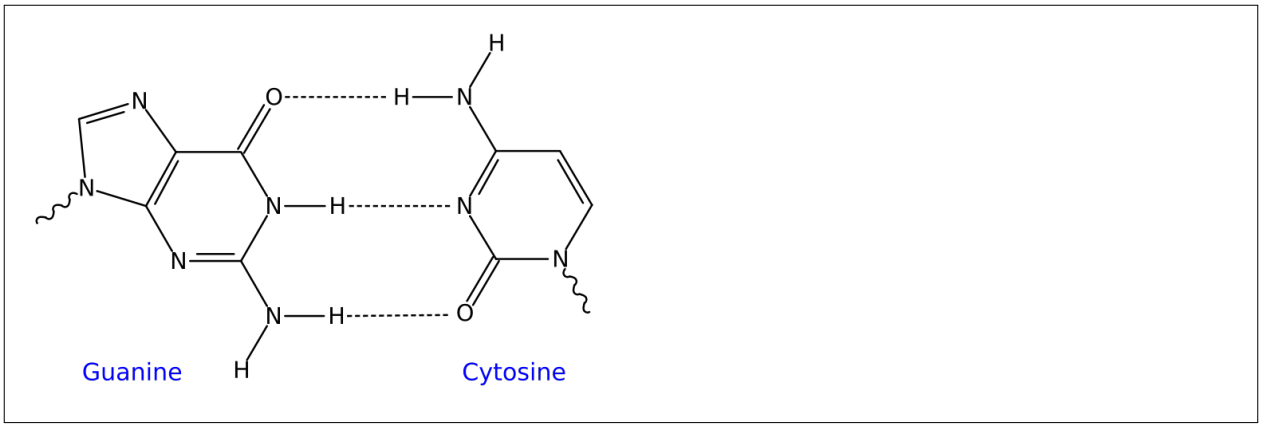

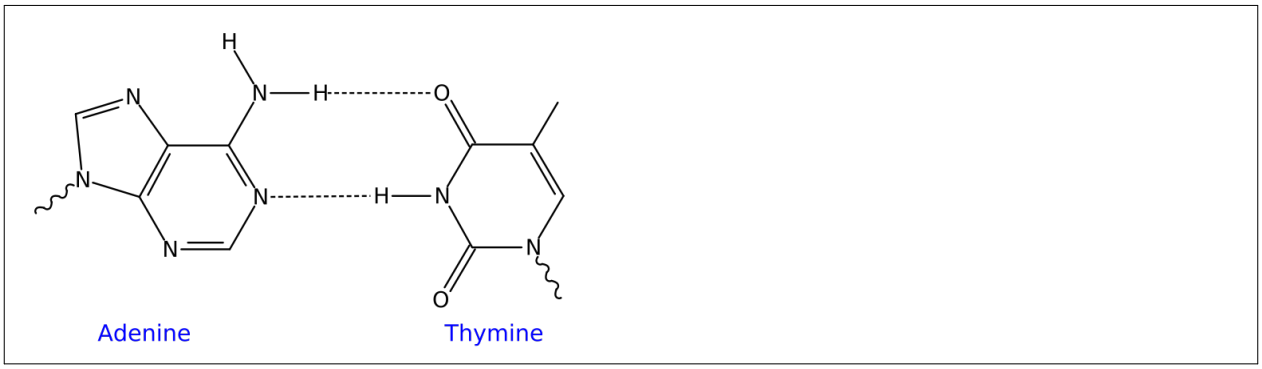

Top, a **GC** base pair with three hydrogen bonds. Bottom, an **AT** base pair with two hydrogen bonds. Non-covalent hydrogen bonds between the pairs are shown as dashed lines.

The two types of base pairs form different numbers of hydrogen bonds, AT forming two hydrogen bonds, and GC forming three hydrogen bonds (see figures, left). DNA with high GC-content is more stable than DNA with low GC-content, but contrary to popular belief, this is not due to the extra hydrogen bond of a GC basepair but rather the contribution of stacking interactions (hydrogen bonding merely provides specificity of the pairing, not stability).[14] As a result, it is both the percentage of GC base pairs and the overall length of a DNA double helix that determine the strength of the association between the two strands of DNA. Long DNA helices with a high GC content have stronger-interacting strands, while short helices with high AT content have weaker-interacting strands.[15] In biology, parts of the DNA double helix that need to separate easily, such as the TATAAT Pribnow box in some promoters, tend to have a high AT content, making the strands easier to pull apart.[16] In the laboratory, the strength of this interaction can be measured by finding the temperature required to break the hydrogen bonds, their melting temperature (also called T_m value). When all the base pairs in a DNA double helix melt, the strands separate and exist in solution as two entirely independent molecules. These single-stranded DNA molecules have no single common shape, but some conformations are more stable than others.[17]

Sense and antisense

A DNA sequence is called "sense" if its sequence is the same as that of a messenger RNA copy that is translated into protein.[18] The sequence on the opposite strand is called the "antisense" sequence. Both sense and antisense sequences can exist on different parts of the same strand of DNA (i.e. both strands contain both sense and antisense sequences). In both prokaryotes and eukaryotes, antisense RNA sequences are produced, but the functions of these RNAs are not entirely clear.[19] One proposal is that antisense RNAs are involved in regulating gene expression through RNA-RNA base pairing.[20]

A few DNA sequences in prokaryotes and eukaryotes, and more in plasmids and viruses, blur the distinction between sense and antisense strands by having overlapping genes.[21] In these cases, some DNA sequences do double duty, encoding one protein when read along one strand, and a second protein when read in the opposite direction along the other strand. In bacteria, this overlap may be involved in the regulation of gene transcription,[22] while in viruses, overlapping genes increase the amount of information that can be encoded within the small viral genome.[23]

Supercoiling

DNA can be twisted like a rope in a process called DNA supercoiling. With DNA in its "relaxed" state, a strand usually circles the axis of the double helix once every 10.4 base pairs, but if the DNA is twisted the strands become more tightly or more loosely wound.[24] If the DNA is twisted in the direction of the helix, this is positive supercoiling, and the bases are held more tightly together. If they are twisted in the opposite direction, this is negative supercoiling, and the bases come apart more easily. In nature, most DNA has slight negative supercoiling that is introduced by enzymes called topoisomerases.[25] These enzymes are also needed to relieve the twisting stresses introduced into DNA strands during processes such as transcription and DNA replication.[26]

Alternate DNA structures

DNA exists in many possible conformations that include A-DNA, B-DNA, and Z-DNA forms, although, only B-DNA and Z-DNA have been directly observed in functional organisms.[9] The conformation that DNA adopts depends on the hydration level, DNA sequence, the amount and direction of supercoiling, chemical modifications of the bases, the type and concentration of metal ions, as well as the presence of polyamines in solution.[27]

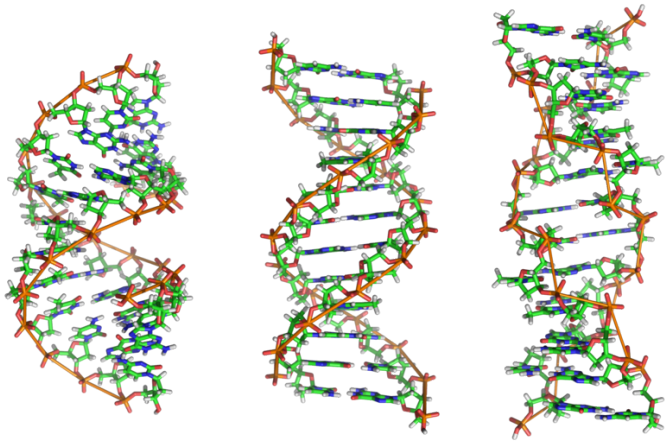

From left to right, the structures of A, B and Z DNA

The first published reports of A-DNA X-ray diffraction patterns— and also B-DNA used analyses based on Patterson transforms that provided only a limited amount of structural information for oriented fibers of DNA.[28] [29] An alternate analysis was then proposed by Wilkins *et al.*, in 1953, for the *in vivo* B-DNA X-ray diffraction/scattering patterns of highly

hydrated DNA fibers in terms of squares of Bessel functions.[30] In the same journal, Watson and Crick presented their → molecular modeling analysis of the DNA X-ray diffraction patterns to suggest that the structure was a double-helix.[6]

Although the `B-DNA form' is most common under the conditions found in cells,[31] it is not a well-defined conformation but a family of related DNA conformations[32] that occur at the high hydration levels present in living cells. Their corresponding X-ray diffraction and scattering patterns are characteristic of molecular paracrystals with a significant degree of disorder.[33] [34]

Compared to B-DNA, the A-DNA form is a wider right-handed spiral, with a shallow, wide minor groove and a narrower, deeper major groove. The A form occurs under non-physiological conditions in partially dehydrated samples of DNA, while in the cell it may be produced in hybrid pairings of DNA and RNA strands, as well as in enzyme-DNA complexes.[35] [36] Segments of DNA where the bases have been chemically modified by methylation may undergo a larger change in conformation and adopt the Z form. Here, the strands turn about the helical axis in a left-handed spiral, the opposite of the more common B form.[37] These unusual structures can be recognized by specific Z-DNA binding proteins and may be involved in the regulation of transcription.[38]

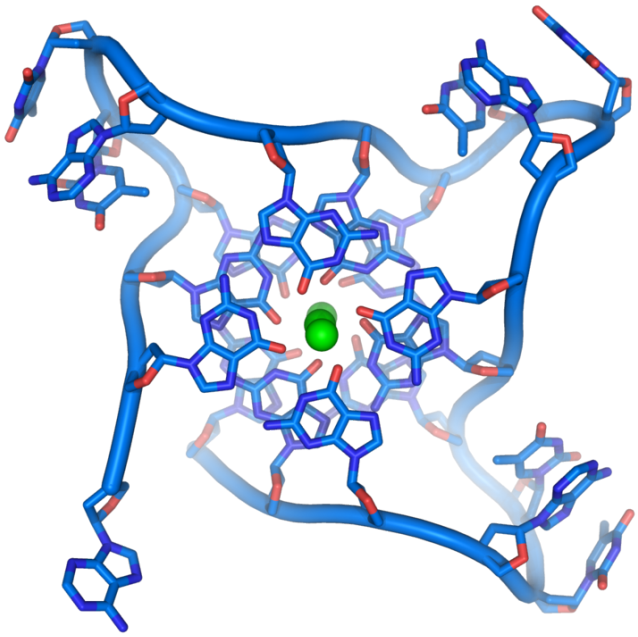

Structure of a DNA quadruplex formed by telomere repeats. The looped conformation of the DNA backbone is very different from the typical helical structure.[39]

Quadruplex structures

At the ends of the linear chromosomes are specialized regions of DNA called telomeres. The main function of these regions is to allow the cell to replicate chromosome ends using the enzyme telomerase, as the enzymes that normally replicate DNA cannot copy the extreme 3′ ends of chromosomes.[40] These specialized chromosome caps also help protect the DNA ends, and stop the DNA repair systems in the cell from treating them as damage to be corrected.[41] In human cells, telomeres are usually lengths of single-stranded DNA containing several thousand repeats of a simple TTAGGG sequence.[42]

These guanine-rich sequences may stabilize chromosome ends by forming structures of stacked sets of four-base units, rather than the usual base pairs found in other DNA molecules. Here, four guanine bases form a flat plate and these flat four-base units then stack on top of each other, to form a stable *G-quadruplex* structure.[43] These structures are stabilized by hydrogen bonding between the edges of the bases and chelation of a metal ion in the centre of each four-base unit.[44] Other structures can also be formed, with the central set of four bases coming from either a single strand folded around the bases, or several different parallel strands, each contributing one base to the central structure.

In addition to these stacked structures, telomeres also form large loop structures called telomere loops, or T-loops. Here, the single-stranded DNA curls around in a long circle stabilized by telomere-binding proteins.[45] At the very end of the T-loop, the single-stranded telomere DNA is held onto a region of double-stranded DNA by the telomere strand disrupting the double-helical DNA and base pairing to one of the two strands. This triple-stranded structure is called a displacement loop or D-loop.[43]

Branched DNA

In DNA fraying occurs when non-complementary regions exist at the end of an otherwise complementary double-strand of DNA. However, branched DNA can occur if a third strand of DNA is introduced and contains adjoining regions able to hybridize with the frayed regions of the pre-existing double-strand. Although the simplest example of branched DNA involves only three strands of DNA, complexes involving additional strands and multiple branches are also possible.[46]

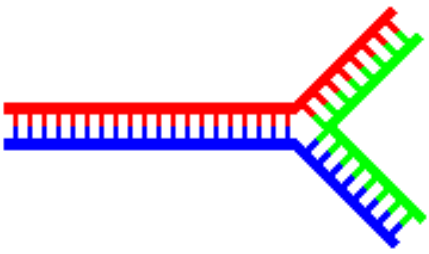

A DNA structure with a single branching point.

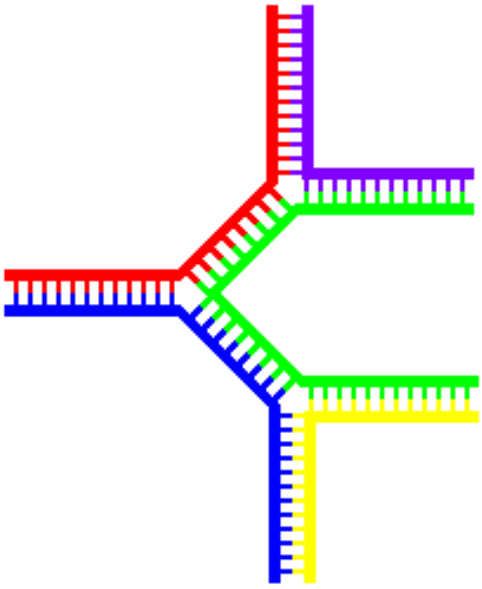

A DNA structure with multiple branches.

Chemical modifications

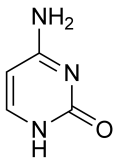

cytosine

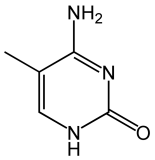

5-methylcytosine

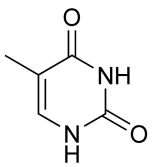

thymine

Structure of cytosine with and without the 5-methyl group. After deamination the 5-methylcytosine has the same structure as thymine

Base modifications

The expression of genes is influenced by how the DNA is packaged in chromosomes, in a structure called chromatin. Base modifications can be involved in packaging, with regions that have low or no gene expression usually containing high levels of methylation of cytosine bases. For example, cytosine methylation, produces 5-methylcytosine, which is important for X-chromosome inactivation.[47] The average level of methylation varies between organisms - the worm *Caenorhabditis elegans* lacks cytosine methylation, while vertebrates have higher levels, with up to 1% of their DNA containing 5-methylcytosine.[48] Despite the importance of 5-methylcytosine, it can deaminate to leave a thymine base, methylated cytosines are therefore particularly prone to mutations.[49] Other base modifications include adenine methylation in bacteria, the presence of 5-hydroxymethylcytosine in the brain,[50] and the glycosylation of uracil to produce the "J-base" in kinetoplastids.[51] [52]

Damage

DNA can be damaged by many different sorts of mutagens, which change the DNA sequence. Mutagens include oxidizing agents, alkylating agents and also high-energy electromagnetic radiation such as ultraviolet light and X-rays. The type of DNA damage produced depends on the type of mutagen. For example, UV light can damage DNA by producing thymine dimers, which are cross-links between pyrimidine bases.[54] On the other hand, oxidants such as free radicals or hydrogen peroxide produce multiple forms of damage, including base modifications, particularly of guanosine, and double-strand breaks.[55] A typical human cell contains about 150,000 bases that have suffered oxidative damage.[56] Of these oxidative lesions, the most dangerous are double-strand breaks, as these are difficult to repair and can produce point mutations, insertions and deletions from the DNA sequence, as well as chromosomal translocations.[57]

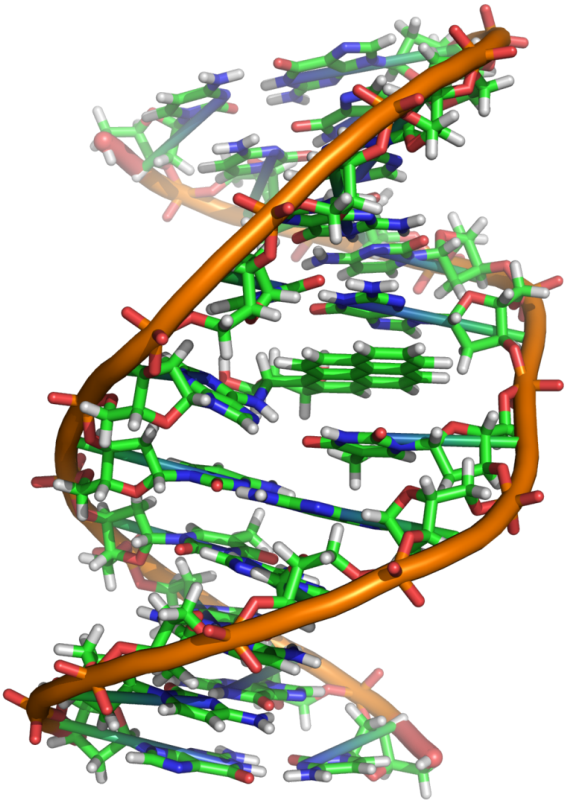

A covalent adduct between benzo[*a*]pyrene, the major mutagen in tobacco smoke, and DNA[53]

Many mutagens fit into the space between two adjacent base pairs, this is called *intercalating*. Most intercalators are aromatic and planar molecules, and include Ethidium bromide, daunomycin, and doxorubicin. In order for an intercalator to fit between base pairs, the bases must separate, distorting the DNA strands by unwinding of the double helix. This inhibits both transcription and DNA replication, causing toxicity and mutations. As a result, DNA intercalators are often carcinogens, and Benzo[*a*]pyrene diol epoxide,

acridines, aflatoxin and ethidium bromide are well-known examples.[58] [59] [60] Nevertheless, due to their ability to inhibit DNA transcription and replication, other similar toxins are also used in chemotherapy to inhibit rapidly growing cancer cells.[61]

Biological functions

DNA usually occurs as linear chromosomes in eukaryotes, and circular chromosomes in prokaryotes. The set of chromosomes in a cell makes up its genome; the human genome has approximately 3 billion base pairs of DNA arranged into 46 chromosomes.[62] The information carried by DNA is held in the sequence of pieces of DNA called genes. Transmission of genetic information in genes is achieved via complementary base pairing. For example, in transcription, when a cell uses the information in a gene, the DNA sequence is copied into a complementary RNA sequence through the attraction between the DNA and the correct RNA nucleotides. Usually, this RNA copy is then used to make a matching protein sequence in a process called translation which depends on the same interaction between RNA nucleotides. Alternatively, a cell may simply copy its genetic information in a process called DNA replication. The details of these functions are covered in other articles; here we focus on the interactions between DNA and other molecules that mediate the function of the genome.

Genes and genomes

Genomic DNA is located in the cell nucleus of eukaryotes, as well as small amounts in mitochondria and chloroplasts. In prokaryotes, the DNA is held within an irregularly shaped body in the cytoplasm called the nucleoid.[63] The genetic information in a genome is held within genes, and the complete set of this information in an organism is called its genotype. A gene is a unit of heredity and is a region of DNA that influences a particular characteristic in an organism. Genes contain an open reading frame that can be transcribed, as well as regulatory sequences such as promoters and enhancers, which control the transcription of the open reading frame.

In many species, only a small fraction of the total sequence of the genome encodes protein. For example, only about 1.5% of the human genome consists of protein-coding exons, with over 50% of human DNA consisting of non-coding repetitive sequences.[64] The reasons for the presence of so much non-coding DNA in eukaryotic genomes and the extraordinary differences in genome size, or *C-value*, among species represent a long-standing puzzle known as the "C-value enigma."[65] However, DNA sequences that do not code protein may still encode functional non-coding RNA molecules, which are involved in the regulation of gene expression.[66]

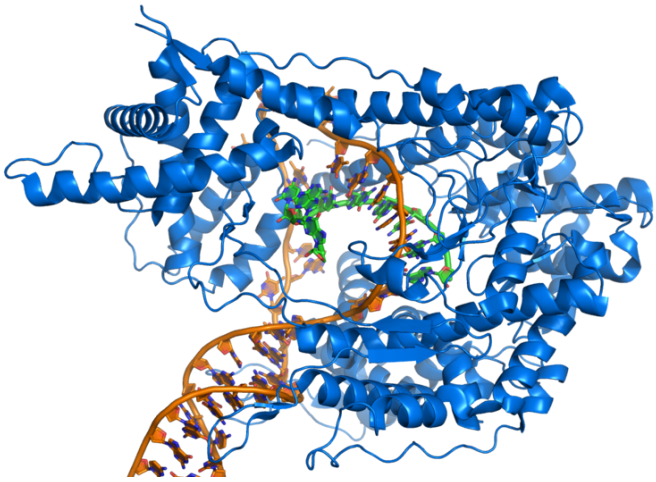

T7 RNA polymerase (blue) producing a mRNA (green) from a DNA template (orange).[67]

Some non-coding DNA sequences play structural roles in chromosomes. Telomeres and centromeres typically contain few genes, but are important for the function and stability of chromosomes.[41] [68] An abundant form of non-coding DNA in humans are pseudogenes, which are copies of genes that have been disabled by mutation.[69] These sequences are usually just molecular fossils, although they can occasionally serve as raw genetic material for the creation of new genes through the process of gene duplication and divergence.[70]

Transcription and translation

A gene is a sequence of DNA that contains genetic information and can influence the phenotype of an organism. Within a gene, the sequence of bases along a DNA strand defines a messenger RNA sequence, which then defines one or more protein sequences. The relationship between the nucleotide sequences of genes and the amino-acid sequences of proteins is determined by the rules of translation, known collectively as the genetic code. The genetic code consists of three-letter 'words' called *codons* formed from a sequence of three nucleotides (e.g. ACT, CAG, TTT).

In transcription, the codons of a gene are copied into messenger RNA by RNA polymerase. This RNA copy is then decoded by a ribosome that reads the RNA sequence by base-pairing the messenger RNA to transfer RNA, which carries amino acids. Since there are 4 bases in 3-letter combinations, there are 64 possible codons (4^3 combinations). These encode the twenty standard amino acids, giving most amino acids more than one possible codon. There are also three 'stop' or 'nonsense' codons signifying the end of the coding region; these are the TAA, TGA and TAG codons.

Replication

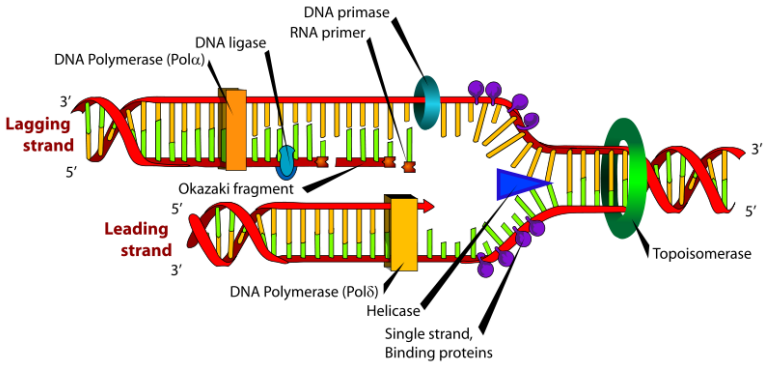

DNA replication. The double helix is unwound by a helicase and topoisomerase. Next, one DNA polymerase produces the leading strand copy. Another DNA polymerase binds to the lagging strand. This enzyme makes discontinuous segments (called Okazaki fragments) before DNA ligase joins them together.

Cell division is essential for an organism to grow, but when a cell divides it must replicate the DNA in its genome so that the two daughter cells have the same genetic information as their parent. The double-stranded structure of DNA provides a simple mechanism for DNA replication. Here, the two strands are separated and then each strand's complementary DNA sequence is recreated by an enzyme called DNA polymerase. This enzyme makes the complementary strand by finding the correct base through complementary base pairing, and bonding it onto the original strand. As DNA polymerases can only extend a DNA strand in a 5′ to 3′ direction, different mechanisms are used to copy the antiparallel strands of the double helix.[71] In this way, the base on the old strand dictates which base appears on the new strand, and the cell ends up with a perfect copy of its DNA.

Interactions with proteins

All the functions of DNA depend on interactions with proteins. These protein interactions can be non-specific, or the protein can bind specifically to a single DNA sequence. Enzymes can also bind to DNA and of these, the polymerases that copy the DNA base sequence in transcription and DNA replication are particularly important.

DNA-binding proteins

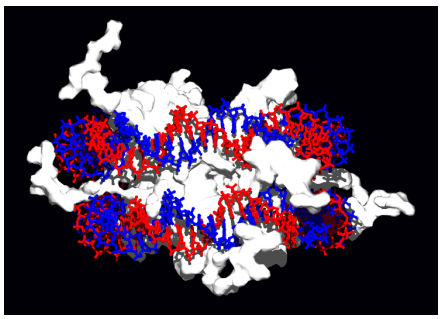

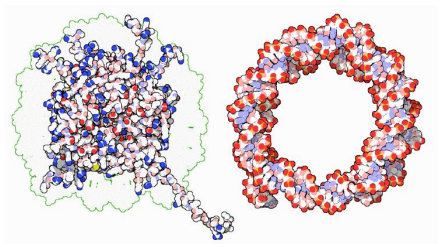

Interaction of DNA with histones (shown in white, top). These proteins' basic amino acids (below left, blue) bind to the acidic phosphate groups on DNA (below right, red).

Structural proteins that bind DNA are well-understood examples of non-specific DNA-protein interactions. Within chromosomes, DNA is held in complexes with structural proteins. These proteins organize the DNA into a compact structure called chromatin. In eukaryotes this structure involves DNA binding to a complex of small basic proteins called histones, while in prokaryotes multiple types of proteins are involved.[72] [73] The histones form a disk-shaped complex called a nucleosome, which contains two complete turns of double-stranded DNA wrapped around its surface. These non-specific interactions are formed through basic residues in the histones making ionic bonds to the acidic sugar-phosphate backbone of the DNA, and are therefore largely independent of the base sequence.[74] Chemical modifications of these basic amino acid residues include methylation, phosphorylation and acetylation.[75] These chemical changes alter the strength of the interaction between the DNA and the histones, making the DNA more or less accessible to transcription factors and changing the rate of transcription.[76] Other non-specific DNA-binding proteins in chromatin include the high-mobility group proteins, which bind to bent or distorted DNA.[77] These proteins are important in bending arrays of nucleosomes and arranging them into the larger structures that make up chromosomes.[78]

A distinct group of DNA-binding proteins are the DNA-binding proteins that specifically bind single-stranded DNA. In humans, replication protein A is the best-understood member of this family and is used in processes where the double helix is separated, including DNA replication, recombination and DNA repair.[79] These binding proteins seem to stabilize single-stranded DNA and protect it from forming stem-loops or being degraded by nucleases.

In contrast, other proteins have evolved to bind to particular DNA sequences. The most intensively studied of these are the various transcription factors, which are proteins that regulate transcription. Each transcription factor binds to one particular set of DNA sequences and activates or inhibits the transcription of genes that have these sequences close to their promoters. The transcription factors do this in two ways. Firstly, they can bind the RNA polymerase responsible for transcription, either directly or through other mediator proteins; this locates the polymerase at the promoter and allows it to begin transcription.[81] Alternatively, transcription factors can bind enzymes that modify the histones at the promoter; this will change the accessibility of the DNA template to the polymerase.[82]

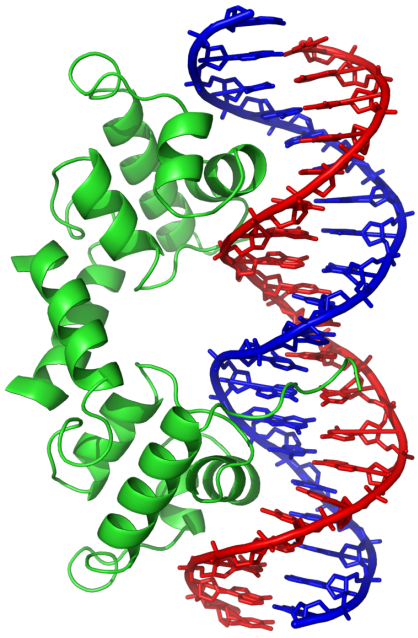

The lambda repressor helix-turn-helix transcription factor bound to its DNA target[80]

As these DNA targets can occur throughout an organism's genome, changes in the activity of one type of transcription factor can affect thousands of genes.[83] Consequently, these proteins are often the targets of the signal transduction processes that control responses to environmental changes or cellular differentiation and development. The specificity of these transcription

factors' interactions with DNA come from the proteins making multiple contacts to the edges of the DNA bases, allowing them to "read" the DNA sequence. Most of these base-interactions are made in the major groove, where the bases are most accessible.[84]

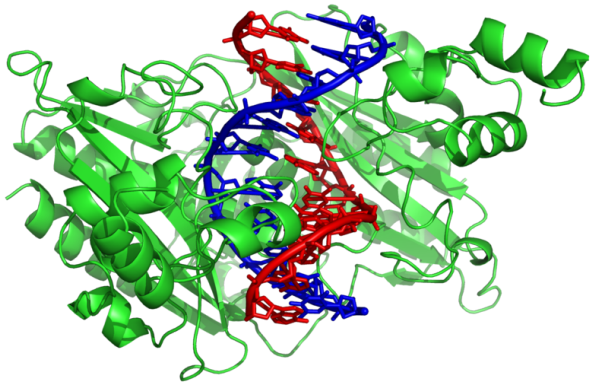

The restriction enzyme EcoRV (green) in a complex with its substrate DNA[85]

DNA-modifying enzymes

Nucleases and ligases

Nucleases are enzymes that cut DNA strands by catalyzing the hydrolysis of the phosphodiester bonds. Nucleases that hydrolyse nucleotides from the ends of DNA strands are called exonucleases, while endonucleases cut within strands. The most frequently used nucleases in molecular biology are the restriction endonucleases, which cut DNA at specific sequences. For instance, the EcoRV enzyme shown to the left recognizes the 6-base sequence 5′-GAT|ATC-3′ and makes a cut at the vertical line. In nature, these enzymes protect bacteria against phage infection by digesting the phage DNA when it enters the bacterial cell, acting as part of the restriction modification system.[86] In technology, these sequence-specific nucleases are used in molecular cloning and DNA fingerprinting.

Enzymes called DNA ligases can rejoin cut or broken DNA strands.[87] Ligases are particularly important in lagging strand DNA replication, as they join together the short segments of DNA produced at the replication fork into a complete copy of the DNA template. They are also used in DNA repair and genetic recombination.[87]

Topoisomerases and helicases

Topoisomerases are enzymes with both nuclease and ligase activity. These proteins change the amount of supercoiling in DNA. Some of these enzyme work by cutting the DNA helix and allowing one section to rotate, thereby reducing its level of supercoiling; the enzyme then seals the DNA break.[25] Other types of these enzymes are capable of cutting one DNA helix and then passing a second strand of DNA through this break, before rejoining the helix.[88] Topoisomerases are required for many processes involving DNA, such as DNA replication and transcription.[26]

Helicases are proteins that are a type of molecular motor. They use the chemical energy in nucleoside triphosphates, predominantly ATP, to break hydrogen bonds between bases and unwind the DNA double helix into single strands.[89] These enzymes are essential for most processes where enzymes need to access the DNA bases.

Polymerases

Polymerases are enzymes that synthesize polynucleotide chains from nucleoside triphosphates. The sequence of their products are copies of existing polynucleotide chains - which are called *templates*. These enzymes function by adding nucleotides onto the 3′ hydroxyl group of the previous nucleotide in a DNA strand. Consequently, all polymerases work in a 5′ to 3′ direction.[90] In the active site of these enzymes, the incoming nucleoside triphosphate base-pairs to the template: this allows polymerases to accurately synthesize the complementary strand of their template. Polymerases are classified according to the type of template that they use.

In DNA replication, a DNA-dependent DNA polymerase makes a copy of a DNA sequence. Accuracy is vital in this process, so many of these polymerases have a proofreading activity. Here, the polymerase recognizes the occasional mistakes in the synthesis reaction by the lack of base pairing between the mismatched nucleotides. If a mismatch is detected, a 3′ to 5′ exonuclease activity is activated and the incorrect base removed.[91] In most organisms DNA polymerases function in a large complex called the replisome that contains multiple accessory subunits, such as the DNA clamp or helicases.[92]

RNA-dependent DNA polymerases are a specialized class of polymerases that copy the sequence of an RNA strand into DNA. They include reverse transcriptase, which is a viral enzyme involved in the infection of cells by retroviruses, and telomerase, which is required for the replication of telomeres.[40] [93] Telomerase is an unusual polymerase because it contains its own RNA template as part of its structure.[41]

Transcription is carried out by a DNA-dependent RNA polymerase that copies the sequence of a DNA strand into RNA. To begin transcribing a gene, the RNA polymerase binds to a sequence of DNA called a promoter and separates the DNA strands. It then copies the gene sequence into a messenger RNA transcript until it reaches a region of DNA called the terminator, where it halts and detaches from the DNA. As with human DNA-dependent DNA polymerases, RNA polymerase II, the enzyme that transcribes most of the genes in the human genome, operates as part of a large protein complex with multiple regulatory and accessory subunits.[94]

Genetic recombination

Structure of the Holliday junction intermediate in genetic recombination. The four separate DNA strands are coloured red, blue, green and yellow.[95]

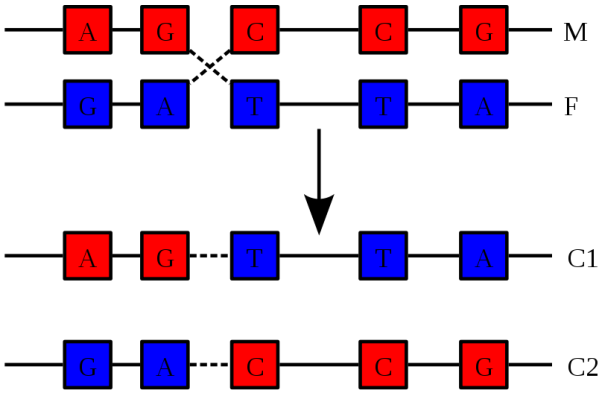

Recombination involves the breakage and rejoining of two chromosomes (M and F) to produce two re-arranged chromosomes (C1 and C2).

A DNA helix usually does not interact with other segments of DNA, and in human cells the different chromosomes even occupy separate areas in the nucleus called "chromosome territories".[96] This physical separation of different chromosomes is important for the ability of DNA to function as a stable repository for information, as one of the few times chromosomes interact is during chromosomal crossover when they recombine. Chromosomal crossover is when two DNA helices break, swap a section and then rejoin.

Recombination allows chromosomes to exchange genetic information and produces new combinations of genes, which increases the efficiency of natural selection and can be important in the rapid evolution of new proteins.[97] Genetic recombination can also be involved in DNA repair, particularly in the cell's response to double-strand breaks.[98]

The most common form of chromosomal crossover is homologous recombination, where the two chromosomes involved share very similar sequences. Non-homologous recombination can be damaging to cells, as it can produce chromosomal translocations and genetic abnormalities. The recombination reaction is catalyzed by enzymes known as *recombinases*, such as RAD51.[99] The first step in recombination is a double-stranded break either caused by an endonuclease or damage to the DNA.[100] A series of steps catalyzed in part by the recombinase then leads to joining of the two helices by at least one Holliday junction, in which a segment of a single strand in each helix is annealed to the complementary strand in the other helix. The Holliday junction is a tetrahedral junction structure that can be moved along the pair of chromosomes, swapping one strand for another. The recombination reaction is then halted by cleavage of the junction and re-ligation of the released DNA.[101]

Evolution

DNA contains the genetic information that allows all modern living things to function, grow and reproduce. However, it is unclear how long in the 4-billion-year history of life DNA has performed this function, as it has been proposed that the earliest forms of life may have used RNA as their genetic material.[90] [102] RNA may have acted as the central part of early cell metabolism as it can both transmit genetic information and carry out catalysis as part of ribozymes.[103] This ancient RNA world where nucleic acid would have been used for both catalysis and genetics may have influenced the evolution of the current genetic code based on four nucleotide bases. This would occur since the number of unique bases in such an organism is a trade-off between a small number of bases increasing replication accuracy and a large number of bases increasing the catalytic efficiency of ribozymes.[104]

Unfortunately, there is no direct evidence of ancient genetic systems, as recovery of DNA from most fossils is impossible. This is because DNA will survive in the environment for less than one million years and slowly degrades into short fragments in solution.[105] Claims for older DNA have been made, most notably a report of the isolation of a viable bacterium from a salt crystal 250-million years old,[106] but these claims are controversial.[107] [108]

Uses in technology

Genetic engineering

Methods have been developed to purify DNA from organisms, such as phenol-chloroform extraction and manipulate it in the laboratory, such as restriction digests and the polymerase chain reaction. Modern biology and biochemistry make intensive use of these techniques in recombinant DNA technology. Recombinant DNA is a man-made DNA sequence that has been assembled from other DNA sequences. They can be transformed into organisms in the form of plasmids or in the appropriate format, by using a viral vector.[109] The genetically modified organisms produced can be used to produce products such as recombinant proteins, used in medical research,[110] or be grown in agriculture.[111] [112]

Forensics

Forensic scientists can use DNA in blood, semen, skin, saliva or hair found at a crime scene to identify a matching DNA of an individual, such as a perpetrator. This process is called genetic fingerprinting, or more accurately, DNA profiling. In DNA profiling, the lengths of variable sections of repetitive DNA, such as short tandem repeats and minisatellites, are compared between people. This method is usually an extremely reliable technique for identifying a matching DNA.[113] However, identification can be complicated if the scene is contaminated with DNA from several people.[114] DNA profiling was developed in 1984 by British geneticist Sir Alec Jeffreys,[115] and first used in forensic science to convict Colin Pitchfork in the 1988 Enderby murders case.[116]

People convicted of certain types of crimes may be required to provide a sample of DNA for a database. This has helped investigators solve old cases where only a DNA sample was obtained from the scene. DNA profiling can also be used to identify victims of mass casualty incidents.[117] On the other hand, many convicted people have been released from prison on the basis of DNA techniques, which were not available when a crime had originally been committed.

Bioinformatics

Bioinformatics involves the manipulation, searching, and data mining of DNA sequence data. The development of techniques to store and search DNA sequences have led to widely applied advances in computer science, especially string searching algorithms, machine learning and database theory.[118] String searching or matching algorithms, which find an occurrence of a sequence of letters inside a larger sequence of letters, were developed to search for specific sequences of nucleotides.[119] In other applications such as text editors, even simple algorithms for this problem usually suffice, but DNA sequences cause these algorithms to exhibit near-worst-case behaviour due to their small number of distinct characters. The related problem of sequence alignment aims to identify homologous sequences and locate the specific mutations that make them distinct. These techniques, especially multiple sequence alignment, are used in studying phylogenetic relationships and protein function.[120] Data sets representing entire genomes' worth of DNA sequences, such as those produced by the Human Genome Project, are difficult to use without annotations, which label the locations of genes and regulatory elements on each chromosome. Regions of DNA sequence that have the characteristic patterns associated with protein- or RNA-coding genes can be identified by gene finding algorithms, which allow researchers to predict the presence of particular gene products in an organism even before they have been isolated experimentally.[121]

DNA nanotechnology

DNA nanotechnology uses the unique molecular recognition properties of DNA and other nucleic acids to create self-assembling branched DNA complexes with useful properties.[123] DNA is thus used as a structural material rather than as a carrier of biological information. This has led to the creation of two-dimensional periodic lattices (both tile-based as well as using the "DNA origami" method) as well as three-dimensional structures in the shapes of polyhedra.[124] Nanomechanical devices and algorithmic self-assembly have also been demonstrated,[125] and these DNA structures have been used to template the arrangement of other molecules such as gold nanoparticles and streptavidin proteins.[126]

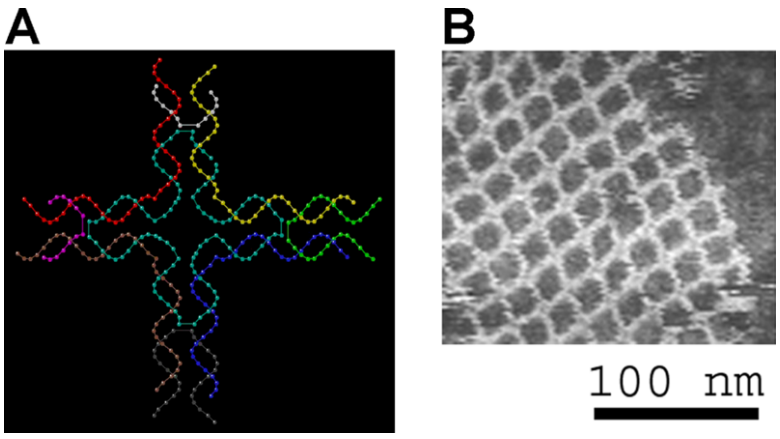

The DNA structure at left (schematic shown) will self-assemble into the structure visualized by atomic force microscopy at right. → DNA nanotechnology is the field which seeks to design nanoscale structures using the molecular recognition properties of DNA molecules. Image from Strong, 2004.[122]

History and anthropology

Because DNA collects mutations over time, which are then inherited, it contains historical information and by comparing DNA sequences, geneticists can infer the evolutionary history of organisms, their phylogeny.[127] This field of phylogenetics is a powerful tool in

evolutionary biology. If DNA sequences within a species are compared, population geneticists can learn the history of particular populations. This can be used in studies ranging from ecological genetics to anthropology; for example, DNA evidence is being used to try to identify the Ten Lost Tribes of Israel.[128] [129]

DNA has also been used to look at modern family relationships, such as establishing family relationships between the descendants of Sally Hemings and Thomas Jefferson. This usage is closely related to the use of DNA in criminal investigations detailed above. Indeed, some criminal investigations have been solved when DNA from crime scenes has matched relatives of the guilty individual.[130]

History of DNA research

DNA was first isolated by the Swiss physician Friedrich Miescher who, in 1869, discovered a microscopic substance in the pus of discarded surgical bandages. As it resided in the nuclei of cells, he called it "nuclein".[131] In 1919, Phoebus Levene identified the base, sugar and phosphate nucleotide unit.[132] Levene suggested that DNA consisted of a string of nucleotide units linked together through the phosphate groups. However, Levene thought the chain was short and the bases repeated in a fixed order. In 1937 William Astbury produced the first X-ray diffraction patterns that showed that DNA had a regular structure.[133]

In 1928, Frederick Griffith discovered that traits of the "smooth" form of the *Pneumococcus* could be transferred to the "rough" form of the same bacteria by mixing killed "smooth" bacteria with the live "rough" form.[134] This system provided the first clear suggestion that DNA carried genetic information—the Avery-MacLeod-McCarty experiment—when Oswald Avery, along with coworkers Colin MacLeod and Maclyn McCarty, identified DNA as the transforming principle in 1943.[135] DNA's role in heredity was confirmed in 1952, when Alfred Hershey and Martha Chase in the Hershey-Chase experiment showed that DNA is the genetic material of the T2 phage.[136]

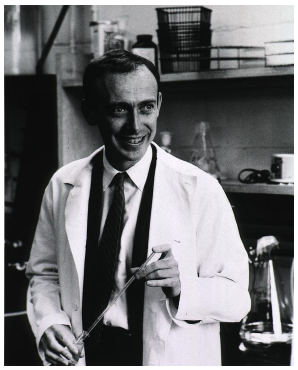

James D. Watson

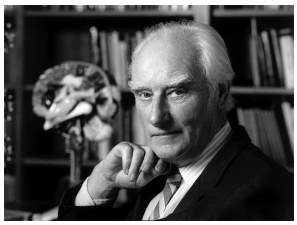

Francis Crick

Francis Crick

Rosalind Franklin

Raymond Gosling

Maurice F.Wilkins

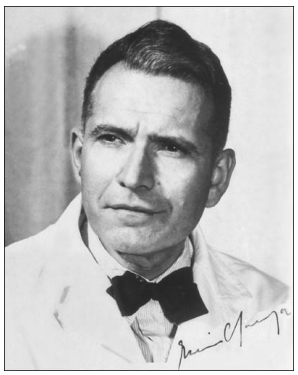

Erwin Chargaff

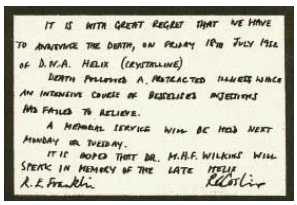

DNA Helix controversy

In 1953 James D. Watson and Francis Crick suggested what is now accepted as the first correct double-helix model of DNA structure in the journal *Nature*.[6] Their double-helix, molecular model of DNA was then based on a single X-ray diffraction image (labeled as "Photo 51")[137] taken by Rosalind Franklin and Raymond Gosling in May 1952, as well as the information that the DNA bases were paired—also obtained through private communications from Erwin Chargaff in the previous years. Chargaff's rules played a very important role in establishing double-helix configurations for B-DNA as well as A-DNA.

Experimental evidence supporting the Watson and Crick model were published in a series of five articles in the same issue of *Nature*.[138] Of these, Franklin and Gosling's paper was the first publication of their own X-ray diffraction data and original analysis method that partially supported the Watson and Crick model[29] [139] ; this issue also contained an article on DNA structure by Maurice Wilkins and two of his colleagues, whose analysis and **in vivo** B-DNA X-ray patterns also supported the presence *in vivo* of the double-helical DNA configurations as proposed by Crick and Watson for their double-helix molecular model of DNA in the previous two pages of *Nature*.[30] In 1962, after Franklin's death, Watson, Crick, and Wilkins jointly received the Nobel Prize in Physiology or Medicine.[140] Unfortunately, Nobel rules of the time allowed only living recipients, but a vigorous debate continues on who should receive credit for the discovery.[141]

In an influential presentation in 1957, Crick laid out the "Central Dogma" of molecular biology, which foretold the relationship between DNA, RNA, and proteins, and articulated the "adaptor hypothesis".[142] Final confirmation of the replication mechanism that was implied by the double-helical structure followed in 1958 through the Meselson-Stahl experiment.[143] Further work by Crick and coworkers showed that the genetic code was based on non-overlapping triplets of bases, called codons, allowing Har Gobind Khorana, Robert W. Holley and Marshall Warren Nirenberg to decipher the genetic code.[144] These findings represent the birth of molecular biology.

See also

- Molecular Structure of Nucleic Acids: A Structure for Deoxyribose Nucleic Acid
- → Molecular models of DNA
- DNA microarray
- DNA sequencing
- Paracrystal model and theory
- X-ray scattering
- Crystallography
- X-ray crystallography
- Genetic disorder
- Junk DNA
- Nucleic acid analogues
- Nucleic acid methods
- Nucleic acid modeling
- Nucleic Acid Notations
- Phosphoramidite
- Plasmid
- Polymerase chain reaction
- *Proteopedia DNA* [145]
- Southern blot
- Triple-stranded DNA

Notes

[1] Saenger, Wolfram (1984). *Principles of Nucleic Acid Structure*. New York: Springer-Verlag. ISBN 0387907629.

[2] Alberts, Bruce; Alexander Johnson, Julian Lewis, Martin Raff, Keith Roberts, and Peter Walters (2002). *Molecular Biology of the Cell; Fourth Edition (http://www.ncbi.nlm.nih.gov/books/bv.fcgi?call=bv.View..ShowTOC&rid=mboc4.TOC&depth=2)*. New York and London: Garland Science. ISBN 0-8153-3218-1. OCLC 145080076 48122761 57023651 69932405 (http://worldcat.org/oclc/145080076+48122761+57023651+69932405). .

[3] Butler, John M. (2001). *Forensic DNA Typing*. Elsevier. ISBN 978-0-12-147951-0. OCLC 223032110 45406517 (http://worldcat.org/oclc/223032110+45406517). pp. 14–15.

[4] Mandelkern M, Elias J, Eden D, Crothers D (1981). "The dimensions of DNA in solution". *J Mol Biol* **152** (1): 153–61. doi: 10.1016/0022-2836(81)90099-1 (http://dx.doi.org/10.1016/0022-2836(81)90099-1). PMID 7338906.

[5] Gregory S, *et al.* (2006). "The DNA sequence and biological annotation of human chromosome 1". *Nature* **441** (7091): 315–21. doi: 10.1038/nature04727 (http://dx.doi.org/10.1038/nature04727). PMID 16710414.

[6] Watson J.D. and Crick F.H.C. (1953). " A Structure for Deoxyribose Nucleic Acid (http://www.nature.com/nature/dna50/watsoncrick.pdf)" (PDF). *Nature* **171**: 737–738. doi: 10.1038/171737a0 (http://dx.doi.org/10.1038/171737a0). PMID 13054692. . Retrieved on 4 May 2009.

[7] Berg J., Tymoczko J. and Stryer L. (2002) *Biochemistry.* W. H. Freeman and Company ISBN 0-7167-4955-6

[8] Abbreviations and Symbols for Nucleic Acids, Polynucleotides and their Constituents (http://www.chem.qmul.ac.uk/iupac/misc/naabb.html) IUPAC-IUB Commission on Biochemical Nomenclature (CBN), Accessed 03 January 2006

[9] Ghosh A, Bansal M (2003). "A glossary of DNA structures from A to Z". *Acta Crystallogr D Biol Crystallogr* **59** (Pt 4): 620–6. doi: 10.1107/S0907444903003251 (http://dx.doi.org/10.1107/S0907444903003251). PMID 12657780.

[10] Created from PDB 1D65 (http://www.rcsb.org/pdb/cgi/explore.cgi?pdbId=1D65)

[11] Wing R, Drew H, Takano T, Broka C, Tanaka S, Itakura K, Dickerson R (1980). "Crystal structure analysis of a complete turn of B-DNA". *Nature* **287** (5784): 755–8. doi: 10.1038/287755a0 (http://dx.doi.org/10.1038/287755a0). PMID 7432492.

[12] Pabo C, Sauer R (1984). "Protein-DNA recognition". *Annu Rev Biochem* **53**: 293–321. doi: 10.1146/annurev.bi.53.070184.001453 (http://dx.doi.org/10.1146/annurev.bi.53.070184.001453). PMID

6236744.

[13] Clausen-Schaumann H, Rief M, Tolksdorf C, Gaub H (2000). " Mechanical stability of single DNA molecules (http://www.pubmedcentral.nih.gov/articlerender.fcgi?tool=pmcentrez&artid=1300792)". *Biophys J* **78** (4): 1997–2007. doi: 10.1016/S0006-3495(00)76747-6 (http://dx.doi.org/10.1016/S0006-3495(00)76747-6). PMID 10733978.

[14] Yakovchuk P, Protozanova E, Frank-Kamenetskii MD (2006). " Base-stacking and base-pairing contributions into thermal stability of the DNA double helix (http://nar.oxfordjournals.org/cgi/pmidlookup?view=long&pmid=16449200)". *Nucleic Acids Res.* **34** (2): 564–74. doi: 10.1093/nar/gkj454 (http://dx.doi.org/10.1093/nar/gkj454). PMID 16449200. PMC: 1360284 (http://www.pubmedcentral.nih.gov/articlerender.fcgi?tool=pmcentrez&artid=1360284). .

[15] Chalikian T, Völker J, Plum G, Breslauer K (1999). " A more unified picture for the thermodynamics of nucleic acid duplex melting: a characterization by calorimetric and volumetric techniques (http://www.pubmedcentral.nih.gov/articlerender.fcgi?tool=pmcentrez&artid=22151)". *Proc Natl Acad Sci USA* **96** (14): 7853–8. doi: 10.1073/pnas.96.14.7853 (http://dx.doi.org/10.1073/pnas.96.14.7853). PMID 10393911.

[16] deHaseth P, Helmann J (1995). "Open complex formation by Escherichia coli RNA polymerase: the mechanism of polymerase-induced strand separation of double helical DNA". *Mol Microbiol* **16** (5): 817–24. doi: 10.1111/j.1365-2958.1995.tb02309.x (http://dx.doi.org/10.1111/j.1365-2958.1995.tb02309.x). PMID 7476180.

[17] Isaksson J, Acharya S, Barman J, Cheruku P, Chattopadhyaya J (2004). "Single-stranded adenine-rich DNA and RNA retain structural characteristics of their respective double-stranded conformations and show directional differences in stacking pattern". *Biochemistry* **43** (51): 15996–6010. doi: 10.1021/bi048221v (http://dx.doi.org/10.1021/bi048221v). PMID 15609994.

[18] Designation of the two strands of DNA (http://www.chem.qmul.ac.uk/iubmb/newsletter/misc/DNA.html) JCBN/NC-IUB Newsletter 1989, Accessed 07 May 2008

[19] Hüttenhofer A, Schattner P, Polacek N (2005). "Non-coding RNAs: hope or hype?". *Trends Genet* **21** (5): 289–97. doi: 10.1016/j.tig.2005.03.007 (http://dx.doi.org/10.1016/j.tig.2005.03.007). PMID 15851066.

[20] Munroe S (2004). "Diversity of antisense regulation in eukaryotes: multiple mechanisms, emerging patterns". *J Cell Biochem* **93** (4): 664–71. doi: 10.1002/jcb.20252 (http://dx.doi.org/10.1002/jcb.20252). PMID 15389973.

[21] Makalowska I, Lin C, Makalowski W (2005). "Overlapping genes in vertebrate genomes". *Comput Biol Chem* **29** (1): 1–12. doi: 10.1016/j.compbiolchem.2004.12.006 (http://dx.doi.org/10.1016/j.compbiolchem.2004.12.006). PMID 15680581.

[22] Johnson Z, Chisholm S (2004). "Properties of overlapping genes are conserved across microbial genomes". *Genome Res* **14** (11): 2268–72. doi: 10.1101/gr.2433104 (http://dx.doi.org/10.1101/gr.2433104). PMID 15520290.

[23] Lamb R, Horvath C (1991). "Diversity of coding strategies in influenza viruses". *Trends Genet* **7** (8): 261–6. PMID 1771674.

[24] Benham C, Mielke S (2005). "DNA mechanics". *Annu Rev Biomed Eng* **7**: 21–53. doi: 10.1146/annurev.bioeng.6.062403.132016 (http://dx.doi.org/10.1146/annurev.bioeng.6.062403.132016). PMID 16004565.

[25] Champoux J (2001). "DNA topoisomerases: structure, function, and mechanism". *Annu Rev Biochem* **70**: 369–413. doi: 10.1146/annurev.biochem.70.1.369 (http://dx.doi.org/10.1146/annurev.biochem.70.1.369). PMID 11395412.

[26] Wang J (2002). "Cellular roles of DNA topoisomerases: a molecular perspective". *Nat Rev Mol Cell Biol* **3** (6): 430–40. doi: 10.1038/nrm831 (http://dx.doi.org/10.1038/nrm831). PMID 12042765.

[27] Basu H, Feuerstein B, Zarling D, Shafer R, Marton L (1988). "Recognition of Z-RNA and Z-DNA determinants by polyamines in solution: experimental and theoretical studies". *J Biomol Struct Dyn* **6** (2): 299–309. PMID 2482766.

[28] Franklin RE, Gosling RG (6 March 1953). " The Structure of Sodium Thymonucleate Fibres I. The Influence of Water Content (http://hekto.med.unc.edu:8080/CARTER/carter_WWW/Bioch_134/PDF_files/Franklin_Gossling.pdf)". *Acta Cryst* **6** (8-9): 673–7. doi: 10.1107/S0365110X53001939 (http://dx.doi.org/10.1107/S0365110X53001939). .
Franklin RE, Gosling RG (September 1953). "The structure of sodium thymonucleate fibres. II. The cylindrically symmetrical Patterson function". *Acta Cryst* **6** (8-9): 678–85. doi: 10.1107/S0365110X53001940 (http://dx.doi.org/10.1107/S0365110X53001940).

[29] Franklin, Rosalind and Gosling, Raymond (1953). " Molecular Configuration in Sodium Thymonucleate. Franklin R. and Gosling R.G (http://www.nature.com/nature/dna50/franklingosling.pdf)" (PDF). *Nature* **171**: 740–1. doi: 10.1038/171740a0 (http://dx.doi.org/10.1038/171740a0). PMID 13054694. .

[30] Wilkins M.H.F., A.R. Stokes A.R. & Wilson, H.R. (1953). " Molecular Structure of Deoxypentose Nucleic Acids (http://www.nature.com/nature/dna50/wilkins.pdf)" (PDF). *Nature* **171**: 738–740. doi: 10.1038/171738a0 (http://dx.doi.org/10.1038/171738a0). PMID 13054693. .

[31] Leslie AG, Arnott S, Chandrasekaran R, Ratliff RL (1980). "Polymorphism of DNA double helices". *J. Mol. Biol.* **143** (1): 49–72. doi: 10.1016/0022-2836(80)90124-2 (http://dx.doi.org/10.1016/0022-2836(80)90124-2). PMID 7441761.

[32] Baianu, I.C. (1980). "Structural Order and Partial Disorder in Biological systems". *Bull. Math. Biol.* **42** (4): 137–141. http://cogprints.org/3822/

[33] Hosemann R., Bagchi R.N., *Direct analysis of diffraction by matter*, North-Holland Publs., Amsterdam – New York, 1962.

[34] Baianu, I.C. (1978). "X-ray scattering by partially disordered membrane systems.". *Acta Cryst.,* **A34** (5): 751–753. doi: 10.1107/S0567739478001540 (http://dx.doi.org/10.1107/S0567739478001540).

[35] Wahl M, Sundaralingam M (1997). "Crystal structures of A-DNA duplexes". *Biopolymers* **44** (1): 45–63. doi:10.1002/(SICI)1097-0282(1997)44:1 (inactive 2009-03-14) . PMID 9097733.

[36] Lu XJ, Shakked Z, Olson WK (2000). "A-form conformational motifs in ligand-bound DNA structures". *J. Mol. Biol.* **300** (4): 819–40. doi: 10.1006/jmbi.2000.3690 (http://dx.doi.org/10.1006/jmbi.2000.3690). PMID 10891271.

[37] Rothenburg S, Koch-Nolte F, Haag F (2001). "DNA methylation and Z-DNA formation as mediators of quantitative differences in the expression of alleles". *Immunol Rev* **184**: 286–98. doi: 10.1034/j.1600-065x.2001.1840125.x (http://dx.doi.org/10.1034/j.1600-065x.2001.1840125.x). PMID 12086319.

[38] Oh D, Kim Y, Rich A (2002). " Z-DNA-binding proteins can act as potent effectors of gene expression in vivo (http://www.pnas.org/cgi/pmidlookup?view=long&pmid=12486233)". *Proc. Natl. Acad. Sci. U.S.A.* **99** (26): 16666–71. doi: 10.1073/pnas.262672699 (http://dx.doi.org/10.1073/pnas.262672699). PMID 12486233. PMC: 139201 (http://www.pubmedcentral.nih.gov/articlerender.fcgi?tool=pmcentrez&artid=139201). .

[39] Created from NDB UD0017 (http://ndbserver.rutgers.edu/atlas/xray/structures/U/ud0017/ud0017.html)

[40] Greider C, Blackburn E (1985). "Identification of a specific telomere terminal transferase activity in Tetrahymena extracts". *Cell* **43** (2 Pt 1): 405–13. doi: 10.1016/0092-8674(85)90170-9 (http://dx.doi.org/10.1016/0092-8674(85)90170-9). PMID 3907856.

[41] Nugent C, Lundblad V (1998). " The telomerase reverse transcriptase: components and regulation (http://www.genesdev.org/cgi/content/full/12/8/1073)". *Genes Dev* **12** (8): 1073–85. doi: 10.1101/gad.12.8.1073 (http://dx.doi.org/10.1101/gad.12.8.1073). PMID 9553037. .

[42] Wright W, Tesmer V, Huffman K, Levene S, Shay J (1997). " Normal human chromosomes have long G-rich telomeric overhangs at one end (http://www.genesdev.org/cgi/content/full/11/21/2801)". *Genes Dev* **11** (21): 2801–9. doi: 10.1101/gad.11.21.2801 (http://dx.doi.org/10.1101/gad.11.21.2801). PMID 9353250. .

[43] Burge S, Parkinson G, Hazel P, Todd A, Neidle S (2006). " Quadruplex DNA: sequence, topology and structure (http://nar.oxfordjournals.org/cgi/pmidlookup?view=long&pmid=17012276)". *Nucleic Acids Res* **34** (19): 5402–15. doi: 10.1093/nar/gkl655 (http://dx.doi.org/10.1093/nar/gkl655). PMID 17012276. PMC: 1636468 (http://www.pubmedcentral.nih.gov/articlerender.fcgi?tool=pmcentrez&artid=1636468). .

[44] Parkinson G, Lee M, Neidle S (2002). "Crystal structure of parallel quadruplexes from human telomeric DNA". *Nature* **417** (6891): 876–80. doi: 10.1038/nature755 (http://dx.doi.org/10.1038/nature755). PMID 12050675.

[45] Griffith J, Comeau L, Rosenfield S, Stansel R, Bianchi A, Moss H, de Lange T (1999). "Mammalian telomeres end in a large duplex loop". *Cell* **97** (4): 503–14. doi: 10.1016/S0092-8674(00)80760-6 (http://dx.doi.org/10.1016/S0092-8674(00)80760-6). PMID 10338214.

[46] Seeman NC (November 2005). "DNA enables nanoscale control of the structure of matter". *Q. Rev. Biophys.* **38** (4): 363–71. doi: 10.1017/S0033583505004087 (http://dx.doi.org/10.1017/S0033583505004087). PMID 16515737.

[47] Klose R, Bird A (2006). "Genomic DNA methylation: the mark and its mediators". *Trends Biochem Sci* **31** (2): 89–97. doi: 10.1016/j.tibs.2005.12.008 (http://dx.doi.org/10.1016/j.tibs.2005.12.008). PMID 16403636.

[48] Bird A (2002). "DNA methylation patterns and epigenetic memory". *Genes Dev* **16** (1): 6–21. doi: 10.1101/gad.947102 (http://dx.doi.org/10.1101/gad.947102). PMID 11782440.

[49] Walsh C, Xu G (2006). "Cytosine methylation and DNA repair". *Curr Top Microbiol Immunol* **301**: 283–315. doi: 10.1007/3-540-31390-7_11 (http://dx.doi.org/10.1007/3-540-31390-7_11). PMID 16570853.

[50] Kriaucionis S, Heintz N (May 2009). "The nuclear DNA base 5-hydroxymethylcytosine is present in Purkinje neurons and the brain". *Science* **324** (5929): 929–30. doi: 10.1126/science.1169786 (http://dx.doi.org/10.1126/science.1169786). PMID 19372393.

[51] Ratel D, Ravanat J, Berger F, Wion D (2006). "N6-methyladenine: the other methylated base of DNA". *Bioessays* **28** (3): 309–15. doi: 10.1002/bies.20342 (http://dx.doi.org/10.1002/bies.20342). PMID 16479578.

[52] Gommers-Ampt J, Van Leeuwen F, de Beer A, Vliegenthart J, Dizdaroglu M, Kowalak J, Crain P, Borst P (1993). "beta-D-glucosyl-hydroxymethyluracil: a novel modified base present in the DNA of the parasitic protozoan T. brucei". *Cell* **75** (6): 1129–36. doi: 10.1016/0092-8674(93)90322-H (http://dx.doi.org/10.1016/0092-8674(93)90322-H). PMID 8261512.
[53] Created from PDB 1JDG (http://www.rcsb.org/pdb/cgi/explore.cgi?pdbId=1JDG)
[54] Douki T, Reynaud-Angelin A, Cadet J, Sage E (2003). "Bipyrimidine photoproducts rather than oxidative lesions are the main type of DNA damage involved in the genotoxic effect of solar UVA radiation". *Biochemistry* **42** (30): 9221–6. doi: 10.1021/bi034593c (http://dx.doi.org/10.1021/bi034593c). PMID 12885257.,
[55] Cadet J, Delatour T, Douki T, Gasparutto D, Pouget J, Ravanat J, Sauvaigo S (1999). "Hydroxyl radicals and DNA base damage". *Mutat Res* **424** (1–2): 9–21. PMID 10064846.
[56] Beckman KB, Ames BN (August 1997). " Oxidative decay of DNA (http://www.jbc.org/cgi/pmidlookup?view=long&pmid=9289489)". *J. Biol. Chem.* **272** (32): 19633–6. PMID 9289489. .
[57] Valerie K, Povirk L (2003). "Regulation and mechanisms of mammalian double-strand break repair". *Oncogene* **22** (37): 5792–812. doi: 10.1038/sj.onc.1206679 (http://dx.doi.org/10.1038/sj.onc.1206679). PMID 12947387.
[58] Ferguson L, Denny W (1991). "The genetic toxicology of acridines". *Mutat Res* **258** (2): 123–60. PMID 1881402.
[59] Jeffrey A (1985). "DNA modification by chemical carcinogens". *Pharmacol Ther* **28** (2): 237–72. doi: 10.1016/0163-7258(85)90013-0 (http://dx.doi.org/10.1016/0163-7258(85)90013-0). PMID 3936066.
[60] Stephens T, Bunde C, Fillmore B (2000). "Mechanism of action in thalidomide teratogenesis". *Biochem Pharmacol* **59** (12): 1489–99. doi: 10.1016/S0006-2952(99)00388-3 (http://dx.doi.org/10.1016/S0006-2952(99)00388-3). PMID 10799645.
[61] Braña M, Cacho M, Gradillas A, de Pascual-Teresa B, Ramos A (2001). "Intercalators as anticancer drugs". *Curr Pharm Des* **7** (17): 1745–80. doi: 10.2174/1381612013397113 (http://dx.doi.org/10.2174/1381612013397113). PMID 11562309.
[62] Venter J, *et al.* (2001). "The sequence of the human genome". *Science* **291** (5507): 1304–51. doi: 10.1126/science.1058040 (http://dx.doi.org/10.1126/science.1058040). PMID 11181995.
[63] Thanbichler M, Wang S, Shapiro L (2005). "The bacterial nucleoid: a highly organized and dynamic structure". *J Cell Biochem* **96** (3): 506–21. doi: 10.1002/jcb.20519 (http://dx.doi.org/10.1002/jcb.20519). PMID 15988757.
[64] Wolfsberg T, McEntyre J, Schuler G (2001). "Guide to the draft human genome". *Nature* **409** (6822): 824–6. doi: 10.1038/35057000 (http://dx.doi.org/10.1038/35057000). PMID 11236998.
[65] Gregory T (2005). " The C-value enigma in plants and animals: a review of parallels and an appeal for partnership (http://aob.oxfordjournals.org/cgi/content/full/95/1/133)". *Ann Bot (Lond)* **95** (1): 133–46. doi: 10.1093/aob/mci009 (http://dx.doi.org/10.1093/aob/mci009). PMID 15596463. .
[66] The ENCODE Project Consortium (2007). "Identification and analysis of functional elements in 1% of the human genome by the ENCODE pilot project". *Nature* **447** (7146): 799–816. doi: 10.1038/nature05874 (http://dx.doi.org/10.1038/nature05874).
[67] Created from PDB 1MSW (http://www.rcsb.org/pdb/explore/explore.do?structureId=1MSW)
[68] Pidoux A, Allshire R (2005). " The role of heterochromatin in centromere function (http://www.pubmedcentral.nih.gov/articlerender.fcgi?tool=pmcentrez&artid=1569473)". *Philos Trans R Soc Lond B Biol Sci* **360** (1455): 569–79. doi: 10.1098/rstb.2004.1611 (http://dx.doi.org/10.1098/rstb.2004.1611). PMID 15905142.
[69] Harrison P, Hegyi H, Balasubramanian S, Luscombe N, Bertone P, Echols N, Johnson T, Gerstein M (2002). " Molecular fossils in the human genome: identification and analysis of the pseudogenes in chromosomes 21 and 22 (http://www.genome.org/cgi/content/full/12/2/272)". *Genome Res* **12** (2): 272–80. doi: 10.1101/gr.207102 (http://dx.doi.org/10.1101/gr.207102). PMID 11827946. .
[70] Harrison P, Gerstein M (2002). "Studying genomes through the aeons: protein families, pseudogenes and proteome evolution". *J Mol Biol* **318** (5): 1155–74. doi: 10.1016/S0022-2836(02)00109-2 (http://dx.doi.org/10.1016/S0022-2836(02)00109-2). PMID 12083509.
[71] Albà M (2001). " Replicative DNA polymerases (http://genomebiology.com/1465-6906/2/REVIEWS3002)". *Genome Biol* **2** (1): REVIEWS3002. doi: 10.1186/gb-2001-2-1-reviews3002 (http://dx.doi.org/10.1186/gb-2001-2-1-reviews3002). PMID 11178285. PMC: 150442 (http://www.pubmedcentral.nih.gov/articlerender.fcgi?tool=pmcentrez&artid=150442). .
[72] Sandman K, Pereira S, Reeve J (1998). "Diversity of prokaryotic chromosomal proteins and the origin of the nucleosome". *Cell Mol Life Sci* **54** (12): 1350–64. doi: 10.1007/s000180050259 (http://dx.doi.org/10.1007/s000180050259). PMID 9893710.
[73] Dame RT (2005). "The role of nucleoid-associated proteins in the organization and compaction of bacterial chromatin". *Mol. Microbiol.* **56** (4): 858–70. doi: 10.1111/j.1365-2958.2005.04598.x (http://dx.doi.org/10.

1111/j.1365-2958.2005.04598.x). PMID 15853876.
[74] Luger K, Mäder A, Richmond R, Sargent D, Richmond T (1997). "Crystal structure of the nucleosome core particle at 2.8 A resolution". *Nature* **389** (6648): 251–60. doi: 10.1038/38444 (http://dx.doi.org/10.1038/38444). PMID 9305837.
[75] Jenuwein T, Allis C (2001). "Translating the histone code". *Science* **293** (5532): 1074–80. doi: 10.1126/science.1063127 (http://dx.doi.org/10.1126/science.1063127). PMID 11498575.
[76] Ito T. "Nucleosome assembly and remodelling". *Curr Top Microbiol Immunol* **274**: 1–22. PMID 12596902.
[77] Thomas J (2001). "HMG1 and 2: architectural DNA-binding proteins". *Biochem Soc Trans* **29** (Pt 4): 395–401. doi: 10.1042/BST0290395 (http://dx.doi.org/10.1042/BST0290395). PMID 11497996.
[78] Grosschedl R, Giese K, Pagel J (1994). "HMG domain proteins: architectural elements in the assembly of nucleoprotein structures". *Trends Genet* **10** (3): 94–100. doi: 10.1016/0168-9525(94)90232-1 (http://dx.doi.org/10.1016/0168-9525(94)90232-1). PMID 8178371.
[79] Iftode C, Daniely Y, Borowiec J (1999). "Replication protein A (RPA): the eukaryotic SSB". *Crit Rev Biochem Mol Biol* **34** (3): 141–80. doi: 10.1080/10409239991209255 (http://dx.doi.org/10.1080/10409239991209255). PMID 10473346.
[80] Created from PDB 1LMB (http://www.rcsb.org/pdb/explore/explore.do?structureId=1LMB)
[81] Myers L, Kornberg R (2000). "Mediator of transcriptional regulation". *Annu Rev Biochem* **69**: 729–49. doi: 10.1146/annurev.biochem.69.1.729 (http://dx.doi.org/10.1146/annurev.biochem.69.1.729). PMID 10966474.
[82] Spiegelman B, Heinrich R (2004). "Biological control through regulated transcriptional coactivators". *Cell* **119** (2): 157–67. doi: 10.1016/j.cell.2004.09.037 (http://dx.doi.org/10.1016/j.cell.2004.09.037). PMID 15479634.
[83] Li Z, Van Calcar S, Qu C, Cavenee W, Zhang M, Ren B (2003). " A global transcriptional regulatory role for c-Myc in Burkitt's lymphoma cells (http://www.pnas.org/cgi/pmidlookup?view=long&pmid=12808131)". *Proc Natl Acad Sci USA* **100** (14): 8164–9. doi: 10.1073/pnas.1332764100 (http://dx.doi.org/10.1073/pnas.1332764100). PMID 12808131. PMC: 166200 (http://www.pubmedcentral.nih.gov/articlerender.fcgi?tool=pmcentrez&artid=166200). .
[84] Pabo C, Sauer R (1984). "Protein-DNA recognition". *Annu Rev Biochem* **53**: 293–321. doi: 10.1146/annurev.bi.53.070184.001453 (http://dx.doi.org/10.1146/annurev.bi.53.070184.001453). PMID 6236744.
[85] Created from PDB 1RVA (http://www.rcsb.org/pdb/explore/explore.do?structureId=1RVA)
[86] Bickle T, Krüger D (1993). " Biology of DNA restriction (http://www.pubmedcentral.nih.gov/articlerender.fcgi?tool=pmcentrez&artid=372918)". *Microbiol Rev* **57** (2): 434–50. PMID 8336674.
[87] Doherty A, Suh S (2000). " Structural and mechanistic conservation in DNA ligases (http://nar.oxfordjournals.org/cgi/pmidlookup?view=long&pmid=11058099)". *Nucleic Acids Res* **28** (21): 4051–8. doi: 10.1093/nar/28.21.4051 (http://dx.doi.org/10.1093/nar/28.21.4051). PMID 11058099. PMC: 113121 (http://www.pubmedcentral.nih.gov/articlerender.fcgi?tool=pmcentrez&artid=113121). .
[88] Schoeffler A, Berger J (2005). "Recent advances in understanding structure-function relationships in the type II topoisomerase mechanism". *Biochem Soc Trans* **33** (Pt 6): 1465–70. doi: 10.1042/BST20051465 (http://dx.doi.org/10.1042/BST20051465). PMID 16246147.
[89] Tuteja N, Tuteja R (2004). "Unraveling DNA helicases. Motif, structure, mechanism and function". *Eur J Biochem* **271** (10): 1849–63. doi: 10.1111/j.1432-1033.2004.04094.x (http://dx.doi.org/10.1111/j.1432-1033.2004.04094.x). PMID 15128295.
[90] Joyce C, Steitz T (1995). " Polymerase structures and function: variations on a theme? (http://www.pubmedcentral.nih.gov/articlerender.fcgi?tool=pmcentrez&artid=177480)". *J Bacteriol* **177** (22): 6321–9. PMID 7592405.
[91] Hubscher U, Maga G, Spadari S (2002). "Eukaryotic DNA polymerases". *Annu Rev Biochem* **71**: 133–63. doi: 10.1146/annurev.biochem.71.090501.150041 (http://dx.doi.org/10.1146/annurev.biochem.71.090501.150041). PMID 12045093.
[92] Johnson A, O'Donnell M (2005). "Cellular DNA replicases: components and dynamics at the replication fork". *Annu Rev Biochem* **74**: 283–315. doi: 10.1146/annurev.biochem.73.011303.073859 (http://dx.doi.org/10.1146/annurev.biochem.73.011303.073859). PMID 15952889.
[93] Tarrago-Litvak L, Andréola M, Nevinsky G, Sarih-Cottin L, Litvak S (01 May 1994). " The reverse transcriptase of HIV-1: from enzymology to therapeutic intervention (http://www.fasebj.org/cgi/reprint/8/8/497)". *Faseb J* **8** (8): 497–503. PMID 7514143. .
[94] Martinez E (2002). "Multi-protein complexes in eukaryotic gene transcription". *Plant Mol Biol* **50** (6): 925–47. doi: 10.1023/A:1021258713850 (http://dx.doi.org/10.1023/A:1021258713850). PMID 12516863.
[95] Created from PDB 1M6G (http://www.rcsb.org/pdb/explore/explore.do?structureId=1M6G)

[96] Cremer T, Cremer C (2001). "Chromosome territories, nuclear architecture and gene regulation in mammalian cells". *Nat Rev Genet* **2** (4): 292–301. doi: 10.1038/35066075 (http://dx.doi.org/10.1038/35066075). PMID 11283701.
[97] Pál C, Papp B, Lercher M (2006). "An integrated view of protein evolution". *Nat Rev Genet* **7** (5): 337–48. doi: 10.1038/nrg1838 (http://dx.doi.org/10.1038/nrg1838). PMID 16619049.
[98] O'Driscoll M, Jeggo P (2006). "The role of double-strand break repair - insights from human genetics". *Nat Rev Genet* **7** (1): 45–54. doi: 10.1038/nrg1746 (http://dx.doi.org/10.1038/nrg1746). PMID 16369571.
[99] Vispé S, Defais M (1997). "Mammalian Rad51 protein: a RecA homologue with pleiotropic functions". *Biochimie* **79** (9-10): 587–92. doi: 10.1016/S0300-9084(97)82007-X (http://dx.doi.org/10.1016/S0300-9084(97)82007-X). PMID 9466696.
[100] Neale MJ, Keeney S (2006). "Clarifying the mechanics of DNA strand exchange in meiotic recombination". *Nature* **442** (7099): 153–8. doi: 10.1038/nature04885 (http://dx.doi.org/10.1038/nature04885). PMID 16838012.
[101] Dickman M, Ingleston S, Sedelnikova S, Rafferty J, Lloyd R, Grasby J, Hornby D (2002). "The RuvABC resolvasome". *Eur J Biochem* **269** (22): 5492–501. doi: 10.1046/j.1432-1033.2002.03250.x (http://dx.doi.org/10.1046/j.1432-1033.2002.03250.x). PMID 12423347.
[102] Orgel L (2004). " Prebiotic chemistry and the origin of the RNA world (http://www.crbmb.com/cgi/reprint/39/2/99.pdf)" (PDF). *Crit Rev Biochem Mol Biol* **39** (2): 99–123. doi: 10.1080/10409230490460765 (http://dx.doi.org/10.1080/10409230490460765). PMID 15217990. .
[103] Davenport R (2001). "Ribozymes. Making copies in the RNA world". *Science* **292** (5520): 1278. doi: 10.1126/science.292.5520.1278a (http://dx.doi.org/10.1126/science.292.5520.1278a). PMID 11360970.
[104] Szathmáry E (1992). " What is the optimum size for the genetic alphabet? (http://www.pnas.org/cgi/reprint/89/7/2614.pdf)" (PDF). *Proc Natl Acad Sci USA* **89** (7): 2614–8. doi: 10.1073/pnas.89.7.2614 (http://dx.doi.org/10.1073/pnas.89.7.2614). PMID 1372984. .
[105] Lindahl T (1993). "Instability and decay of the primary structure of DNA". *Nature* **362** (6422): 709–15. doi: 10.1038/362709a0 (http://dx.doi.org/10.1038/362709a0). PMID 8469282.
[106] Vreeland R, Rosenzweig W, Powers D (2000). "Isolation of a 250 million-year-old halotolerant bacterium from a primary salt crystal". *Nature* **407** (6806): 897–900. doi: 10.1038/35038060 (http://dx.doi.org/10.1038/35038060). PMID 11057666.
[107] Hebsgaard M, Phillips M, Willerslev E (2005). "Geologically ancient DNA: fact or artefact?". *Trends Microbiol* **13** (5): 212–20. doi: 10.1016/j.tim.2005.03.010 (http://dx.doi.org/10.1016/j.tim.2005.03.010). PMID 15866038.
[108] Nickle D, Learn G, Rain M, Mullins J, Mittler J (2002). "Curiously modern DNA for a "250 million-year-old" bacterium". *J Mol Evol* **54** (1): 134–7. doi: 10.1007/s00239-001-0025-x (http://dx.doi.org/10.1007/s00239-001-0025-x). PMID 11734907.
[109] Goff SP, Berg P (1976). "Construction of hybrid viruses containing SV40 and lambda phage DNA segments and their propagation in cultured monkey cells". *Cell* **9** (4 PT 2): 695–705. doi: 10.1016/0092-8674(76)90133-1 (http://dx.doi.org/10.1016/0092-8674(76)90133-1). PMID 189942.
[110] Houdebine L. "Transgenic animal models in biomedical research". *Methods Mol Biol* **360**: 163–202. PMID 17172731.
[111] Daniell H, Dhingra A (2002). "Multigene engineering: dawn of an exciting new era in biotechnology". *Curr Opin Biotechnol* **13** (2): 136–41. doi: 10.1016/S0958-1669(02)00297-5 (http://dx.doi.org/10.1016/S0958-1669(02)00297-5). PMID 11950565.
[112] Job D (2002). "Plant biotechnology in agriculture". *Biochimie* **84** (11): 1105–10. doi: 10.1016/S0300-9084(02)00013-5 (http://dx.doi.org/10.1016/S0300-9084(02)00013-5). PMID 12595138.
[113] Collins A, Morton N (1994). " Likelihood ratios for DNA identification (http://www.pnas.org/cgi/reprint/91/13/6007.pdf)" (PDF). *Proc Natl Acad Sci USA* **91** (13): 6007–11. doi: 10.1073/pnas.91.13.6007 (http://dx.doi.org/10.1073/pnas.91.13.6007). PMID 8016106. .
[114] Weir B, Triggs C, Starling L, Stowell L, Walsh K, Buckleton J (1997). "Interpreting DNA mixtures". *J Forensic Sci* **42** (2): 213–22. PMID 9068179.
[115] Jeffreys A, Wilson V, Thein S (1985). "Individual-specific 'fingerprints' of human DNA". *Nature* **316** (6023): 76–9. doi: 10.1038/316076a0 (http://dx.doi.org/10.1038/316076a0). PMID 2989708.
[116] Colin Pitchfork — first murder conviction on DNA evidence also clears the prime suspect (http://www.forensic.gov.uk/forensic_t/inside/news/list_casefiles.php?case=1) Forensic Science Service Accessed 23 December 2006
[117] "DNA Identification in Mass Fatality Incidents" (http://massfatality.dna.gov/Introduction/). National Institute of Justice. September 2006. .
[118] Baldi, Pierre; Brunak, Soren (2001), *Bioinformatics: The Machine Learning Approach*, MIT Press, ISBN 978-0-262-02506-5, OCLC 45951728 57562233 (http://worldcat.org/oclc/45951728+57562233).

[119] Gusfield, Dan. *Algorithms on Strings, Trees, and Sequences: Computer Science and Computational Biology*. Cambridge University Press, 15 January 1997. ISBN 978-0-521-58519-4.
[120] Sjölander K (2004). " Phylogenomic inference of protein molecular function: advances and challenges (http://bioinformatics.oxfordjournals.org/cgi/reprint/20/2/170)". *Bioinformatics* **20** (2): 170–9. doi: 10.1093/bioinformatics/bth021 (http://dx.doi.org/10.1093/bioinformatics/bth021). PMID 14734307. .
[121] Mount DM (2004). *Bioinformatics: Sequence and Genome Analysis* (2 ed.). Cold Spring Harbor, NY: Cold Spring Harbor Laboratory Press. ISBN 0879697121. OCLC 55106399 (http://worldcat.org/oclc/55106399).
[122] http://dx.doi.org/10.1371/journal.pbio.0020073
[123] Rothemund PW (March 2006). "Folding DNA to create nanoscale shapes and patterns". *Nature* **440** (7082): 297–302. doi: 10.1038/nature04586 (http://dx.doi.org/10.1038/nature04586). PMID 16541064.
[124] Andersen ES, Dong M, Nielsen MM, *et al.* (May 2009). "Self-assembly of a nanoscale DNA box with a controllable lid". *Nature* **459** (7243): 73–6. doi: 10.1038/nature07971 (http://dx.doi.org/10.1038/nature07971). PMID 19424153.
[125] Ishitsuka Y, Ha T (May 2009). "DNA nanotechnology: a nanomachine goes live". *Nat Nanotechnol* **4** (5): 281–2. doi: 10.1038/nnano.2009.101 (http://dx.doi.org/10.1038/nnano.2009.101). PMID 19421208.
[126] Aldaye FA, Palmer AL, Sleiman HF (September 2008). "Assembling materials with DNA as the guide". *Science* **321** (5897): 1795–9. doi: 10.1126/science.1154533 (http://dx.doi.org/10.1126/science.1154533). PMID 18818351.
[127] Wray G (2002). " Dating branches on the tree of life using DNA (http://genomebiology.com/1465-6906/3/REVIEWS0001)". *Genome Biol* **3** (1): REVIEWS0001. doi: 10.1046/j.1525-142X.1999.99010.x (http://dx.doi.org/10.1046/j.1525-142X.1999.99010.x). PMID 11806830. PMC: 150454 (http://www.pubmedcentral.nih.gov/articlerender.fcgi?tool=pmcentrez&artid=150454). .
[128] *Lost Tribes of Israel*, NOVA, PBS airdate: 22 February 2000. Transcript available from PBS.org, (http://www.pbs.org/wgbh/nova/transcripts/2706israel.html) (last accessed on 4 March 2006)
[129] Kleiman, Yaakov. "The Cohanim/DNA Connection: The fascinating story of how DNA studies confirm an ancient biblical tradition". (http://www.aish.com/societywork/sciencenature/the_cohanim_-_dna_connection.asp) *aish.com* (January 13, 2000). Accessed 4 March 2006.
[130] Bhattacharya, Shaoni. "Killer convicted thanks to relative's DNA". (http://www.newscientist.com/article.ns?id=dn4908) *newscientist.com* (20 April 2004). Accessed 22 December 06
[131] Dahm R (January 2008). "Discovering DNA: Friedrich Miescher and the early years of nucleic acid research". *Hum. Genet.* **122** (6): 565–81. doi: 10.1007/s00439-007-0433-0 (http://dx.doi.org/10.1007/s00439-007-0433-0). PMID 17901982.
[132] Levene P, (01 December 1919). " The structure of yeast nucleic acid (http://www.jbc.org/cgi/reprint/40/2/415)". *J Biol Chem* **40** (2): 415–24. .
[133] Astbury W, (1947). "Nucleic acid". *Symp. SOC. Exp. Bbl* **1** (66).
[134] Lorenz MG, Wackernagel W (01 September 1994). " Bacterial gene transfer by natural genetic transformation in the environment (http://mmbr.asm.org/cgi/pmidlookup?view=long&pmid=7968924)". *Microbiol. Rev.* **58** (3): 563–602. PMID 7968924. PMC: 372978 (http://www.pubmedcentral.nih.gov/articlerender.fcgi?tool=pmcentrez&artid=372978). .
[135] Avery O, MacLeod C, McCarty M (1944). " Studies on the chemical nature of the substance inducing transformation of pneumococcal types. Inductions of transformation by a desoxyribonucleic acid fraction isolated from pneumococcus type III (http://www.jem.org/cgi/reprint/149/2/297)". *J Exp Med* **79** (2): 137–158. doi: 10.1084/jem.79.2.137 (http://dx.doi.org/10.1084/jem.79.2.137). .
[136] Hershey A, Chase M (1952). " Independent functions of viral protein and nucleic acid in growth of bacteriophage (http://www.jgp.org/cgi/reprint/36/1/39.pdf)" (PDF). *J Gen Physiol* **36** (1): 39–56. doi: 10.1085/jgp.36.1.39 (http://dx.doi.org/10.1085/jgp.36.1.39). PMID 12981234. .
[137] The B-DNA X-ray pattern on the right of this linked image (http://osulibrary.oregonstate.edu/specialcollections/coll/pauling/dna/pictures/sci9.001.5.html) was obtained by Rosalind Franklin and Raymond Gosling in May 1952 at high hydration levels of DNA and it has been labeled as "Photo 51"
[138] Nature Archives Double Helix of DNA: 50 Years (http://www.nature.com/nature/dna50/archive.html)
[139] Original X-ray diffraction image (http://osulibrary.oregonstate.edu/specialcollections/coll/pauling/dna/pictures/franklin-typeBphoto.html)
[140] The Nobel Prize in Physiology or Medicine 1962 (http://nobelprize.org/nobel_prizes/medicine/laureates/1962/) Nobelprize .org Accessed 22 December 06
[141] Brenda Maddox (23 January 2003). " The double helix and the 'wronged heroine' (http://www.biomath.nyu.edu/index/course/hw_articles/nature4.pdf)" (PDF). *Nature* **421**: 407–408. doi: 10.1038/nature01399 (http://dx.doi.org/10.1038/nature01399). PMID 12540909. .
[142] Crick, F.H.C. On degenerate templates and the adaptor hypothesis (PDF). (http://genome.wellcome.ac.uk/assets/wtx030893.pdf) genome.wellcome.ac.uk (Lecture, 1955). Accessed 22 December 2006

[143] Meselson M, Stahl F (1958). "The replication of DNA in *Escherichia coli*". *Proc Natl Acad Sci USA* **44** (7): 671–82. doi: 10.1073/pnas.44.7.671 (http://dx.doi.org/10.1073/pnas.44.7.671). PMID 16590258.
[144] The Nobel Prize in Physiology or Medicine 1968 (http://nobelprize.org/nobel_prizes/medicine/laureates/1968/) Nobelprize.org Accessed 22 December 06
[145] http://proteopedia.org/wiki/index.php/DNA

Further reading

- Calladine, Chris R.; Drew, Horace R.; Luisi, Ben F. and Travers, Andrew A. (2003). *Understanding DNA: the molecule & how it works*. Amsterdam: Elsevier Academic Press. ISBN 0-12-155089-3.
- Dennis, Carina; Julie Clayton (2003). *50 years of DNA*. Basingstoke: Palgrave Macmillan. ISBN 1-4039-1479-6.
- Judson, Horace Freeland (1996). *The eighth day of creation: makers of the revolution in biology*. Plainview, N.Y: CSHL Press. ISBN 0-87969-478-5.
- Olby, Robert C. (1994). *The path to the double helix: the discovery of DNA*. New York: Dover Publications. ISBN 0-486-68117-3., first published in October 1974 by MacMillan, with foreword by Francis Crick;the definitive DNA textbook,revised in 1994 with a 9 page postscript.
- Olby, Robert C. (2009). *Francis Crick: A Biography*. Plainview, N.Y: Cold Spring Harbor Laboratory Press. ISBN 0-87969-798-9.
- Ridley, Matt (2006). *Francis Crick: discoverer of the genetic code*. [Ashland, OH: Eminent Lives, Atlas Books. ISBN 0-06-082333-X.
- Berry, Andrew; Watson, James D. (2003). *DNA: the secret of life*. New York: Alfred A. Knopf. ISBN 0-375-41546-7.
- Stent, Gunther Siegmund; Watson, James D. (1980). *The double helix: a personal account of the discovery of the structure of DNA*. New York: Norton. ISBN 0-393-95075-1.
- Wilkins, Maurice (2003). *The third man of the double helix the autobiography of Maurice Wilkins*. Cambridge, Eng: University Press. ISBN 0-19-860665-6.

External links

- DNA (http://www.dmoz.org/Science/Biology/Biochemistry_and_Molecular_Biology/Biomolecules/Nucleic_Acids/DNA//) at the Open Directory Project
- DNA binding site prediction on protein (http://pipe.scs.fsu.edu/displar.html)
- DNA coiling to form chromosomes (http://biostudio.com/c_ education mac.htm)
- DNA from the Beginning (http://www.dnaftb.org/dnaftb/) Another DNA Learning Center site on DNA, genes, and heredity from Mendel to the human genome project.
- DNA Lab, demonstrates how to extract DNA from wheat using readily available equipment and supplies. (http://ca.youtube.com/watch?v=iyb7fwduuGM)
- DNA the Double Helix Game (http://nobelprize.org/educational_games/medicine/dna_double_helix/) From the official Nobel Prize web site
- DNA under electron microscope (http://www.fidelitysystems.com/Unlinked_DNA.html)
- Dolan DNA Learning Center (http://www.dnalc.org/)
- Double Jelix: 50 years of DNA (http://www.nature.com/nature/dna50/archive.html), *Nature*
- Double Helix 1953–2003 (http://www.ncbe.reading.ac.uk/DNA50/) National Centre for Biotechnology Education

- Francis Crick and James Watson talking on the BBC in 1962, 1972, and 1974 (http://www.bbc.co.uk/bbcfour/audiointerviews/profilepages/crickwatson1.shtml)
- Genetic Education Modules for Teachers (http://www.genome.gov/10506718) — *DNA from the Beginning* Study Guide
- Guide to DNA cloning (http://www.blackwellpublishing.com/trun/artwork/Animations/cloningexp/cloningexp.html)
- Olby R (January 2003). " Quiet debut for the double helix (http://chem-faculty.ucsd.edu/joseph/CHEM13/DNA1.pdf)". *Nature* **421** (6921): 402–5. doi: 10.1038/nature01397 (http://dx.doi.org/10.1038/nature01397). PMID 12540907. http://chem-faculty.ucsd.edu/joseph/CHEM13/DNA1.pdf.
- PDB Molecule of the Month *pdb23_1 (http://www.rcsb.org/pdb/static.do?p=education_discussion/molecule_of_the_month/pdb23_1.html)*
- Rosalind Franklin's contributions to the study of DNA (http://mason.gmu.edu/~emoody/rfranklin.html)
- The Register of Francis Crick Personal Papers 1938 - 2007 (http://orpheus.ucsd.edu/speccoll/testing/html/mss0660a.html#abstract) at Mandeville Special Collections Library, Geisel Library, University of California, San Diego
- The Secret Life of DNA - DNA Music compositions (http://www.tjmitchell.com/stuart/dna.html)
- U.S. National DNA Day (http://www.genome.gov/10506367) — watch videos and participate in real-time chat with top scientists
- " Clue to chemistry of heredity found (http://www.nytimes.com/packages/pdf/science/dna-article.pdf)". *The New York Times*. Saturday, June 13, 1953. http://www.nytimes.com/packages/pdf/science/dna-article.pdf. The first American newspaper coverage of the discovery of the DNA structure.

DNA nanotechnology

Part of a series of articles on **Molecular self-assembly**
Self-assembled monolayer Supramolecular assembly → DNA nanotechnology
See also Nanotechnology

DNA nanotechnology is a subfield of nanotechnology which seeks to use the unique molecular recognition properties of → DNA and other nucleic acids to create novel, controllable structures out of DNA. The DNA is thus used as a structural material rather than as a carrier of genetic information, making it an example of bionanotechnology. This has possible applications in molecular self-assembly and in DNA computing.

Introduction: DNA crossover molecules

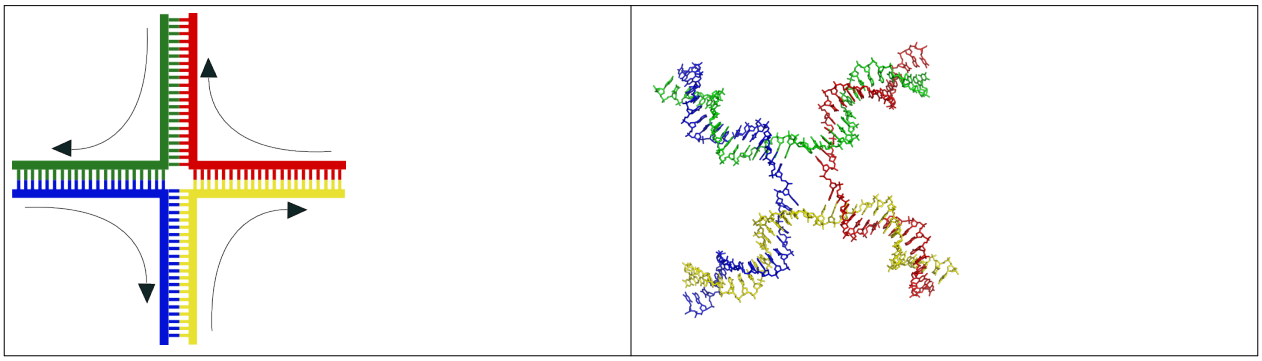

Structure of the 4-arm junction.
Left: A schematic. **Right**: A more realistic model.[1]
Each of the four separate DNA single strands are shown in different colors.

DNA nanotechnology makes use of branched DNA structures to create DNA complexes with useful properties. → DNA is normally a linear molecule, in that its axis is unbranched. However, DNA molecules containing junctions can also be made. For example, a four-arm junction can be made using four individual DNA strands which are complementary to each other in the correct pattern. Due to Watson-Crick base pairing, only portions of the strands which are complementary to each other will attach to each other to form duplex DNA. This four-arm junction is an immobile form of a Holliday junction.

Junctions can be used in more complex molecules. The most important of these is the "double-crossover" or DX motif. Here, two DNA duplexes lie next to each other, and share two junction points where strands cross from one duplex into the other. This molecule has the advantage that the junction points are now constrained to a single orientation as opposed to being flexible as in the four-arm junction. This makes the DX motif suitible as a structural building block for larger DNA complexes.[3]

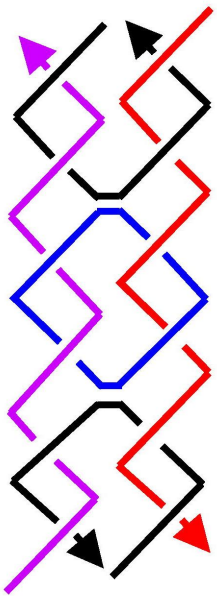

A double-crossover (DX) molecule. This molecule consists of five → DNA single strands which form two double-helical domains, on the left and the right in this image. There are two crossover points where the strands cross from one domain into the other. Image from Mao, 2004. [2]

Tile-based arrays

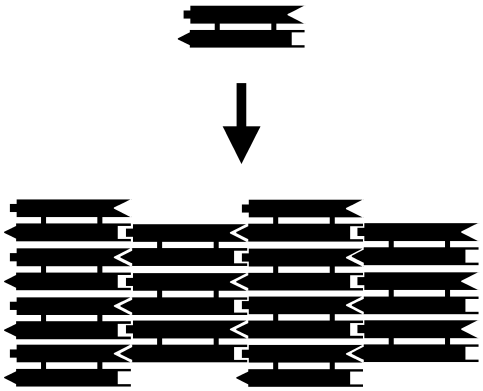

Assembly of a DX array. Each bar represents a double-helical domain of → DNA, with the shapes representing comlimentary sticky ends. The DX molecule at top will combine into the two-dimensional DNA array shown at bottom. Image from Mao, 2004. [4]

DX arrays

DX, Double Crossover, molecules can be equipped with sticky ends in order to combine them into a two-dimenstional periodic lattice. Each DX molecule has four termini, one at each end of the two double-helical domains, and these can be equipped with sticky ends that program them to combine into a specific pattern. More than one type of DX can be used which can be made to arrange in rows or any other tessellated pattern. They thus form extended flat sheets which are essentially two-dimensional crystals of DNA.[5]

DNA nanotubes

In addition to flat sheets, DX arrays have been made to form hollow tubes of 4-20 nm diameter. These DNA nanotubes are somewhat similar in size and shape to carbon nanotubes, but the carbon nanotubes are stronger and better conductors, whereas the DNA nanotubes are more easily modified and connected to other structures.[6]

Other tile arrays

Two-dimensional arrays have been made out of other motifs as well, including the Holliday junction rhombus array as well as various DX-based arrays in the shapes of triangles and hexagons.[7] Another motif, the six-helix bundle, has the ability to form three-dimensional DNA arrays as well.[8]

DNA origami

As an alternative to the tile-based approach, two-dimensional DNA structures can be made from a single, long DNA strand of arbitrary sequence which is folded into the desired shape by using shorter, "staple" strands. This allows the creation of two-dimensional shapes at the nanoscale using → DNA. Demonstrated designs have included the smiley face and a coarse map of North America. DNA origami was the cover story of *Nature* on March 15, 2006.[9]

DNA polyhedra

A number of three-dimensional DNA molecules have been made which have the connectivity of a polyhedron such as an octahedron or cube. In other words, the DNA duplexes trace the edges of a polyhedron with a DNA junction at each vertex. The earliest demonstrations of DNA polyhedra involved multiple ligations and solid-phase synthesis steps to create catenated polyhedra. More recently, there have been demonstrations of a DNA truncated octahedron made from a long single strand designed to fold into the correct conformation, as well as a tetrahedron which can be produced from four DNA strands in a single step.[10]

DNA nanomechanical devices

DNA complexes have been made which change their conformation upon some stimulus. These are intended to have applications in nanorobotics. One of the first such devices, called "molecular tweezers," changes from an open to a closed state based upon the presence of control strands.

DNA machines have also been made which show a twisting motion. One of these makes use of the transition between the B-DNA and Z-DNA forms to respond to a change in buffer conditions. Another relies on the presence of control strands to switch from a paranemic-crossover (PX) conformation to a double-junction (JX2) conformation.[11]

Stem Loop Controllers

A design called a *stem loop*, consisting of a single strand of DNA which has a loop at an end, are a dynamic structure that opens and closes when a piece of DNA bonds to the loop part. This effect has been exploited to create several logic gates. [12] [13] These logic gates have been used to create the computers MAYA I and MAYA II which can play tick-tac-toe to some extent.[14]

Applications

Algorithmic self-assembly

DNA nanotechnology has been applied to the related field of DNA computing. A DX array has been demonstrated whose assembly encodes an XOR operation, which allows the DNA array to implement a cellular automaton which generates a fractal called the Sierpinski gasket. This shows that computation can be incorporated into the assembly of DNA arrays, increasing its scope beyond simple periodic arrays.

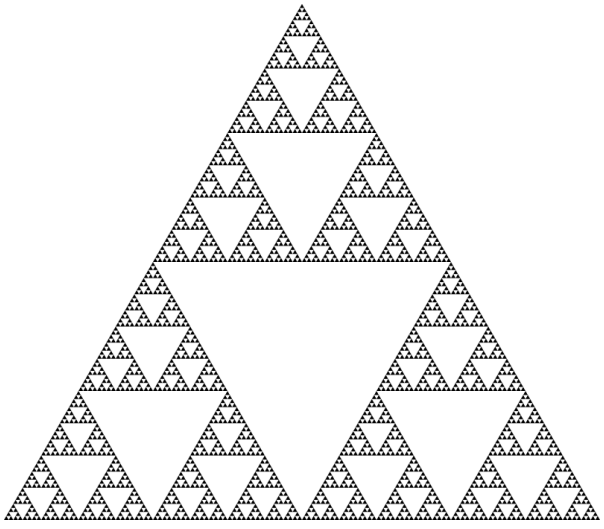

The Sierpinski gasket.

Note that DNA computing overlaps with, but is distinct from, DNA nanotechnology. The latter uses the specificity of Watson-Crick basepairing to make novel structures out of DNA. These structures can be used for DNA computing, but they do not have to be. Additionally, DNA computing can be done without using the types of molecules made possible by DNA Nanotechnology.[16]

Nanoarchitecture

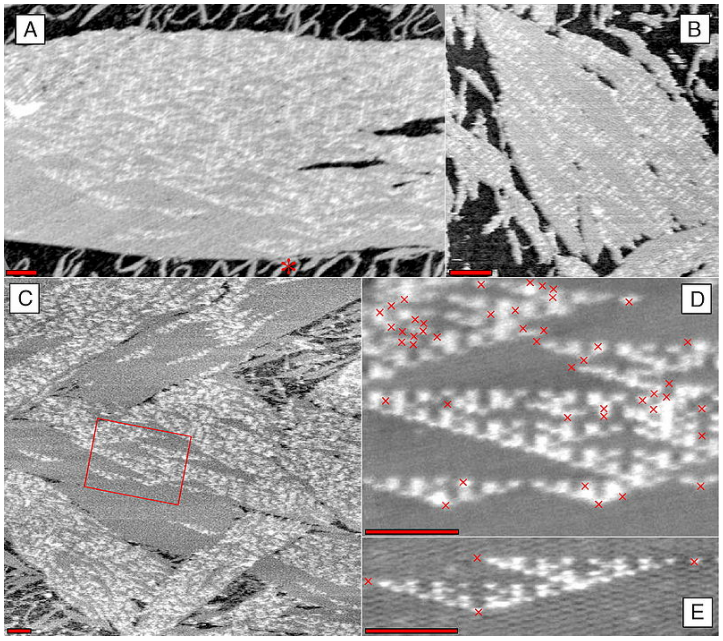

DNA arrays that display a representation of the Sierpinski gasket on their surfaces. Click the image for further details. Image from Rothemund *et al.*, 2004. [15]

The idea of using DNA arrays to template the assembly of other functional molecules has been around for a while, but only recently has progress been made in reducing these kinds of schemes to practice. In 2006, researchers covalently attached gold nanoparticles to a DX-based tile and showed that self-assembly of the DNA structures also assembled the nanoparticles hosted on them. A non-covalent hosting scheme was shown in 2007, using Dervan polyamides on a DX array to arrange streptavidin proteins on specific kinds of tiles on the DNA array.[17] Previously in 2006 LaBean demonstrated the letters "D" "N" and "A" created on a 4x4 DX array using streptavidin. [18]

DNA has also been used to assemble a single walled carbon nanotube Field-effect_transistor.[19]

See also

- Mechanical properties of DNA

External links

- Chengde Mao page at Purdue University [20]
- John Reif lab at Duke University [21]
- Nadrian Seeman lab at NYU [22]
- William M. Shih lab at Harvard Medical School [23]
- Andrew Turberfield lab at Oxford University [24]
- Erik Winfree lab at Caltech [25]
- Hao Yan lab at Arizona State University [26]
- Bernard Yurke formerly at Bell Labs [27] now at Boise State University [28]
- Thom LaBean at Duke University [29]
- Software for 3D DNA design, modeling and/or simulation:
  - Ascalaph Designer [30]
  - caDNAno [31]
  - GIDEON [32]
  - NanoEngineer-1 [33]
- International Society for Nanoscale Science, Computation and Engineering [34]

References

Note: Click on the doi to access the text of the referenced article.

[1] Created from PDB 1M6G (http://www.rcsb.org/pdb/explore/explore.do?structureId=1M6G)

[2] http://dx.doi.org/10.1371/journal.pbio.0020431

- Seeman, Nadrian C. (1 November 1999). "DNA Engineering and its Application to Nanotechnology". *Trends in Biotechnology* **17** (11): 437–443. doi: 10.1016/S0167-7799(99)01360-8 (http://dx.doi.org/10.1016/S0167-7799(99)01360-8). ISSN 0167-7799 (http://worldcat.org/issn/0167-7799).
- Seeman, Nadrian C. (January 2001). "DNA Nicks and Nodes and Nanotechnology". *Nano Letters* **1** (1): 22–26. doi: 10.1021/nl000182v (http://dx.doi.org/10.1021/nl000182v). ISSN 1530-6984 (http://worldcat.org/issn/1530-6984).
- Mao, Chengde (December 2004). "The Emergence of Complexity: Lessons from DNA". *PLoS Biology* **2** (12): 2036–2038. doi: 10.1371/journal.pbio.0020431 (http://dx.doi.org/10.1371/journal.pbio.0020431). ISSN 1544-9173 (http://worldcat.org/issn/1544-9173).
- Kumara, Mudalige T. (July 2008). "Assembly pathway analysis of DNA nanostructures and the construction of parallel motifs". *Nano Letters* **8** (7): 1971–1977. doi: 10.1021/nl800907y (http://dx.doi.org/10.1021/nl800907y). ISSN .

[4] http://dx.doi.org/10.1371/journal.pbio.0020431

- Winfree, Erik; Liu, Furong; Wenzler, Lisa A. & Seeman, Nadrian C. (6 August 1998). "Design and self-assembly of two-dimensional DNA crystals". *Nature* **394**: 529–544. doi: 10.1038/28998 (http://dx.doi.org/10.1038/28998). ISSN 0028-0836 (http://worldcat.org/issn/0028-0836).
- Liu, Furong; Sha, Ruojie & Seeman, Nadrian C. (10 February 1999). "Modifying the Surface Features of Two-Dimensional DNA Crystals". *Journal of the American Chemical Society* **121** (5): 917–922. doi: 10.1021/ja982824a (http://dx.doi.org/10.1021/ja982824a). ISSN 0002-7863 (http://worldcat.org/issn/0002-7863).
- Rothemund, Paul W. K.; Ekani-Nkodo, Axel; Papadakis, Nick; Kumar, Ashish; Fygenson, Deborah Kuchnir & Winfree, Erik (22 December 2004). "Design and Characterization of Programmable DNA Nanotubes". *Journal of the American Chemical Society* **126** (50): 16344–16352. doi: 10.1021/ja044319l (http://dx.doi.org/10.1021/ja044319l). ISSN 0002-7863 (http://worldcat.org/issn/0002-7863).
- Mao, Chengde; Sun, Weiqiong & Seeman, Nadrian C. (16 June 1999). "Designed Two-Dimensional DNA Holliday Junction Arrays Visualized by Atomic Force Microscopy". *Journal of the American Chemical Society* **121** (23): 5437–5443. doi: 10.1021/ja9900398 (http://dx.doi.org/10.1021/ja9900398). ISSN 0002-7863 (http://worldcat.org/issn/0002-7863).
- Constantinou, Pamela E.; Wang, Tong; Kopatsch, Jens; Israel, Lisa B.; Zhang, Xiaoping; Ding, Baoquan; Sherman, William B.; Wang, Xing; Zheng, Jianping; Sha, Ruojie & Seeman, Nadrian C. (2006). "Double cohesion in structural DNA nanotechnology". *Organic and Biomolecular Chemistry* **4**: 3414–3419. doi: 10.1039/b605212f (http://dx.doi.org/10.1039/b605212f).
- Mathieu, Frederick; Liao, Shiping; Kopatsch, Jens; Wang, Tong; Mao, Chengde & Seeman, Nadrian C. (April 2005). "Six-Helix Bundles Designed from DNA". *Nano Letters* **5** (4): 661–665. doi: 10.1021/nl050084f (http://dx.doi.org/10.1021/nl050084f). ISSN 1530-6984 (http://worldcat.org/issn/1530-6984).
- Rothemund, Paul W. K. (2006). "Folding DNA to create nanoscale shapes and patterns". *Nature* **440**: 297–302. doi: 10.1038/nature04586 (http://dx.doi.org/10.1038/nature04586). ISSN 0028-0836 (http://worldcat.org/issn/0028-0836).
- Zhang, Yuwen; Seeman, Nadrian C. (1994). "Construction of a DNA-truncated octahedron". *Journal of the American Chemical Society* **116** (5): 1661–1669. doi: 10.1021/ja00084a006 (http://dx.doi.org/10.1021/ja00084a006). ISSN 0002-7863 (http://worldcat.org/issn/0002-7863).
- Shih, William M.; Quispe, Joel D.; Joyce, Gerald F. (12 February 2004). "A 1.7-kilobase single-stranded DNA that folds into a nanoscale octahedron". *Nature* **427**: 618–621. doi: 10.1038/nature02307 (http://dx.doi.org/10.1038/nature02307). ISSN 0028-0836 (http://worldcat.org/issn/0028-0836).
- Goodman, R.P.; Schaap, I.A.T.; Tardin, C.F.; Erben, C.M.; Berry, R.M.; Schmidt, C.F.; Turberfield, A.J. (9 December 2005). "Rapid chiral assembly of rigid DNA building blocks for molecular nanofabrication". *Science* **310** (5754): 1661–1665. doi: 10.1126/science.1120367 (http://dx.doi.org/10.1126/science.1120367). ISSN 0036-8075 (http://worldcat.org/issn/0036-8075).
- Yurke, Bernard; Turberfield, Andrew J.; Mills, Allen P., Jr; Simmel, Friedrich C. & Neumann, Jennifer L. (10 August 2000). "A DNA-fuelled molecular machine made of DNA". *Nature* **406**: 605–609. doi:

10.1038/35020524 (http://dx.doi.org/10.1038/35020524). ISSN 0028-0836 (http://worldcat.org/issn/0028-0836).

- Mao, Chengde; Sun, Weiqiong; Shen, Zhiyong & Seeman, Nadrian C. (14 January 1999). "A DNA Nanomechanical Device Based on the B-Z Transition". *Nature* **397**: 144–146. doi: 10.1038/16437 (http://dx.doi.org/10.1038/16437). ISSN .
- Yan, Hao; Zhang, Xiaoping; Shen, Zhiyong & Seeman, Nadrian C. (3 January 2002). "A robust DNA mechanical device controlled by hybridization topology". *Nature* **415**: 62–65. doi: 10.1038/415062a (http://dx.doi.org/10.1038/415062a). ISSN .

[12] DNA Logic Gates (https://digamma.cs.unm.edu/wiki/bin/view/McogPublicWeb/MolecularLogicGates)
[13] (http://www.duke.edu/~jme17/Joshua_E._Mendoza-Elias/Research_Ideas.html)
[14] MAYA II (https://digamma.cs.unm.edu/wiki/bin/view/McogPublicWeb/MolecularAutomataMAYAII)
[15] http://dx.doi.org/10.1371/journal.pbio.0020424

- Rothemund, Paul W. K.; Papadakis, Nick & Winfree, Erik (December 2004). "Algorithmic Self-Assembly of DNA Sierpinski Triangles". *PLoS Biology* **2** (12): 2041–2053. doi: 10.1371/journal.pbio.0020424 (http://dx.doi.org/10.1371/journal.pbio.0020424). ISSN 1544-9173 (http://worldcat.org/issn/1544-9173).
- Robinson, Bruche H.; Seeman, Nadrian C. (August 1987). "The Design of a Biochip: A Self-Assembling Molecular-Scale Memory Device". *Protein Engineering* **1** (4): 295–300. ISSN 0269-2139 (http://worldcat.org/issn/0269-2139). Link (http://peds.oxfordjournals.org/cgi/content/abstract/1/4/295)
- Zheng, Jiwen; Constantinou, Pamela E.; Micheel, Christine; Alivisatos, A. Paul; Kiehl, Richard A. & Seeman Nadrian C. (2006). "2D Nanoparticle Arrays Show the Organizational Power of Robust DNA Motifs". *Nano Letters* **6**: 1502–1504. doi: 10.1021/nl060994c (http://dx.doi.org/10.1021/nl060994c). ISSN 1530-6984 (http://worldcat.org/issn/1530-6984).
- Cohen, Justin D.; Sadowski, John P.; Dervan, Peter B. (2007). "Addressing Single Molecules on DNA Nanostructures". *Angewandte Chemie* **46** (42): 7956–7959. doi: 10.1002/anie.200702767 (http://dx.doi.org/10.1002/anie.200702767). ISSN 0570-0833 (http://worldcat.org/issn/0570-0833).

[18] Park, Sung Ha; Sung Ha Park, Constantin Pistol, Sang Jung Ahn, John H. Reif, Alvin R. Lebeck, Chris Dwyer, Thomas H. LaBean (October 2006). " Finite-Size, Fully Addressable DNA Tile Lattices Formed by Hierarchical Assembly Procedures (http://www3.interscience.wiley.com/journal/113390879/abstract)". *Angewandte Chemie* **118** (40): 749–753. doi: 10.1002/ange.200690141 (http://dx.doi.org/10.1002/ange.200690141). ISSN 1521-3757 (http://worldcat.org/issn/1521-3757). .
[19] Keren, K.; Kinneret Keren, Rotem S. Berman, Evgeny Buchstab, Uri Sivan, Erez Braun (November 2003). " DNA-Templated Carbon Nanotube Field-Effect Transistor (http://www.sciencemag.org/cgi/content/abstract/sci;302/5649/1380)". *Science* **302** (6549): 1380–1382. doi: 10.1126/science.1091022 (http://dx.doi.org/10.1126/science.1091022). ISSN 1095-9203 (http://worldcat.org/issn/1095-9203). .
[20] http://www.chem.purdue.edu/people/faculty/faculty.asp?itemID=46
[21] http://www.cs.duke.edu/~reif/BMC/Reif.BMCproject.html
[22] http://seemanlab4.chem.nyu.edu/
[23] http://research2.dfci.harvard.edu/shih/SHIH_LAB/Home.html
[24] http://www.physics.ox.ac.uk/cm/people/turberfield.htm
[25] http://dna.caltech.edu/
[26] http://chemistry.asu.edu/faculty/hao_yan.asp
[27] http://www.bell-labs.com/org/physicalsciences/profiles/yurke.html
[28] http://coen.boisestate.edu/departments/faculty.asp?ID=134
[29] http://www.cs.duke.edu/~thl/
[30] http://www.agilemolecule.com/Ascalaph/Ascalaph_Designer.html
[31] http://cadnano.org
[32] http://www.subirac.com
[33] http://www.nanoengineer-1.net
[34] http://www.isnsce.org/

2D-FT NMRI and Spectroscopy

2D-FT Nuclear magnetic resonance imaging (**2D-FT NMRI**), or **Two-dimensional Fourier transform** nuclear magnetic resonance imaging (**NMRI**), is primarily a non—invasive imaging technique most commonly used in biomedical research and medical radiology/nuclear medicine/MRI to visualize structures and functions of the living systems and single cells. For example it can provides fairly detailed images of a human body in any selected cross-sectional plane, such as longitudinal, transversal, sagital, etc. The basic NMR phenomenon or physical principle[1] is essentially the same in N(MRI), nuclear magnetic resonance/→ FT (NMR) spectroscopy, topical NMR, or even in Electron Spin Resonance /EPR; however, the details are significantly different at present for EPR, as only in the early days of NMR the static magnetic field was scanned for obtaining spectra, as it is still the case in many EPR or ESR spectrometers. NMRI, on the other hand, often utilizes a linear magnetic field gradient to obtain an image that combines the visualization of molecular structure and dynamics. It is this dynamic aspect of NMRI, as well as its highest sensitivity for the ^{1}H nucleus that distinguishes it very dramatically from X-ray CAT scanning that 'misses' hydrogens because of their very low X-ray scattering factor.

Thus, NMRI provides much greater contrast especially for the different soft tissues of the body than computed tomography (CT) as its most sensitive option observes the nuclear spin distribution and dynamics of highly mobile molecules that contain the naturally abundant, stable hydrogen isotope ^{1}H as in plasma water molecules, blood, disolved metabolites and fats. This approach makes it most useful in cardiovascular, oncological (cancer), neurological (brain), musculoskeletal, and cartilage imaging. Unlike CT, it uses no ionizing radiation, and also unlike nuclear imaging it does not employ any radioactive isotopes. Some of the first MRI images reported were published in 1973[2] and the first study performed on a human took place on July 3, 1977.[3] Earlier papers were also published by Sir Peter Mansfield[4] in UK (Nobel Laureate in 2003), and R. Damadian in the USA[5] , (together with an approved patent for 'fonar', or magnetic imaging). The detailed physical theory of NMRI was published by Peter Mansfield in 1973[6] . Unpublished 'high-resolution' (50 micron resolution) images of other living systems, such as hydrated wheat grains, were also obtained and communicated in UK in 1977-1979, and were subsequently confirmed by articles published in *Nature* by Peter Callaghan.

NMR Principle

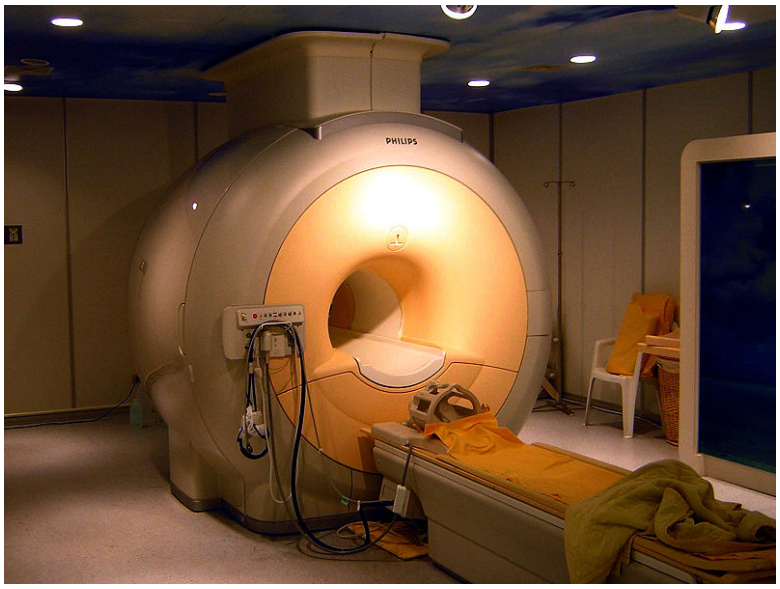

Advanced 4.7 T clinical diagnostics and biomedical research NMR Imaging instrument.

Certain nuclei such as ^{1}H nuclei, or `fermions' have spin-1/2, because there are two spin states, referred to as "up" and "down" states. The nuclear magnetic resonance absorption phenomenon occurs when samples containing such nuclear spins are placed in a static magnetic field and a very short radiofrequency pulse is applied with a center, or carrier, frequency matching that of the transition between the up and down states of the spin-1/2 ^{1}H nuclei that were polarized by the static magnetic field. [7] Very low field schemes have also been recently reported.[8]

Chemical Shifts

NMR is a very useful family of techniques for chemical and biochemical research because of the chemical shift; this effect consists in a frequency shift of the nuclear magnetic resonance for specific chemical groups or atoms as a result of the partial shielding of the corresponding nuclei from the applied, static external magnetic field by the electron orbitals (or molecular orbitals) surrounding such nuclei present in the chemical groups. Thus, the higher the electron density surrounding a specific nucleus the larger the chemical shift will be. The resulting magnetic field at the nucleus is thus lower than the applied external magnetic field and the resonance frequencies observed as a result of such shielding are lower than the value that would be observed in the absence of any electronic orbital shielding. Furthermore, in order to obtain a chemical shift value independent of the strength of the applied magnetic field and allow for the direct comparison of spectra obtained at different magnetic field values, the chemical shift is defined by the ratio of the strength of the local magnetic field value at the observed (electron orbital-shielded) nucleus by the external magnetic field strength, $\mathbf{H}_{loc}/\ \mathbf{H}_{0}$. The first NMR observations of the chemical shift, with the correct physical chemistry interpretation, were reported for ^{19}F containing compounds in the early 1950s by Herbert S. Gutowsky and Charles P. Slichter from the University of Illinois at Urbana (USA).

A related effect in metals is called the Knight shift, which is due only to the conduction electrons. Such conduction electrons present in metals induce an "additional" local field at the nuclear site, due to the spin re-orientation of the conduction electrons in the presence of the applied (constant), external magnetic field. This is only broadly `similar' to the chemical shift in either solutions or diamagnetic solids.

NMR Imaging Principles

A number of methods have been devised for combining magnetic field gradients and radiofrequency pulsed excitation to obtain an image. Two major maethods involve either 2D -FT or 3D-FT[9] reconstruction from projections, somewhat similar to Computed Tomography, with the exception of the image interpretation that in the former case must include dynamic and relaxation/contrast enhancement information as well. Other schemes involve building the NMR image either point-by-point or line-by-line. Some schemes use instead gradients in the rf field rather than in the static magnetic field. The majority of NMR images routinely obtained are either by the Two-Dimensional Fourier Transform (2D-FT) technique [10] (with slice selection), or by the Three-Dimensional Fourier Transform (3D—FT) techniques that are however much more time consuming at present. 2D-FT NMRI is sometime called in common parlance a "spin-warp". An NMR image corresponds to a spectrum consisting of a number of `spatial frequencies' at different locations in the sample investigated, or in a patient.[11] A two–dimensional Fourier transformation of such a "real" image may be considered as a representation of such "real waves" by a matrix of spatial frequencies known as the k–space. We shall see next in some mathematical detail how the 2D-FT computation works to obtain 2D-FT NMR images.

Two-dimensional Fourier transform imaging and spectroscopy

A two-dimensional Fourier transform (2D-FT) is computed numerically or carried out in two stages, both involving `standard', one-dimensional Fourier transforms. However, the second stage Fourier transform is not the inverse Fourier transform (which would result in the original function that was transformed at the first stage), but a Fourier transform in a second variable—which is `shifted' in value—relative to that involved in the result of the first Fourier transform. Such 2D-FT analysis is a very powerful method for both NMRI and two-dimensional nuclear magnetic resonance spectroscopy (2D-FT NMRS)[12] that allows the three-dimensional reconstruction of polymer and biopolymer structures at atomic resolution.[13] for molecular weights (Mw) of dissolved biopolymers in aqueous solutions (for example) up to about 50,000 Mw. For larger biopolymers or polymers, more complex methods have been developed to obtain limited structural resolution needed for partial 3D-reconstructions of higher molecular structures, e.g. for up 900,000 Mw or even oriented microcrystals in aqueous suspensions or single crystals; such methods have also been reported for *in vivo* 2D-FT NMR spectroscopic studies of algae, bacteria, yeast and certain mammalian cells, including human ones. The 2D-FT method is also widely utilized in optical spectroscopy, such as *2D-FT NIR hyperspectral imaging* (2D-FT NIR-HS), or in MRI imaging for research and clinical, diagnostic applications in Medicine. In the latter case, 2D-FT NIR-HS has recently allowed the identification of single, malignant cancer cells surrounded by healthy human breast tissue at about 1 micron resolution, well-beyond the resolution obtainable by 2D-FT NMRI for such systems in the limited time available for such diagnostic investigations (and also in magnetic fields up to the FDA approved magnetic field strength $\mathbf{H}_0$ of 4.7 T, as shown in the top image of the state-of-the-art NMRI instrument). A more precise mathematical definition of the `double' (2D) Fourier transform involved in both 2D NMRI and 2D-FT NMRS is specified next, and a precise example follows this generally accepted definition.

2D-FT Definition

A *2D-FT, or two-dimensional Fourier transform*, is a standard Fourier transformation of a function of two variables, **f**(x_1, x_2), carried first in the first variable x_1, followed by the Fourier transform in the second variable x_2 of the resulting function **F**(s_1,x_2). Note that in the case of both 2D-FT NMRI and 2D-FT NMRS the two independent variables in this definition are in the time domain, whereas the results of the two successive Fourier transforms have, of course, frequencies as the independent variable in the NMRS, and ultimately spatial coordinates for both 2D NMRI and 2D-FT NMRS following computer structural recontructions based on special algorithms that are different from FT or 2D-FT. Moreover, such structural algorithms are different for 2D NMRI and 2D-FT NMRS: in the former case they involve macroscopic, or anatomical structure detrmination, whereas in the latter case of 2D-FT NMRS the atomic structure reconstruction algorithms are based on the quantum theory of a microphysical (quantum) process such as nuclear Overhauser enhancement NOE, or specific magnetic dipole-dipole interactions[14] between neighbor nuclei.

Example 1

A 2D Fourier transformation and phase correction is applied to a set of 2D NMR (FID) signals: **s**(t_1,t_2) yielding a real 2D-FT NMR `spectrum' (collection of 1D FT-NMR spectra) represented by a matrix **S** whose elements are

$$\mathbf{S}\ (\nu_1, \nu_2) = \mathbf{Re} \int \int cos(\nu_1 t_1) exp^{(-i\nu_2 t_2)} s(t_1, t_2) dt_1 dt_2$$

where : ν_1 and : ν_2 denote the discrete indirect double-quantum and single-quantum(detection) axes, respectively, in the 2D NMR experiments. Next, the *covariance matrix* is calculated in the frequency domain according to the following equation

C $(\nu_2', \nu_2) = S^T S = \sum_{\nu^1} [S(\nu_1, \nu_2') S(\nu_1, \nu_2)],$ with : ν_2, ν_2' taking all possible single-quantum frequency values and with the summation carried out over all discrete, double quantum frequencies : ν_1.

Example 2

Atomic Structure from 2D-FT STEM Images [15] of electron distributions in a high-temperature cuprate superconductor `paracrystal' reveal both the domains (or `location') and the local symmetry of the 'pseudo-gap' in the electron-pair correlation band responsible for the high—temperature superconductivity effect (obtained at Cornell University). So far there have been three Nobel prizes awarded for 2D-FT NMR/MRI during 1992-2003, and an additional, earlier Nobel prize for 2D-FT of X-ray data (`CAT scans'); recently the advanced possibilities of 2D-FT techniques in Chemistry, Physiology and Medicine [16] received very significant recognition.[17]

Brief explanation of NMRI diagnostic uses in Pathology

As an example, a diseased tissue such as a malign tumor, can be detected by 2D-FT NMRI because the hydrogen nuclei of molecules in different tissues return to their equilibrium spin state at different relaxation rates, and also because of the manner in which a malign tumor spreads and grows rapidly along the blood vessels adjacent to the tumor, also inducing further vascularization to occur. By changing the pulse delays in the RF pulse

sequence employed, and/or the RF pulse sequence itself, one may obtain a `relaxation—based contrast', or contrast enhancement between different types of body tissue, such as normal vs. diseased tissue cells for example. Excluded from such diagnostic observations by NMRI are all patients with ferromagnetic metal implants, (e.g., cochlear implants), and all cardiac pacemaker patients who cannot undergo any NMRI scan because of the very intense magnetic and RF fields employed in NMRI which would strongly interfere with the correct functioning of such pacemakers. It is, however, conceivable that future developments may also include along with the NMRI diagnostic treatments with special techniques involving applied magnetic fields and very high frequency RF. Already, surgery with special tools is being experimented on in the presence of NMR imaging of subjects.Thus, NMRI is used to image almost every part of the body, and is especially useful for diagnosis in neurological conditions, disorders of the muscles and joints, for evaluating tumors, such as in lung or skin cancers, abnormalities in the heart (especially in children with hereditary disorders), blood vessels, CAD, atherosclerosis and cardiac infarcts [18] (courtesy of Dr. Robert R. Edelman)

See also

- Nuclear magnetic resonance (NMR)
- Edward Mills Purcell
- Felix Bloch
- Medical imaging
- Paul C. Lauterbur
- Magnetic resonance microscopy
- Peter Mansfield
- Computed tomography (CT)
- Solid-state NMR
- Knight shift
- John Hasbrouck Van Vleck
- Chemical shift
- Herbert S. Gutowsky
- John S. Waugh
- Charles Pence Slichter
- Protein nuclear magnetic resonance spectroscopy
- Kurt Wüthrich
- Nuclear Overhauser effect
- Fourier transform spectroscopy(FTS)
- Jean Jeneer
- Richard R. Ernst
- FT-NIRS (NIR)
- Magnetic resonance elastography
- Relaxation
- Earth's field NMR (EFNMR)
- Robinson oscillator

Footnotes

[1] Antoine Abragam. 1968. *Principles of Nuclear Magnetic Resonance.*, 895 pp., Cambridge University Press: Cambridge, UK.

[2] Lauterbur, P.C., Nobel Laureate in 2003 (1973). "Image Formation by Induced Local Interactions: Examples of Employing Nuclear Magnetic Resonance". *Nature* **242**: 190–1. doi: 10.1038/242190a0 (http://dx.doi.org/10.1038/242190a0).

[3] Howstuffworks "How MRI Works" (http://www.howstuffworks.com/mri.htm/printable)

[4] Peter Mansfield. 2003. Nobel Laureate in Physiology and Medicine for (2D and 3D) MRI (http://www.parteqinnovations.com/pdf-doc/fandr-Gaz1006.pdf)

[5] Damadian, R. V. "Tumor Detection by Nuclear Magnetic Resonance," Science, 171 (March 19, 1971): 1151-1153 (http://www.sciencemag.org/cgi/content/abstract/171/3976/1151)

[6] NMR 'diffraction' in solids? P. Mansfield et al. 1973 J. Phys. C: Solid State Phys. 6 L422-L426 doi: 10.1088/0022-3719 (http://www.iop.org/EJ/article/0022-3719/6/22/007/jcv6i22pL422.pdf)

[7] Antoine Abragam. 1968. *Principles of Nuclear Magnetic Resonance.*, 895 pp., Cambridge University Press: Cambridge, UK.

[8] Raftery D (August 2006). " MRI without the magnet (http://www.pubmedcentral.nih.gov/articlerender.fcgi?tool=pmcentrez&artid=1568902)". *Proc Natl Acad Sci USA.* **103** (34): 12657–8. doi: 10.1073/pnas.0605625103 (http://dx.doi.org/10.1073/pnas.0605625103). PMID 16912110.

[9] Wu Y, Chesler DA, Glimcher MJ, *et al.* (February 1999). " Multinuclear solid-state three-dimensional MRI of bone and synthetic calcium phosphates (http://www.pnas.org/cgi/pmidlookup?view=long&pmid=9990066)". *Proc. Natl. Acad. Sci. U.S.A.* **96** (4): 1574–8. doi: 10.1073/pnas.96.4.1574 (http://dx.doi.org/10.1073/pnas.96.4.1574). PMID 9990066. PMC: 15521 (http://www.pubmedcentral.nih.gov/articlerender.fcgi?tool=pmcentrez&artid=15521). .

[10] http://www.math.cuhk.edu.hk/course/mat2071a/lec1_08.ppt

[11] *Haacke, E Mark; Brown, Robert F; Thompson, Michael; Venkatesan, Ramesh (1999). *Magnetic resonance imaging: physical principles and sequence design*. New York: J. Wiley & Sons. ISBN 0-471-35128-8.

[12] Richard R. Ernst. 1992. Nuclear Magnetic Resonance Fourier Transform (2D-FT) Spectroscopy. Nobel Lecture (http://nobelprize.org/nobel_prizes/chemistry/laureates/1991/ernst-lecture.pdf), on December 9, 1992.

[13] http://en.wikipedia.org/wiki/Nuclear_magnetic_resonance#Nuclear_spin_and_magnets Kurt Wüthrich in 1982-1986 : 2D-FT NMR of solutions

[14] Charles P. Slichter.1996. *Principles of Magnetic Resonance.* Springer: Berlin and New York, Third Edition., 651pp. ISBN 0-387-50157-6.

[15] http://www.physorg.com/news129395045.html

[16] http://nobelprize.org/nobel_prizes/chemistry/laureates/1991/ernst-lecture.pdf

[17] Protein structure determination in solution by NMR spectroscopy (http://www.ncbi.nlm.nih.gov/entrez/query.fcgi?cmd=Retrieve&db=pubmed&dopt=Abstract&list_uids=2266107&query_hl=33&itool=pubmed_docsum) Kurt Wüthrich. J Biol Chem. 1990 December 25;265(36):22059-62.

[18] http://www.mr-tip.com/serv1.php?type=img&img=Cardiac%20Infarct%20Short%20Axis%20Cine%204

References

- Antoine Abragam. 1968. *Principles of Nuclear Magnetic Resonance.*, 895 pp., Cambridge University Press: Cambridge, UK.
- Charles P. Slichter.1996. *Principles of Magnetic Resonance.* Springer: Berlin and New York, Third Edition., 651pp. ISBN 0-387-50157-6.
- Kurt Wüthrich. 1986, *NMR of Proteins and Nucleic Acids.*, J. Wiley and Sons: New York, Chichester, Brisbane, Toronto, Singapore. (Nobel Laureate in 2002 for 2D-FT NMR Studies of Structure and Function of Biological Macromolecules (http://nobelprize.org/nobel_prizes/chemistry/laureates/2002/wutrich-lecture.pdf)
- Protein structure determination in solution by NMR spectroscopy (http://www.ncbi.nlm.nih.gov/entrez/query.fcgi?cmd=Retrieve&db=pubmed&dopt=Abstract&list_uids=2266107&query_hl=33&itool=pubmed_docsum) Kurt Wüthrich. J Biol Chem. 1990 December 25;265(36):22059-62

- 2D-FT NMRI Instrument image: A JPG color image of a 2D-FT NMRI `monster' Instrument (http://upload.wikimedia.org/wikipedia/en/b/bf/HWB-NMRv900.jpg).
- Richard R. Ernst. 1992. Nuclear Magnetic Resonance Fourier Transform (2D-FT) Spectroscopy. Nobel Lecture (http://nobelprize.org/nobel_prizes/chemistry/laureates/1991/ernst-lecture.pdf), on December 9, 1992.
- Peter Mansfield. 2003. Nobel Laureate in Physiology and Medicine for (2D and 3D) MRI (http://www.parteqinnovations.com/pdf-doc/fandr-Gaz1006.pdf)
- D. Benett. 2007. PhD Thesis. Worcester Polytechnic Institute. PDF of 2D-FT Imaging Applications to NMRI in Medical Research. (http://www.wpi.edu/Pubs/ETD/Available/etd-081707-080430/unrestricted/dbennett.pdf) Worcester Polytechnic Institute. (Includes many 2D-FT NMR images of human brains.)
- Paul Lauterbur. 2003. Nobel Laureate in Physiology and Medicine for (2D and 3D) MRI. (http://nobelprize.org/nobel_prizes/medicine/laureates/2003/)
- Jean Jeener. 1971. Two-dimensional Fourier Transform NMR, presented at an Ampere International Summer School, Basko Polje, unpublished. A verbatim quote follows from Richard R. Ernst's Nobel Laureate Lecture delivered on December 2, 1992, "A new approach to measure two-dimensional (2D) spectra." has been proposed by Jean Jeener at an Ampere Summer School in Basko Polje, Yugoslavia, 1971 (Jean Jeneer,1971)). He suggested a 2D Fourier transform experiment consisting of two $\pi/2$ pulses with a variable time t_1 between the pulses and the time variable t_2 measuring the time elapsed after the second pulse as shown in Fig. 6 that expands the principles of Fig. 1. Measuring the response $s(t_1,t_2)$ of the two-pulse sequence and Fourier-transformation with respect to both time variables produces a two-dimensional spectrum $S(O_1,O_2)$ of the desired form. This two-pulse experiment by Jean Jeener is the forefather of a whole class of $2D$ experiments that can also easily be expanded to multidimensional spectroscopy.
- Dudley, Robert, L (1993). "High-Field NMR Instrumentation". *Ch. 10 in Physical Chemistry of Food Processes* (New York: Van Nostrand-Reinhold) **2**: 421-30. ISBN 0-442-00582-2.
- Baianu, I.C.; Kumosinski, Thomas (August 1993). "NMR Principles and Applications to Structure and Hydration,". *Ch.9 in Physical Chemistry of Food Processes* (New York: Van Nostrand-Reinhold) **2**: 338-420. ISBN 0-442-00582-2.
- Haacke, E Mark; Brown, Robert F; Thompson, Michael; Venkatesan, Ramesh (1999). *Magnetic resonance imaging: physical principles and sequence design*. New York: J. Wiley & Sons. ISBN 0-471-35128-8.
- Raftery D (August 2006). " MRI without the magnet (http://www.pubmedcentral.nih.gov/articlerender.fcgi?tool=pmcentrez&artid=1568902)". *Proc Natl Acad Sci USA.* **103** (34): 12657–8. doi: 10.1073/pnas.0605625103 (http://dx.doi.org/10.1073/pnas.0605625103). PMID 16912110.
- Wu Y, Chesler DA, Glimcher MJ, *et al.* (February 1999). " Multinuclear solid-state three-dimensional MRI of bone and synthetic calcium phosphates (http://www.pnas.org/cgi/pmidlookup?view=long&pmid=9990066)". *Proc. Natl. Acad. Sci. U.S.A.* **96** (4): 1574–8. doi: 10.1073/pnas.96.4.1574 (http://dx.doi.org/10.1073/pnas.96.4.1574). PMID 9990066. PMC: 15521 (http://www.pubmedcentral.nih.gov/articlerender.fcgi?tool=pmcentrez&artid=15521). http://www.pnas.org/cgi/pmidlookup?view=long&

pmid=9990066.

External links

- Cardiac Infarct or "heart attack" Imaged in Real Time by 2D-FT NMRI (http://www.mr-tip.com/exam_gifs/cardiac_infarct_short_axis_cine_6.gif)
- Interactive Flash Animation on MRI (http://www.e-mri.org) - *Online Magnetic Resonance Imaging physics and technique course*
- Herbert S. Gutowsky
- Jiri Jonas and Charles P. Slichter: NMR Memoires at NAS about Herbert Sander Gutowsky; NAS = National Academy of Sciences, USA, (http://books.nap.edu/html/biomems/hgutowsky.pdf)
- 3D Animation Movie about MRI Exam (http://www.patiencys.com/MRI/)
- International Society for Magnetic Resonance in Medicine (http://www.ismrm.org)
- Danger of objects flying into the scanner (http://www.simplyphysics.com/flying_objects.html)

Related Wikipedia websites

- Medical imaging
- Computed tomography
- Magnetic resonance microscopy
- → Fourier transform spectroscopy
- FT-NIRS
- Magnetic resonance elastography
- Nuclear magnetic resonance (NMR)
- Chemical shift
- Relaxation
- Robinson oscillator
- Earth's field NMR (EFNMR)
- Rabi cycle

This article incorporates material by the original author from 2D-FT MR- Imaging and related Nobel awards (http:/ / planetphysics. org/ encyclopedia/ 2DFTImaging. html) on PlanetPhysics (http://planetphysics.org/), which is licensed under the GFDL.

NMR spectroscopy

Nuclear magnetic resonance spectroscopy, most commonly known as **NMR spectroscopy**, is the name given to a technique which exploits the magnetic properties of certain nuclei. This phenomenon and its origins are detailed in a separate section on nuclear magnetic resonance. The most important applications for the organic chemist are proton NMR and carbon-13 NMR spectroscopy. In principle, NMR is applicable to any nucleus possessing spin.

A 900MHz NMR instrument with a 21.2 T magnet at HWB-NMR, Birmingham, UK, being loaded with a sample.

Many types of information can be obtained from an NMR spectrum. Much like using infrared spectroscopy to identify functional groups, analysis of a 1D NMR spectrum provides information on the number and type of chemical entities in a molecule. However, NMR provides much more information than IR.

The impact of NMR spectroscopy on the natural sciences has been substantial. It can, among other things, be used to study mixtures of analytes, to understand dynamic effects such as change in temperature and reaction mechanisms, and is an invaluable tool in understanding protein and nucleic acid structure and function. It can be applied to a wide variety of samples, both in the solution and the solid state.

Basic NMR techniques

When placed in a magnetic field, NMR active nuclei (such as ^{1}H or ^{13}C) absorb at a frequency characteristic of the isotope. The resonant frequency, energy of the absorption and the intensity of the signal are proportional to the strength of the magnetic field. For example, in a 21 tesla magnetic field, protons resonate at 900 MHz. It is common to refer to a 21 T magnet as a 900 MHz magnet, although different nuclei resonate at a different frequency at this field strength.

In the Earth's magnetic field the same nuclei resonate at audio frequencies. This effect is used in Earth's field NMR spectrometers and other instruments. Because these instruments are portable and inexpensive, they are often used for teaching and field work.

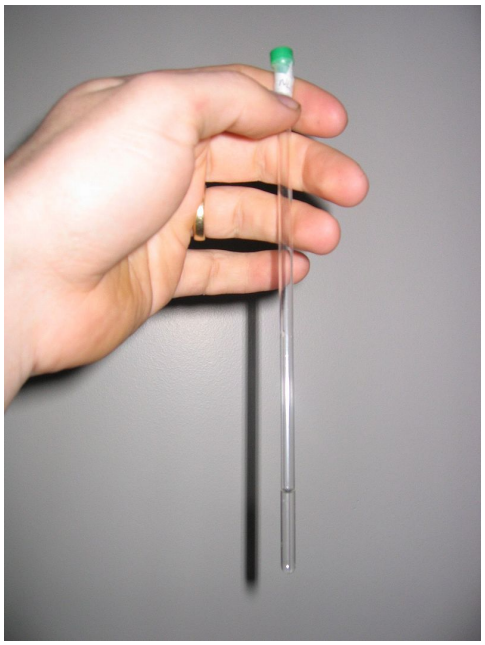

The NMR sample is prepared in a thin-walled glass tube - an NMR tube.

Chemical shift

Depending on the local chemical environment, different protons in a molecule resonate at slightly different frequencies. Since both this frequency shift and the fundamental resonant frequency are directly proportional to the strength of the magnetic field, the shift is converted into a *field-independent* dimensionless value known as the chemical shift. The chemical shift is reported as a relative measure from some reference resonance frequency. (For the nuclei ^{1}H, ^{13}C, and ^{29}Si, TMS (tetramethylsilane) is commonly used as a reference.) This difference between the frequency of the signal and the frequency of the reference is divided by frequency of the reference signal to give the chemical shift. The frequency shifts are extremely small in comparison to the fundamental NMR frequency. A typical frequency shift might be 100 Hz, compared to a fundamental NMR frequency of 100 MHz, so the chemical shift is generally expressed in parts per million (ppm).[1]

By understanding different chemical environments, the chemical shift can be used to obtain some structural information about the molecule in a sample. The conversion of the raw data to this information is called *assigning* the spectrum. For example, for the ^{1}H-NMR spectrum for ethanol (CH_3CH_2OH), one would expect three specific signals at three specific chemical shifts: one for the CH_3 group, one for the CH_2 group and one for the OH group. A typical CH_3 group has a shift around 1 ppm, a CH_2 attached to an OH has a shift of around 4 ppm and an OH has a shift around 2–3 ppm depending on the solvent used.

Because of molecular motion at room temperature, the three methyl protons *average* out during the course of the NMR experiment (which typically requires a few ms). These protons become degenerate and form a peak at the same chemical shift.

The shape and size of peaks are indicators of chemical structure too. In the example above—the proton spectrum of ethanol—the CH_3 peak would be three times as large as the OH. Similarly the CH_2 peak would be twice the size of the OH peak but only 2/3 the size of the CH_3 peak.

Modern analysis software allows analysis of the size of peaks to understand how many protons give rise to the peak. This is known as integration—a mathematical process which calculates the area under a graph (essentially what a spectrum is). The analyst must integrate the peak and not measure its height because the peaks also have *width*—and thus its size is dependent on its area not its height. However, it should be mentioned that the number of protons, or any other observed nucleus, is only proportional to the intensity, or the integral, of the NMR signal, in the very simplest one-dimensional NMR experiments. In more elaborate experiments, for instance, experiments typically used to obtain carbon-13 NMR spectra, the integral of the signals depends on the relaxation rate of the nucleus, and its scalar and dipolar coupling constants. Very often these factors are poorly understood - therefore, the integral of the NMR signal is very difficult to interpret in more complicated NMR experiments.

J-coupling

Multiplicity	Intensity Ratio
Singlet (s)	1
Doublet (d)	1:1
Triplet (t)	1:2:1
Quartet (q)	1:3:3:1
Quintet	1:4:6:4:1
Sextet	1:5:10:10:5:1
Septet	1:6:15:20:15:6:1

Some of the most useful information for structure determination in a one-dimensional NMR spectrum comes from **J-coupling** or **scalar coupling** (a special case of spin-spin coupling) between NMR active nuclei. This coupling arises from the interaction of different spin states through the chemical bonds of a molecule and results in the splitting of NMR signals. These splitting patterns can be complex or simple and, likewise, can be straightforwardly interpretable or deceptive. This coupling provides detailed insight into the connectivity of atoms in a molecule.

Coupling to n equivalent (spin ½) nuclei splits the signal into a n+1 **multiplet** with intensity ratios following Pascal's triangle as described on the right. Coupling to additional spins will lead to further splittings of each component of the multiplet e.g. coupling to two different spin ½ nuclei with significantly different coupling constants will lead to a *doublet of doublets* (abbreviation: dd). Note that coupling between nuclei that are chemically equivalent (that is, have the same chemical shift) has no effect of the NMR spectra and couplings between nuclei that are distant (usually more than 3 bonds apart for protons in flexible molecules) are usually too small to cause observable splittings. *Long-range* couplings over more than three bonds can often be observed in cyclic and aromatic compounds, leading to more complex splitting patterns.

For example, in the proton spectrum for ethanol described above, the CH_3 group is split into a *triplet* with an intensity ratio of 1:2:1 by the two neighboring CH_2 protons. Similarly, the CH_2 is split into a *quartet* with an intensity ratio of 1:3:3:1 by the three neighboring CH_3 protons. In principle, the two CH_2 protons would also be split again into a *doublet* to form a *doublet of quartets* by the hydroxyl proton, but intermolecular exchange of the

acidic hydroxyl proton often results in a loss of coupling information.

Coupling to any spin ½ nuclei such as phosphorus-31 or fluorine-19 works in this fashion (although the magnitudes of the coupling constants may be very different). But the splitting patterns differ from those described above for nuclei with spin greater than ½ because the spin quantum number has more than two possible values. For instance, coupling to deuterium (a spin 1 nucleus) splits the signal into a *1:1:1 triplet* because the spin 1 has three spin states. Similarly, a spin 3/2 nucleus splits a signal into a *1:1:1:1 quartet* and so on.

Coupling combined with the chemical shift (and the integration for protons) tells us not only about the chemical environment of the nuclei, but also the number of *neighboring* NMR active nuclei within the molecule. In more complex spectra with multiple peaks at similar chemical shifts or in spectra of nuclei other than hydrogen, coupling is often the only way to distinguish different nuclei.

Second-order (or strong) coupling

The above description assumes that the coupling constant is small in comparison with the difference in NMR frequencies between the inequivalent spins. If the shift separation decreases (or the coupling strength increases), the multiplet intensity patterns are first distorted, and then become more complex and less easily analyzed (especially if more than two spins are involved). Intensification of some peaks in a multiplet is achieved at the expense of the remainder, which sometimes almost disappear in the background noise, although the integrated area under the peaks remains constant. In most high-field NMR, however, the distortions are usually modest and the characteristic distortions (*roofing*) can in fact help to identify related peaks.

Second-order effects decrease as the frequency difference between multiplets increases, so that high-field (i.e. high-frequency) NMR spectra display less distortion than lower frequency spectra. Early spectra at 60 MHz were more prone to distortion than spectra from later machines typically operating at frequencies at 200 MHz or above.

Magnetic inequivalence

More subtle effects can occur if chemically equivalent spins (i.e. nuclei related by symmetry and so having the same NMR frequency) have different coupling relationships to external spins. Spins that are chemically equivalent but are not indistinguishable (based on their coupling relationships) are termed magnetically inequivalent. For example, the 4 H sites of 1,2-dichlorobenzene divide into two chemically equivalent pairs by symmetry, but an individual member of one of the pairs has different couplings to the spins making up the other pair. Magnetic inequivalence can lead to highly complex spectra which can only be analyzed by computational modeling. Such effects are more common in NMR spectra of aromatic and other non-flexible systems, while conformational averaging about C-C bonds in flexible molecules tends to equalize the couplings between protons on adjacent carbons, reducing problems with magnetic inequivalence.

Correlation spectroscopy

Correlation spectroscopy is one of several types of → two-dimensional nuclear magnetic resonance (NMR) spectroscopy. This type of NMR experiment is best known by its acronym, COSY. Other types of → two-dimensional NMR include J-spectroscopy, exchange spectroscopy (EXSY), Nuclear Overhauser effect spectroscopy (NOESY), total correlation spectroscopy (TOCSY) and heteronuclear correlation experiments, such as HSQC, HMQC, and HMBC. Two-dimensional NMR spectra provide more information about a molecule than one-dimensional NMR spectra and are especially useful in determining the structure of a molecule, particularly for molecules that are too complicated to work with using one-dimensional NMR. The first two-dimensional experiment, COSY, was proposed by Jean Jeener, a professor at Université Libre de Bruxelles, in 1971. This experiment was later implemented by Walter P. Aue, Enrico Bartholdi and Richard R. Ernst, who published their work in 1976.[2]

Solid-state nuclear magnetic resonance

A variety of physical circumstances does not allow molecules to be studied in solution, and at the same time not by other spectroscopic techniques to an atomic level, either. In solid-phase media, such as crystals, microcrystalline powders, gels, anisotropic solutions, etc., it is in particular the dipolar coupling and chemical shift anisotropy that become dominant to the behaviour of the nuclear spin systems. In conventional solution-state NMR spectroscopy, these additional interactions would lead to a significant broadening of spectral lines. A variety of techniques allows to establish high-resolution conditions, that can, at least for ^{13}C spectra, be comparable to solution-state NMR spectra.

Two important concepts for high-resolution solid-state NMR spectroscopy are the limitation of possible molecular orientation by sample orientation, and the reduction of anisotropic nuclear magnetic interactions by sample spinning. Of the latter approach, fast spinning around the magic angle is a very prominent method, when the system comprises spin 1/2 nuclei. A number of intermediate techniques, with samples of partial alignment or reduced mobility, is currently being used in NMR spectroscopy.

Applications in which solid-state NMR effects occur are often related to structure investigations on membrane proteins, protein fibrils or all kinds of polymers, and chemical analysis in inorganic chemistry, but also include "exotic" applications like the plant leaves and fuel cells.

NMR spectroscopy applied to proteins

Much of the recent innovation within NMR spectroscopy has been within the field of protein NMR, which has become a very important technique in structural biology. One common goal of these investigations is to obtain high resolution 3-dimensional structures of the protein, similar to what can be achieved by X-ray crystallography. In contrast to X-ray crystallography, NMR is primarily limited to relatively small proteins, usually smaller than 35 kDa, though technical advances allow ever larger structures to be solved. NMR spectroscopy is often the only way to obtain high resolution information on partially or wholly intrinsically unstructured proteins.

Proteins are orders of magnitude larger than the small organic molecules discussed earlier in this article, but the same NMR theory applies. Because of the increased number of each

element present in the molecule, the basic 1D spectra become crowded with overlapping signals to an extent where analysis is impossible. Therefore, multidimensional (2, 3 or 4D) experiments have been devised to deal with this problem. To facilitate these experiments, it is desirable to isotopically label the protein with ^{13}C and ^{15}N because the predominant naturally occurring isotope ^{12}C is not NMR-active, whereas the nuclear quadrupole moment of the predominant naturally occurring ^{14}N isotope prevents high resolution information to be obtained from this nitrogen isotope. The most important method used for structure determination of proteins utilizes NOE experiments to measure distances between pairs of atoms within the molecule. Subsequently, the obtained distances are used to generate a 3D structure of the molecule using a computer program.

See also

- In vivo magnetic resonance spectroscopy
- Low field NMR
- Magnetic Resonance Imaging
- Nuclear Magnetic Resonance
- NMR spectra database
- NMR tube - includes sample preparation
- Protein nuclear magnetic resonance spectroscopy

References

[1] James Keeler. "Chapter 2: NMR and energy levels" (http://www-keeler.ch.cam.ac.uk/lectures/Irvine/chapter2.pdf) (reprinted at University of Cambridge). *Understanding NMR Spectroscopy*. University of California, Irvine. . Retrieved on 2007-05-11.

[2] Martin, G.E; Zekter, A.S., *Two-Dimensional NMR Methods for Establishing Molecular Connectivity*; VCH Publishers, Inc: New York, 1988 (p.59)

External links

- Protein NMR- A Practical Guide (http://www.protein-nmr.org.uk) Practical guide to NMR, in particular protein NMR assignment
- James Keeler. "Understanding NMR Spectroscopy" (http://www-keeler.ch.cam.ac.uk/lectures/Irvine/) (reprinted at University of Cambridge). University of California, Irvine. http://www-keeler.ch.cam.ac.uk/lectures/Irvine/. Retrieved on 2007-05-11.
- The Basics of NMR (http://www.cis.rit.edu/htbooks/nmr/) - A non-technical overview of NMR theory, equipment, and techniques by Dr. Joseph Hornak, Professor of Chemistry at RIT
- NMRWiki.ORG (http://nmrwiki.org) project, a Wiki dedicated to NMR, MRI, and EPR.
- NMR spectroscopy for organic chemistry (http://www.organicworldwide.net/nmr.html)
- The Spectral Game (http://spectralgame.com) NMR spectroscopy game.

Free NMR processing, analysis and simulation software

- WINDNMR-Pro (http://www.chem.wisc.edu/areas/reich/plt/windnmr.htm) - simulation software for interactive calculation of first and second-order spin-coupled multiplets and a variety of DNMR lineshapes.
- CARA (http://www.nmr.ch) - resonance assignment software developed at the Wüthrich group
- NMRShiftDB (http://www.nmrshiftdb.org) - open database and NMR prediction website

- Spinworks (http://www.umanitoba.ca/chemistry/nmr/spinworks/)

Fourier transform spectroscopy

Fourier transform spectroscopy is a measurement technique whereby spectra are collected based on measurements of the temporal coherence of a radiative source, using time-domain measurements of the electromagnetic radiation or other type of radiation. It can be applied to a variety of types of spectroscopy including optical spectroscopy, infrared spectroscopy (FT IR, FT-NIRS), → Fourier transform (FT) nuclear magnetic resonance, mass spectrometry and electron spin resonance spectroscopy. There are several methods for measuring the temporal coherence of the light, including the continuous wave *Michelson* or *Fourier transform* spectrometer and the pulsed Fourier transform spectrograph (which is more sensitive and has a much shorter sampling time than conventional spectroscopic techniques, but is only applicable in a laboratory environment).

Continuous wave *Michelson* or *Fourier transform* spectrograph

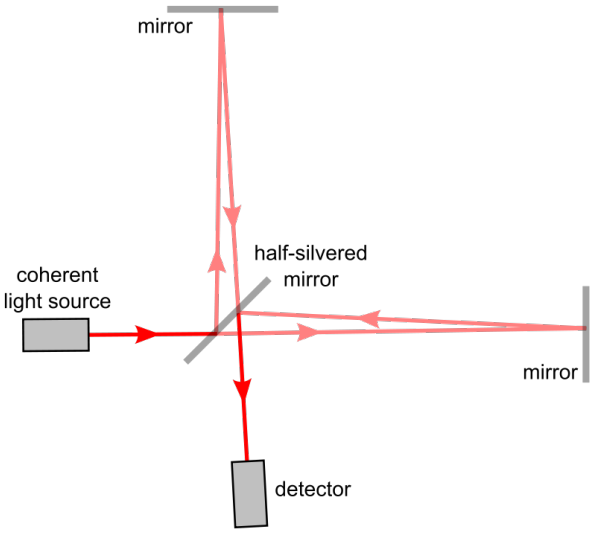

The Fourier transform spectrometer is just a Michelson interferometer but one of the two fully-reflecting mirrors is movable, allowing a variable delay (in the travel-time of the light) to be included in one of the beams.

The Michelson spectrograph is similar to the instrument used in the Michelson-Morley experiment. Light from the source is split into two beams by a half-silvered mirror, one is reflected off a fixed mirror and one off a moving mirror which introduces a time delay -- the Fourier transform spectrometer is just a Michelson interferometer with a movable mirror. The beams interfere, allowing the temporal coherence of the light to be measured at each different time delay setting, effectively converting the time domain into a spatial coordinate. By making measurements of the signal at many discrete positions of the moving mirror, the spectrum can be reconstructed using a Fourier transform of the temporal coherence of the light. Michelson spectrographs are capable of very high spectral resolution observations of very bright sources. The Michelson or Fourier transform spectrograph was popular for infra-red applications at a time when infra-red astronomy only had single pixel detectors. Imaging Michelson spectrometers are a possibility, but in general have been supplanted by imaging Fabry-Perot instruments which are easier to construct.

Pulsed *Fourier transform* spectrometer

A pulsed *Fourier transform* spectrometer does not employ transmittance techniques. In the most general description of pulsed FT spectrometry, a sample is exposed to an energizing event which causes a periodic response. The frequency of the periodic response, as governed by the field conditions in the spectrometer, is indicative of the measured properties of the analyte.

Examples of Pulsed Fourier transform spectrometry

In magnetic spectroscopy (EPR, NMR), an RF pulse in a strong ambient magnetic field is used as the energizing event. This turns the magnetic particles at an angle to the ambient field, resulting in gyration. The gyrating spins then induce a periodic current in a detector coil. Each spin exhibits a characteristic frequency of gyration (relative to the field strength) which reveals information about the analyte.

In FT-mass spectrometry, the energizing event is the injection of the charged sample into the strong electromagnetic field of a cyclotron. These particles travel in circles, inducing a current in a fixed coil on one point in their circle. Each traveling particle exhibits a characteristic cyclotron frequency-field ratio revealing the masses in the sample.

The Free Induction Decay

Pulsed FT spectrometry gives the advantage of requiring a single, time-dependent measurement which can easily deconvolute a set of similar but distinct signals. The resulting composite signal, is called a *free induction decay,* because typically the signal will decay due to inhomogeneities in sample frequency, or simply unrecoverable loss of signal due to entropic loss of the property being measured.

Fellgett Advantage

One of the most important advantages of Fourier transform spectroscopy was shown by P.B. Fellgett, an early advocate of the method. The Fellgett advantage, also known as the multiplex principle, states that a multiplex spectrometer such as the Fourier transform spectroscopy will produce a gain of the order of the square root of m in the signal-to-noise ratio of the resulting spectrum, when compared with an equivalent scanning monochromator, where m is the number of elements comprising the resulting spectrum when the measurement noise is dominated by detector noise.

Converting spectra from time domain to frequency domain

$$S(t) = \int_{-\infty}^{\infty} I(\nu) e^{-i\nu 2\pi t}\, d\nu$$

The sum is performed over all contributing frequencies to give a signal S(t) in the time domain.

$$I(\nu) = 2Re \int_{-\infty}^{\infty} S(t) e^{2i\pi\nu t} dt$$

gives non-zero value when S(t) contains a component that matches the oscillating function. Remember that

$$e^{ix} = \cos x + i \sin x$$

See also

- Applied spectroscopy
- → 2D-FT NMRI and Spectroscopy
- Forensic chemistry
- Forensic polymer engineering
- nuclear magnetic resonance
- Infra-red spectroscopy

References and notes

Further reading

- Ellis, D.I. and Goodacre, R. (2006). "Metabolic fingerprinting in disease diagnosis: biomedical applications of infrared and Raman spectroscopy". *The Analyst* **131**: 875–885. doi:10.1039/b602376m [1].

External links

- Description of how a Fourier transform spectrometer works [2]
- The Michelson or Fourier transform spectrograph [3]
- Internet Journal of Vibrational Spectroscopy - How FTIR works [4]
- Fourier Transform Spectroscopy Topical Meeting and Tabletop Exhibit [5]

References

[1] http://dx.doi.org/10.1039%2Fb602376m
[2] http://scienceworld.wolfram.com/physics/FourierTransformSpectrometer.html
[3] http://www.astro.livjm.ac.uk/courses/phys362/notes/
[4] http://www.ijvs.com/volume5/edition5/section1.html#Feature
[5] http://www.osa.org/meetings/topicalmeetings/fts/default.aspx

Chemical imaging

Chemical imaging is the simultaneous measurement of spectra (chemical information) and images or pictures (spatial information)[1] [2] The technique is most often applied to either solid or gel samples, and has applications in chemistry, biology[3] [4] [5] [6] [7] [8] , medicine[9] [10] , pharmacy[11] (see also for example: Chemical Imaging Without Dyeing [12]), food science, biotechnology[13] [14] , agriculture and industry (see for example:NIR Chemical Imaging in Pharmaceutical Industry [15] and Pharmaceutical Process Analytical Technology: [16]). NIR, IR and Raman chemical imaging is also referred to as hyperspectral, spectroscopic, spectral or multispectral imaging (also see microspectroscopy). However, other ultra-sensitive and selective, chemical imaging techniques are also in use that involve either UV-visible or fluorescence microspectroscopy. Chemical imaging techniques can be used to analyze samples of all sizes, from the single molecule[17] [18] to the cellular level in biology and medicine[19] [20] [21] , and to images of planetary systems in astronomy, but different instrumentation is employed for making observations on such widely different systems.

Chemical imaging instrumentation is composed of three components: a radiation source to illuminate the sample, a spectrally selective element, and usually a detector array (the camera) to collect the images. When many stacked spectral channels (wavelengths) are collected for different locations of the microspectrometer focus on a line or planar array in the focal plane, the data is called hyperspectral; fewer wavelength data sets are called multispectral. The data format is called a hypercube. The data set may be visualized as a three-dimensional block of data spanning two spatial dimensions (x and y), with a series of wavelengths (lambda) making up the third (spectral) axis. The hypercube can be visually and mathematically treated as a series of spectrally resolved images (each image plane corresponding to the image at one wavelength) or a series of spatially resolved spectra. The analyst may choose to view the spectrum measured at a particular spatial location; this is useful for chemical identification. Alternatively, selecting an image plane at a particular wavelength can highlight the spatial distribution of sample components, provided that their spectral signatures are different at the selected wavelength.

Many materials, both manufactured and naturally occurring, derive their functionality from the spatial distribution of sample components. For example, extended release pharmaceutical formulations can be achieved by using a coating that acts as a barrier layer. The release of active ingredient is controlled by the presence of this barrier, and imperfections in the coating, such as discontinuities, may result in altered performance. In the semi-conductor industry, irregularities or contaminants in silicon wafers or printed micro-circuits can lead to failure of these components. The functionality of biological systems is also dependent upon chemical gradients – a single cell, tissue, and even whole organs function because of the very specific arrangement of components. It has been shown that even small changes in chemical composition and distribution may be an early indicator of disease.

Any material that depends on chemical gradients for functionality may be amenable to study by an analytical technique that couples spatial and chemical characterization. To efficiently and effectively design and manufacture such materials, the ‘what’ and the ‘where’ must both be measured. The demand for this type of analysis is increasing as manufactured materials become more complex. Chemical imaging techniques not only

permit visualization of the spatially resolved chemical information that is critical to understanding modern manufactured products, but it is also a non-destructive technique so that samples are preserved for further testing.

History

Commercially available laboratory-based chemical imaging systems emerged in the early 1990s (ref. 1-5). In addition to economic factors, such as the need for sophisticated electronics and extremely high-end computers, a significant barrier to commercialization of infrared imaging was that the focal plane array (FPA) needed to read IR images were not readily available as commercial items. As high-speed electronics and sophisticated computers became more commonplace, and infrared cameras became readily commercially available, laboratory chemical imaging systems were introduced.

Initially used for novel research in specialized laboratories, chemical imaging became a more commonplace analytical technique used for general R&D, quality assurance (QA) and quality control (QC) in less than a decade. The rapid acceptance of the technology in a variety of industries (pharmaceutical, polymers, semiconductors, security, forensics and agriculture) rests in the wealth of information characterizing both chemical composition and morphology. The parallel nature of chemical imaging data makes it possible to analyze multiple samples simultaneously for applications that require high throughput analysis in addition to characterizing a single sample.

Principles

Chemical imaging shares the fundamentals of vibrational spectroscopic techniques, but provides additional information by way of the simultaneous acquisition of spatially resolved spectra. It combines the advantages of digital imaging with the attributes of spectroscopic measurements. Briefly, vibrational spectroscopy measures the interaction of light with matter. Photons that interact with a sample are either absorbed or scattered; photons of specific energy are absorbed, and the pattern of absorption provides information, or a fingerprint, on the molecules that are present in the sample.

On the other hand, in terms of the observation setup, chemical imaging can be carried out in one of the following modes: (optical) absorption, emission (fluorescence), (optical) transmission or scattering (Raman). A consensus currently exists that the fluorescence (emission) and Raman scattering modes are the most sensitive and powerful, but also the most expensive.

In a transmission measurement, the radiation goes through a sample and is measured by a detector placed on the far side of the sample. The energy transferred from the incoming radiation to the molecule(s) can be calculated as the difference between the quantity of photons that were emitted by the source and the quantity that is measured by the detector. In a diffuse reflectance measurement, the same energy difference measurement is made, but the source and detector are located on the same side of the sample, and the photons that are measured have re-emerged from the illuminated side of the sample rather than passed through it. The energy may be measured at one or multiple wavelengths; when a series of measurements are made, the response curve is called a spectrum.

A key element in acquiring spectra is that the radiation must somehow be energy selected – either before or after interacting with the sample. Wavelength selection can be

accomplished with a fixed filter, tunable filter, spectrograph, an interferometer, or other devices. For a fixed filter approach, it is not efficient to collect a significant number of wavelengths, and multispectral data are usually collected. Interferometer-based chemical imaging requires that entire spectral ranges be collected, and therefore results in hyperspectral data. Tunable filters have the flexibility to provide either multi- or hyperspectral data, depending on analytical requirements.

Spectra may be measured one point at a time using a single element detector (single-point mapping), as a line-image using a linear array detector (typically 16 to 28 pixels) (linear array mapping), or as a two-dimensional image using a Focal Plane Array (FPA)(typically 256 to 16,384 pixels) (FPA imaging). For single-point the sample is moved in the x and y directions point-by-point using a computer-controlled stage. With linear array mapping, the sample is moved line-by-line with a computer-controlled stage. FPA imaging data are collected with a two-dimensional FPA detector, hence capturing the full desired field-of-view at one time for each individual wavelength, without having to move the sample. FPA imaging, with its ability to collected tens of thousands of spectra simultaneously is orders of magnitude faster than linear arrays which are can typically collect 16 to 28 spectra simultaneously, which are in turn much faster than single-point mapping.

Terminology

Some words common in spectroscopy, optical microscopy and photography have been adapted or their scope modified for their use in chemical imaging. They include: resolution, field of view and magnification. There are two types of resolution in chemical imaging. The spectral resolution refers to the ability to resolve small energy differences; it applies to the spectral axis. The spatial resolution is the minimum distance between two objects that is required for them to be detected as distinct objects. The spatial resolution is influenced by the field of view, a physical measure of the size of the area probed by the analysis. In imaging, the field of view is a product of the magnification and the number of pixels in the detector array. The magnification is a ratio of the physical area of the detector array divided by the area of the sample field of view. Higher magnifications for the same detector image a smaller area of the sample.

Types of vibrational chemical imaging instruments

Chemical imaging has been implemented for mid-infrared, near-infrared spectroscopy and Raman spectroscopy. As with their bulk spectroscopy counterparts, each imaging technique has particular strengths and weaknesses, and are best suited to fulfill different needs.

Mid-infrared chemical imaging

Mid-infrared (MIR) spectroscopy probes fundamental molecular vibrations, which arise in the spectral range 2,500-25,000 nm. Commercial imaging implementations in the MIR region typically employ Fourier Transform Infrared (→ FT-IR) interferometers and the range is more commonly presented in wavenumber, 4,000 – 400 cm^{-1}. The MIR absorption bands tend to be relatively narrow and well-resolved; direct spectral interpretation is often possible by an experienced spectroscopist. MIR spectroscopy can distinguish subtle changes in chemistry and structure, and is often used for the identification of unknown materials. The absorptions in this spectral range are relatively strong; for this reason, sample presentation is important to limit the amount of material interacting with the

incoming radiation in the MIR region. Most data collected in this range is collected in transmission mode through thin sections (~10 micrometres) of material. Water is a very strong absorber of MIR radiation and wet samples often require advanced sampling procedures (such as attenuated total reflectance). Commercial instruments include point and line mapping, and imaging. All employ an FT-IR interferometer as wavelength selective element and light source.

For types of MIR microscope, see Microscopy#infrared microscopy.

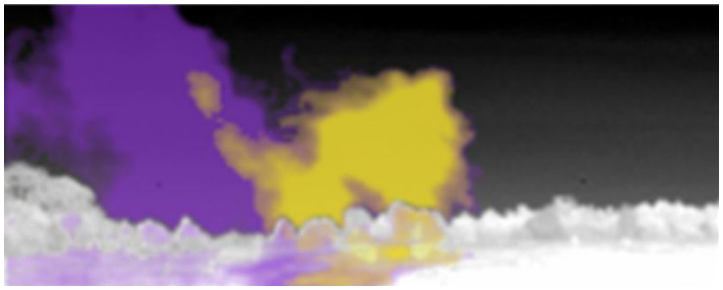

Remote chemical imaging of a simultaneous release of SF_6 and NH_3 at 1.5km using the FIRST imaging spectrometer[22]

Atmospheric windows in the infrared spectrum are also employed to perform chemical imaging remotely. In these spectral regions the atmospheric gases (mainly water and CO_2) present low absorption and allow infrared viewing over kilometer distances. Target molecules can then be viewed using the selective absorption/emission processes described above. An example of the chemical imaging of a simultaneous release of SF_6 and NH_3 is shown in the image.

Near-infrared chemical imaging

The analytical near infrared (NIR) region spans the range from approximately 700-2,500 nm. The absorption bands seen in this spectral range arise from overtones and combination bands of O-H, N-H, C-H and S-H stretching and bending vibrations. Absorption is one to two orders of magnitude smaller in the NIR compared to the MIR; this phenomenon eliminates the need for extensive sample preparation. Thick and thin samples can be analyzed without any sample preparation, it is possible to acquire NIR chemical images through some packaging materials, and the technique can be used to examine hydrated samples, within limits. Intact samples can be imaged in transmittance or diffuse reflectance.

The lineshapes for overtone and combination bands tend to be much broader and more overlapped than for the fundamental bands seen in the MIR. Often, multivariate methods are used to separate spectral signatures of sample components. NIR chemical imaging is particularly useful for performing rapid, reproducible and non-destructive analyses of known materials[23] [24] . NIR imaging instruments are typically based on one of two platforms: imaging using a tunable filter and broad band illumination, and line mapping employing an FT-IR interferometer as the wavelength filter and light source.

Raman chemical imaging

The Raman shift chemical imaging spectral range spans from approximately 50 to 4,000 cm^{-1}; the actual spectral range over which a particular Raman measurement is made is a function of the laser excitation frequency. The basic principle behind Raman spectroscopy differs from the MIR and NIR in that the x-axis of the Raman spectrum is measured as a function of energy shift (in cm^{-1}) relative to the frequency of the laser used as the source of radiation. Briefly, the Raman spectrum arises from inelastic scattering of incident photons, which requires a change in polarizability with vibration, as opposed to infrared absorption, which requires a change in dipole moment with vibration. The end result is spectral

information that is similar and in many cases complementary to the MIR. The Raman effect is weak - only about one in 10^7 photons incident to the sample undergoes Raman scattering. Both organic and inorganic materials possess a Raman spectrum; they generally produce sharp bands that are chemically specific. Fluorescence is a competing phenomenon and, depending on the sample, can overwhelm the Raman signal, for both bulk spectroscopy and imaging implementations.

Raman chemical imaging requires little or no sample preparation. However, physical sample sectioning may be used to expose the surface of interest, with care taken to obtain a surface that is as flat as possible. The conditions required for a particular measurement dictate the level of invasiveness of the technique, and samples that are sensitive to high power laser radiation may be damaged during analysis. It is relatively insensitive to the presence of water in the sample and is therefore useful for imaging samples that contain water such as biological material.

Fluorescence imaging (visible and NIR)

This emission microspectroscopy mode is the most sensitive in both visible and FT-NIR microspectroscopy, and has therefore numerous biomedical, biotechnological and agricultural applications. There are several powerful, highly specific and sensitive fluorescence techniques that are currently in use, or still being developed; among the former are FLIM, FRAP, FRET and FLIM-FRET; among the latter are NIR fluorescence and probe-sensitivity enhanced NIR fluorescence microspectroscopy and nanospectroscopy techniques (see "Further reading" section).

Sampling and samples

The value of imaging lies in the ability to resolve spatial heterogeneities in solid-state or gel/gel-like samples. Imaging a liquid or even a suspension has limited use as constant sample motion serves to average spatial information, unless ultra-fast recording techniques are employed as in fluorescence correlation microspectroscopy or FLIM obsevations where a single molecule may be monitored at extremely high (photon) detection speed. High-throughput experiments (such as imaging multi-well plates) of liquid samples can however provide valuable information. In this case, the parallel acquisition of thousands of spectra can be used to compare differences between samples, rather than the more common implementation of exploring spatial heterogeneity within a single sample.

Similarly, there is no benefit in imaging a truly homogeneous sample, as a single point spectrometer will generate the same spectral information. Of course the definition of homogeneity is dependent on the spatial resolution of the imaging system employed. For MIR imaging, where wavelengths span from 3-10 micrometres, objects on the order of 5 micrometres may theoretically be resolved. The sampled areas are limited by current experimental implementations because illumination is provided by the interferometer. Raman imaging may be able to resolve particles less than 1 micrometre in size, but the sample area that can be illuminated is severely limited. With Raman imaging, it is considered impractical to image large areas and, consequently, large samples. FT-NIR chemical/hyperspectral imaging usually resolves only larger objects (>10 micrometres), and is better suited for large samples because illumination sources are readily available. However, FT-NIR microspectroscopy was recently reported to be capable of about 1.2 micron (micrometer) resolution in biological samples[25] Furthermore, two-photon

excitation FCS experiments were reported to have attained 15 nanometer resolution on biomembrane thin films with a special coincidence photon-counting setup.

Detection limit

The concept of the detection limit for chemical imaging is quite different than for bulk spectroscopy, as it depends on the sample itself. Because a bulk spectrum represents an average of the materials present, the spectral signatures of trace components are simply overwhelmed by dilution. In imaging however, each pixel has a corresponding spectrum. If the physical size of the trace contaminant is on the order of the pixel size imaged on the sample, its spectral signature will likely be detectable. If however, the trace component is dispersed homogeneously (relative to pixel image size) throughout a sample, it will not be detectable. Therefore, detection limits of chemical imaging techniques are strongly influenced by particle size, the chemical and spatial heterogeneity of the sample, and the spatial resolution of the image.

Data analysis

Data analysis methods for chemical imaging data sets typically employ mathematical algorithms common to single point spectroscopy or to image analysis. The reasoning is that the spectrum acquired by each detector is equivalent to a single point spectrum; therefore pre-processing, chemometrics and pattern recognition techniques are utilized with the similar goal to separate chemical and physical effects and perform a qualitative or quantitative characterization of individual sample components. In the spatial dimension, each chemical image is equivalent to a digital image and standard image analysis and robust statistical analysis can be used for feature extraction.

See also

- Multispectral image
- Microspectroscopy
- Imaging spectroscopy

References

[1] http://www.imaging.net/chemical-imaging/ Chemical imaging

[2] http://www.malvern.com/LabEng/products/sdi/bibliography/sdi_bibliography.htm E. N. Lewis, E. Lee and L. H. Kidder, Combining Imaging and Spectroscopy: Solving Problems with Near-Infrared Chemical Imaging. Microscopy Today, Volume 12, No. 6, 11/2004.

[3] C.L. Evans and X.S. Xie.2008. Coherent Anti-Stokes Raman Scattering Microscopy: Chemical Imaging for Biology and Medicine., doi:10.1146/annurev.anchem.1.031207.112754 *Annual Review of Analytical Chemistry*, **1**: 883-909.

[4] Diaspro, A., and Robello, M. (1999). Multi-photon Excitation Microscopy to Study Biosystems. European Microscopy and Analysis., 5:5-7.

[5] D.S. Mantus and G. H. Morrison. 1991. Chemical imaging in biology and medicine using ion microscopy., *Microchimica Acta*, **104**, (1-6) January 1991, doi: 10.1007/BF01245536

[6] Bagatolli, L.A., and Gratton, E. (2000). Two-photon fluorescence microscopy of coexisting lipid domains in giant unilamellar vesicles of binary phospholipid mixtures. Biophys J., 78:290-305.

[7] Schwille, P., Haupts, U., Maiti, S., and Webb. W.(1999). Molecular dynamics in living cells observed by fluorescence correlation spectroscopy with one- and two-photon excitation. Biophysical Journal, 77(10):2251-2265.

[8] 1.Lee, S. C. et al., (2001). One Micrometer Resolution NMR Microscopy. J. Magn. Res., 150: 207-213.

[9] Near Infrared Microspectroscopy, Fluorescence Microspectroscopy,Infrared Chemical Imaging and High Resolution Nuclear Magnetic Resonance Analysis of Soybean Seeds, Somatic Embryos and Single Cells., Baianu, I.C. et al. 2004., In *Oil Extraction and Analysis.*, D. Luthria, Editor pp.241-273, AOCS Press., Champaign, IL.
[10] Single Cancer Cell Detection by Near Infrared Microspectroscopy, Infrared Chemical Imaging and Fluorescence Microspectroscopy.2004.I. C. Baianu, D. Costescu, N. E. Hofmann and S. S. Korban, q-bio/0407006 (July 2004) (http://arxiv.org/abs/q-bio/0407006)
[11] J. Dubois, G. Sando, E. N. Lewis, Near-Infrared Chemical Imaging, A Valuable Tool for the Pharmaceutical Industry, G.I.T. Laboratory Journal Europe, No. 1-2, 2007.
[12] http://witec.de/en/download/Raman/ImagingMicroscopy04.pdf
[13] Raghavachari, R., Editor. 2001. *Near-Infrared Applications in Biotechnology*, Marcel-Dekker, New York, NY.
[14] Applications of Novel Techniques to Health Foods, Medical and Agricultural Biotechnology.(June 2004) I. C. Baianu, P. R. Lozano, V. I. Prisecaru and H. C. Lin q-bio/0406047 (http://arxiv.org/abs/q-bio/0406047)
[15] http://www.spectroscopyeurope.com/NIR_14_3.pdf
[16] http://www.fda.gov/cder/OPS/PAT.htm
[17] Eigen, M., and Rigler, R. (1994). Sorting single molecules: Applications to diagnostics and evolutionary biotechnology, Proc. Natl. Acad. Sci. USA 91:5740.
[18] Rigler R. and Widengren J. (1990). Ultrasensitive detection of single molecules by fluorescence correlation spectroscopy, *BioScience* (Ed. Klinge & Owman) p.180.
[19] Single Cancer Cell Detection by Near Infrared Microspectroscopy, Infrared Chemical Imaging and Fluorescence Microspectroscopy.2004.I. C. Baianu, D. Costescu, N. E. Hofmann, S. S. Korban and et al., q-bio/0407006 (July 2004) (http://arxiv.org/abs/q-bio/0407006)
[20] Oehlenschläger F., Schwille P. and Eigen M. (1996). Detection of HIV-1 RNA by nucleic acid sequence-based amplification combined with fluorescence correlation spectroscopy, *Proc. Natl. Acad. Sci. USA* **93**:1281.
[21] Near Infrared Microspectroscopy, Fluorescence Microspectroscopy,Infrared Chemical Imaging and High Resolution Nuclear Magnetic Resonance Analysis of Soybean Seeds, Somatic Embryos and Single Cells., Baianu, I.C. et al. 2004., In *Oil Extraction and Analysis.*, D. Luthria, Editor pp.241-273, AOCS Press., Champaign, IL.
[22] M. Chamberland, V. Farley, A. Vallières, L. Belhumeur, A. Villemaire, J. Giroux et J. Legault, High-Performance Field-Portable Imaging Radiometric Spectrometer Technology For Hyperspectral imaging Applications, Proc. SPIE 5994, 59940N, September 2005.
[23] Novel Techniques for Microspectroscopy and Chemical Imaging Analysis of Soybean Seeds and Embryos.(2002). Baianu, I.C., Costescu, D.M., and You, T. *Soy2002 Conference*, Urbana, Illinois.
[24] Near Infrared Microspectroscopy, Chemical Imaging and NMR Analysis of Oil in Developing and Mutagenized Soybean Embryos in Culture. (2003). Baianu, I.C., Costescu, D.M., Hofmann, N., and Korban, S.S. *AOCS Meeting, Analytical Division*.
[25] Near Infrared Microspectroscopy, Fluorescence Microspectroscopy,Infrared Chemical Imaging and High Resolution Nuclear Magnetic Resonance Analysis of Soybean Seeds, Somatic Embryos and Single Cells., Baianu, I.C. et al. 2004., In *Oil Extraction and Analysis.*, D. Luthria, Editor pp.241-273, AOCS Press., Champaign, IL.

Further reading

1. E. N. Lewis, P. J. Treado, I. W. Levin, Near-Infrared and Raman Spectroscopic Imaging, American Laboratory, 06/1994:16 (1994)
2. E. N. Lewis, P. J. Treado, R. C. Reeder, G. M. Story, A. E. Dowrey, C. Marcott, I. W. Levin, FTIR spectroscopic imaging using an infrared focal-plane array detector, Analytical Chemistry, 67:3377 (1995)
3. P. Colarusso, L. H. Kidder, I. W. Levin, J. C. Fraser, E. N. Lewis Infrared Spectroscopic Imaging: from Planetary to Cellular Systems, Applied Spectroscopy, 52 (3):106A (1998)
4. P. J. Treado I. W. Levin, E. N. Lewis, Near-Infrared Spectroscopic Imaging Microscopy of Biological Materials Using an Infrared Focal-Plane Array and an Acousto-Optic Tunable Filter (AOTF), Applied Spectroscopy, 48:5 (1994)
5. Hammond, S.V., Clarke, F. C., Near-infrared microspectroscopy. In: Handbook of Vibrational Spectroscopy, Vol. 2, J.M. Chalmers and P.R. Griffiths Eds. John Wiley and Sons, West Sussex, UK, 2002, p.1405-1418

6. L.H. Kidder, A.S. Haka, E.N. Lewis, Instrumentation for FT-IR Imaging. In: Handbook of Vibrational Spectroscopy, Vol. 2, J.M. Chalmers and P.R. Griffiths Eds. John Wiley and Sons, West Sussex, UK, 2002, pp.1386-1404
7. J. Zhang; A. O'Connor; J. F. Turner II, Cosine Histogram Analysis for Spectral Image Data Classification,Applied Spectroscopy, Volume 58, Number 11, November 2004, pp. 1318-1324(7)
8. J. F. Turner II; J. Zhang; A. O'Connor, A Spectral Identity Mapper for Chemical Image Analysis, Applied Spectroscopy, Volume 58, Number 11, November 2004, pp. 1308-1317(10)
9. H. R. MORRIS, J. F. TURNER II, B. MUNRO, R. A. RYNTZ, P. J. TREADO, Chemical imaging of thermoplastic olefin (TPO) surface architecture, Langmuir, 1999, vol. 15, no8, pp. 2961-2972
10. J. F. Turner II, Chemical imaging and spectroscopy using tunable filters: Instrumentation, methodology, and multivariate analysis, Thesis (PhD). UNIVERSITY OF PITTSBURGH, Source DAI-B 59/09, p. 4782, Mar 1999, 286 pages.
11. P. Schwille.(2001). in *Fluorescence Correlation Spectroscopy. Theory and applications.* R. Rigler & E.S. Elson, eds., p. 360. Springer Verlag: Berlin.
12. Schwille P., Oehlenschläger F. and Walter N. (1996). Analysis of RNA-DNA hybridization kinetics by fluorescence correlation spectroscopy, *Biochemistry* **35**:10182.
13. FLIM | Fluorescence Lifetime Imaging Microscopy: Fluorescence, fluorophore chemical imaging, confocal emission microspectroscopy, FRET, cross-correlation fluorescence microspectroscopy (http://www.nikoninstruments.com/infocenter.php?n=FLIM).
14. FLIM Applications: (http://www.nikoninstruments.com/infocenter.php?n=FLIM) "FLIM is able to discriminate between fluorescence emanating from different fluorophores and autoflorescing molecules in a specimen, even if their emission spectra are similar. It is, therefore, ideal for identifying fluorophores in multi-label studies. FLIM can also be used to measure intracellular ion concentrations without extensive calibration procedures (for example, Calcium Green) and to obtain information about the local environment of a fluorophore based on changes in its lifetime." FLIM is also often used in microspectroscopic/chemical imaging, or microscopic, studies to monitor spatial and temporal protein-protein interactions, properties of membranes and interactions with nucleic acids in living cells.
15. Gadella TW Jr., *FRET and FLIM techniques*, 33. Imprint: Elsevier, ISBN 978-0-08-054958-3. (2008) 560 pages
16. Langel FD, et al., Multiple protein domains mediate interaction between Bcl10 and Malt1, *J. Biol. Chem.*, (2008) 283(47):32419-31
17. Clayton AH. , The polarized AB plot for the frequency-domain analysis and representation of fluorophore rotation and resonance energy homotransfer. J *Microscopy*. (2008) 232(2):306-12
18. Clayton AH, et al., Predominance of activated EGFR higher-order oligomers on the cell surface. *Growth Factors* (2008) 20:1
19. Plowman et al., Electrostatic Interactions Positively Regulate K-Ras Nanocluster Formation and Function. *Molecular and Cellular Biology* (2008) 4377–4385
20. Belanis L, et al., Galectin-1 Is a Novel Structural Component and a Major Regulator of H-Ras Nanoclusters. *Molecular Biology of the Cell* (2008) 19:1404–1414
21. Van Manen HJ, Refractive index sensing of green fluorescent proteins in living cells using fluorescence lifetime imaging microscopy. Biophys J. (2008) 94(8):L67-9

22. Van der Krogt GNM, et al., A Comparison of Donor-Acceptor Pairs for Genetically Encoded FRET Sensors: Application to the Epac cAMP Sensor as an Example, PLoS ONE, (2008) 3(4):e1916
23. Dai X, et al., Fluorescence intensity and lifetime imaging of free and micellar-encapsulated doxorubicin in living cells. *Nanomedicine*. (2008) **4**(1):49-56.

External links

- NIR Chemical Imaging in Pharmaceutical Industry (http://www.spectroscopyeurope.com/NIR_14_3.pdf)
- Pharmaceutical Process Analytical Technology: (http://www.fda.gov/cder/OPS/PAT.htm)
- NIR Chemical Imaging for Counterfeit Pharmaceutical Product Analysis (http://www.spectroscopymag.com/spectroscopy/Near-IR+Spectroscopy/NIR-Chemical-Imaging-for-Counterfeit-Pharmaceutica/ArticleStandard/Article/detail/406629)
- Chemical Imaging: Potential New Crime Busting Tool (http://www.sciencedaily.com/releases/2007/08/070802103435.htm)
- Chemical Imaging Without Dyeing (http://witec.de/en/download/Raman/ImagingMicroscopy04.pdf) - Chemical Imaging Without Dyeing

Hyperspectral imaging

Hyperspectral imaging collects and processes information from across the electromagnetic spectrum. Unlike the human eye, which just sees visible light, hyperspectral imaging is more like the eyes of the mantis shrimp, which can see visible light as well as from the ultraviolet to infrared. Hyperspectral capabilities enable the mantis shrimp to recognize different types of coral, prey, or predators, all which may appear as the same color to the human eye.

Humans build sensors and processing systems to provide the same type of capability for application in agriculture, mineralogy, physics, and surveillance. Hyperspectral sensors look at objects using a vast portion of the electromagnetic spectrum. Certain objects leave unique 'fingerprints' across the electromagnetic spectrum. These 'fingerprints' are known as spectral signatures and enable identification of the materials that make up a scanned object. For example, having the spectral signature for oil helps mineralogists find new oil fields.

Acquisition and Analysis

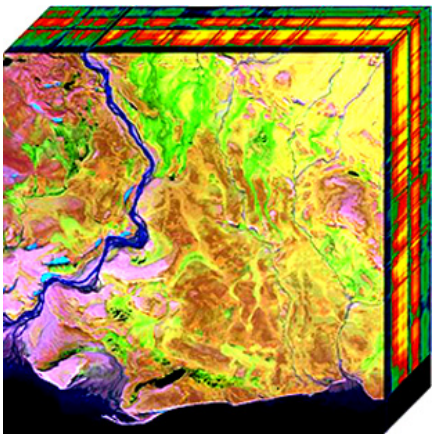

Example of a hyperspectral cube

Hyperspectral sensors collect information as a set of 'images'. Each image represents a range of the electromagnetic spectrum and is also known as a spectral band. These 'images' are then combined and form a three dimensional hyperspectral cube for processing and analysis.

Hyperspectral cubes are generated from airborne sensors like the NASA's *Airborne Visible/Infrared Imaging Spectrometer* (AVIRIS), or from satellites like NASA's Hyperion.[1] However, for many development and validation studies handheld sensors are used.[2]

The precision of these sensors is typically measured in spectral resolution, which is the width of each band of the spectrum that is captured. If the scanner picks up on a large number of fairly narrow frequency bands, it is possible to identify objects even if said objects are only captured in a handful of pixels. However, spatial resolution is a factor in addition to spectral resolution. If the pixels are too large, then multiple objects are captured in the same pixel and become difficult to identify. If the pixels are too small, then the energy captured by each sensor-cell is low, and the decreased signal-to-noise ratio reduces the reliability of measured features.

MicroMSI, Opticks and Envi are three remote sensing applications that support the processing and analysis of hyperspectral data. The acquisition and processing of hyperspectral images is also referred to as imaging spectroscopy.

Differences between Hyperspectral and Multispectral

Hyperspectral Imaging is part of a class of techniques commonly referred to as spectral imaging or spectral analysis. Hyperspectral Imaging is related to multispectral imaging. The distinction between hyperspectral and multispectral is usually defined as the number of spectral bands. Multispectral data contains from tens to hundreds of bands. Hyperspectral data contains hundreds to thousands of bands. However, hyperspectral imaging may be best defined by the manner in which the data is collected. Hyperspectral data is a set of contiguous bands (usually by one sensor). Multispectral is a set of optimally chosen spectral bands that are typically not contiguous and can be collected from multiple sensors.

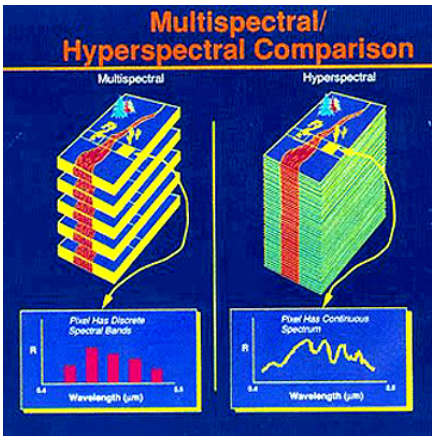

Hyperspectral and Multispectral Differences.

Applications

Hyperspectral remote sensing is used in a wide array of real-life applications. Although originally developed for mining and geology (The ability of hyperspectral imaging to identify various minerals makes it ideal for the mining and oil industries, where it can be used to look for ore and oil[2] [3] it has now spread into fields as wide-spread as ecology and surveillance, as well as historical manuscript research such as the imaging of the Archimedes Palimpsest. This technology is continually becoming more available to the public, and has been used in a wide variety of ways. Organizations such as NASA and the USGS have catalogues of various minerals and their spectral signatures, and have posted them online to make them readily available for researchers.

Agriculture

Although the costs of acquiring hyperspectral images is typically high, for specific crops and in specific climates hyperspectral remote sensing is used more and more for monitoring the development and health of crops. In Australia work is underway to use imaging spectrometers to detect grape variety, and develop an early warning system for disease outbreaks.[4] Furthermore work is underway to use hyperspectral data to detect the chemical composition of plants[5] which can be used to detect the nutrient and water status of wheat in irrigated systems[6]

Mineralogy

The original field of development for hyperspectral remote sensing, hyperspectral sensing of minerals is now well developed. Many minerals can be identified from images, and their relation to the presence of valuable minerals such as gold and diamonds is well understood. Currently the move is towards understanding the relation between oil and gas leakages from pipelines and natural wells; their effect on the vegetation and the spectral signatures. Recent work includes the PhD dissertations of Werff[7] and Noomen[8] .

Physics

Physicists use an electron microscopy technique that involves microanalysis using either Energy dispersive X-ray spectroscopy (EDS), Electron energy loss spectroscopy (EELS), Infrared Spectroscopy(IR), Raman Spectroscopy, or cathodoluminescence (CL) spectroscopy, in which the entire spectrum measured at each point is recorded. EELS hyperspectral imaging is performed in a scanning transmission electron microscope (STEM); EDS and CL mapping can be performed in STEM as well, or in a scanning electron microscope or electron probe microanalyzer (EPMA). Often, multiple techniques (EDS, EELS, CL) are used simultaneously.

In a "normal" mapping experiment, an image of the sample will be made that is simply the intensity of a particular emission mapped in an XY raster. For example, an EDS map could be made of a steel sample, in which iron x-ray intensity is used for the intensity grayscale of the image. Dark areas in the image would indicate not-iron-bearing impurities. This could potentially give misleading results; if the steel contained tungsten inclusions, for example, the high atomic number of tungsten could result in bremsstrahlung radiation that made the iron-free areas *appear* to be rich in iron.

By hyperspectral mapping, instead, the entire spectrum at each mapping point is acquired, and a quantitative analysis can be performed by computer post-processing of the data, and

a quantitative map of iron content produced. This would show which areas contained no iron, despite the anomalous x-ray counts caused by bremsstrahlung. Because EELS core-loss edges are small signals on top of a large background, hyperspectral imaging allows large improvements to the quality of EELS chemical maps.

Similarly, in CL mapping, small shifts in the peak emission energy could be mapped, which would give information regarding slight chemical composition changes or changes in the stress state of a sample.

Surveillance

Hyperspectral surveillance is the implementation of hyperspectral scanning technology for surveillance purposes. Hyperspectral imaging is particularly useful in military surveillance because of measures that military entities now take to avoid airborne surveillance. Airborne surveillance has been in effect since soldiers used tethered balloons to spy on troops during the American Civil War, and since that time we have learned not only to hide from the naked eye, but to mask our heat signature to blend in to the surroundings and avoid infrared scanning, as well. The idea that drives hyperspectral surveillance is that hyperspectral scanning draws information from such a large portion of the light spectrum that any given object should have unique spectral signature in at least a few of the many bands that get scanned.[1]

Advantages and Disadvantages

The primary advantages to hyperspectral imaging is that, because an entire spectrum is acquired at each point, the operator needs no a priori knowledge of the sample, and post-processing allows all available information from the dataset to be mined.

The primary disadvantages are cost and complexity. Fast computers, sensitive detectors, and large data storage capacities are needed for analyzing hyperspectral data. Significant data storage capacity is necessary since hyperspectral cubes are large multi-dimensional datasets, potentially exceeding hundreds of megabytes. All of these factors greatly increase the cost of acquiring and processing hyperspectral data. Also, one of the hurdles that researchers have had to face is finding ways to program hyperspectral satellites to sort through data on their own and transmit only the most important images, as both transmission and storage of that much data could prove difficult and costly.[1] As a relatively new analytical technique, the full potential of hyperspectral imaging has not yet been realized.

See also

- Airborne Real-time Cueing Hyperspectral Enhanced Reconnaissance
- Full Spectral Imaging
- Multi-spectral image
- → Chemical imaging
- Remote Sensing
- Sensor fusion

External Links

ITT Visual Information Solutions - ENVI Hyperspectral Image Processing Software [9]

References

[1] Schurmer, J.H., (Dec 2003) *Hyperspectral imaging from space (http://www.afrlhorizons.com/Briefs/Dec03/VS0302.html)*, Air Force Research Laboratories Technology Horizons

[2] Ellis, J., (Jan 2001) *Searching for oil seeps and oil-impacted soil with hyperspectral imagery (http://www.eomonline.com/Common/currentissues/Jan01/ellis.htm),* Earth Observation Magazine.

[3] Smith, R.B. (July 14, 2006), *Introduction to hyperspectral imaging with TMIPS (http://www.microimages.com/getstart/pdf/hyprspec.pdf)*, MicroImages Tutorial Web site

[4] Lacar, F.M., et al., *Use of hyperspectral imagery for mapping grape varieties in the Barossa Valley, South Australia (http://hdl.handle.net/2440/39292)*, Geoscience and remote sensing symposium (IGARSS'01) - IEEE 2001 International, vol.6 2875-2877p. doi: 10.1109/IGARSS.2001.978191 (http://dx.doi.org/10.1109/IGARSS.2001.978191)

[5] Ferwerda, J.G. (2005), *Charting the quality of forage: measuring and mapping the variation of chemical components in foliage with hyperspectral remote sensing (http://www.itc.nl/library/Papers_2005/phd/ferwerda.pdf)*, Wageningen University , ITC Dissertation 126, 166p. ISBN 90-8504-209-7

[6] Tilling, A.K., et al., (2006) *Remote sensing to detect nitrogen and water stress in wheat (http://www.regional.org.au/au/asa/2006/plenary/technology/4584_tillingak.htm)*, The Australian Society of Agronomy

[7] Werff H. (2006), *Knowledge based remote sensing of complex objects: recognition of spectral and spatial patterns resulting from natural hydrocarbon seepages (http://www.itc.nl/library/papers_2006/phd/vdwerff.pdf)*, Utrecht University, ITC Dissertation 131, 138p. ISBN 90-6164-238-8

[8] Noomen, M.F. (2007), *Hyperspectral reflectance of vegetation affected by underground hydrocarbon gas seepage (http://www.itc.nl/library/papers_2007/phd/noomen.pdf)*, Enschede, ITC 151p. ISBN 978-90-8504-671-4.

[9] http://www.ittvis.com/ProductServices/ENVI.aspx

FT-IR

1. REDIRECT → Fourier transform spectroscopy

CARS

Coherent anti-Stokes Raman spectroscopy, also called Coherent anti-Stokes Raman scattering spectroscopy (CARS), is a form of spectroscopy used primarily in chemistry, physics and related fields. It is sensitive to the same vibrational signatures of molecules as seen in Raman spectroscopy, typically the nuclear vibrations of chemical bonds. Unlike Raman spectroscopy, CARS employs multiple photons to address the molecular vibrations, and produces a signal in which the emitted waves are coherent with one another. As a result, CARS is orders of magnitude stronger than spontaneous Raman emission. CARS is a third-order nonlinear optical process involving three laser beams: a pump beam of frequency ω_p, a Stokes beam of frequency ω_S and a probe beam at frequency ω_{pr}. These beams interact with the sample and generate a coherent optical signal at the anti-Stokes frequency (ω_p-ω_S+ω_{pr}). The latter is resonantly enhanced when the frequency difference between the pump and the Stokes beams (ω_p-ω_S) coincides with the frequency of a Raman resonance, which is the basis of the technique's intrinsic vibrational contrast mechanism.[1] [2]

History

The acronym CARS, which invokes a seemingly inadvertent relation to automobiles, is actually closely related to the birth story of the technique. In 1965, a paper was published by two researchers of the Scientific Laboratory at the Ford Motor Company, P. D. Maker and R. W. Terhune, in which the CARS phenomenon was reported for the first time.[3] Maker and Terhune used a pulsed ruby laser to investigate the third order response of several materials. They first passed the ruby beam of frequency ω through a Raman shifter to create a second beam at ω-ω_v, and then directed the two beams simultaneously onto the sample. When the pulses from both beams overlapped in space and time, the Ford researchers observed a signal at ω+ω_v, which is the blue-shifted CARS signal. They also demonstrated that the signal increases significantly when the difference frequency ω_v between the incident beams matches a Raman frequency of sample. Maker and Terhune called their technique simply 'three wave mixing experiments'. The name coherent anti-Stokes Raman spectroscopy was assigned almost ten years later, by Begley et al. at Stanford University in 1974.[4] Since then, this vibrationally sensitive nonlinear optical technique is commonly known as CARS.

Principle

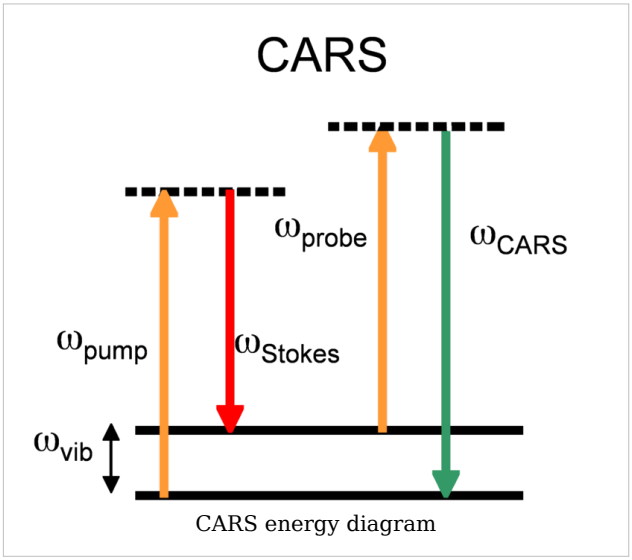

CARS energy diagram

The CARS process can be physically explained by using either a classical oscillator model or by using a quantum mechanical model that incorporates the energy levels of the molecule. Classically, the Raman active vibrator is modeled as a (damped) harmonic oscillator with a characteristic frequency of ω_v. In CARS, this oscillator is not driven by a single optical wave, but by the difference frequency (ω_p-ω_S) between the pump and the Stokes beams instead. This driving mechanism is similar to hearing the low combination tone when striking two different high tone piano keys: your ear is sensitive to the difference frequency of the high tones. Similarly, the Raman oscillator is susceptible to the difference frequency of two optical waves. When the difference frequency ω_p-ω_S approaches ω_v, the oscillator is driven very efficiently. On a molecular level, this implies that the electron cloud surrounding the chemical bond is vigorously oscillating with the frequency ω_p-ω_S. These electron motions alter the optical properties of the sample, i.e. there is a periodic modulation of the refractive index of the material. This periodic modulation can be probed by a third laser beam, the probe beam. When the probe beam is propagating through the periodically altered medium, it acquires the same modulation. Part of the probe, originally at ω_{pr} will now get modified to ω_{pr}+ω_p-ω_S, which is the observed anti-Stokes emission. Under certain beam geometries, the anti-Stokes emission may diffract away from the probe beam, and can be detected in a separate direction.

While intuitive, this classical picture does not take into account the quantum mechanical energy levels of the molecule. Quantum mechanically, the CARS process can be understood as follows. Our molecule is initially in the ground state, the lowest energy state of the molecule. The pump beam excites the molecule to a virtual state. A virtual state is not an eigenstate of the molecule, rather it exhibits an infinitely short lifetime, and thus the molecule cannot remain in this state. If a Stokes beam is simultaneously present along with the pump, the virtual state can be used as an instantaneous gateway to address a vibrational eigenstate of the molecule. The joint action of the pump and the Stokes has effectively established a coupling between the ground state and the vibrationally excited state of the molecule. The molecule is now in two states at the same time: it resides in a coherent superposition of states. This coherence between the states can be probed by the probe beam, which promotes the system to a virtual state. Again, the molecule cannot stay in the virtual state and will fall back instantaneously to the ground state under the emission of a photon at the anti-Stokes frequency. The molecule is no longer in a superposition, as it resides again in one state, the ground state. In the quantum mechanical model, no energy is deposited in the molecule during the CARS process. Instead, the molecule acts like a medium for converting the frequencies of the three incoming waves into a CARS signal (a parametric process). There are, however, related coherent Raman process that occur simultaneously which do deposit energy into the molecule.

Comparison to Raman spectroscopy

CARS is often compared to Raman spectroscopy as both techniques probe the same Raman active modes. Raman can be done using a single CW laser whereas CARS requires (generally) two pulsed laser sources. The Raman signal is detected on the red side of the incoming radiation where it might have to compete with other fluorescent processes. The CARS signal is detected on the blue side, which is free from fluorescence, but it comes with a non-resonant contribution. The differences between the signals from Raman and CARS (there are many variants of both techniques) stems largely from the fact that Raman relies on a spontaneous transition whereas CARS relies on a coherently driven transition. The total Raman signal collected from a sample is the incoherent addition of the signal from individual molecules. It is therefore linear in the concentration of those molecules and the signal is emitted in all directions. The total CARS signal comes from a coherent addition of the signal from individual molecules. For the coherent addition to be additive, phase-matching must be fulfilled. For tight focusing conditions this is generally not a restriction. Once phase-matching is fulfilled the signal amplitude grows linear with distance so that the power grows quadratically. This signal forms a collimated beam that is therefore easily collected. The fact that the CARS signal is quadratic in the distance makes it quadratic with respect to the concentration and therefore especially sensitive to the majority constituent. The total CARS signal also contains an inherent non-resonant background. This non-resonant signal can be considered as the result of (several) far off-resonance transitions that also add coherently. The resonant amplitude contains a phase shift of Pi over the resonance whereas the non-resonant part does not. The spectral line shape of the CARS intensity therefore resembles a Fano-profile which is shifted with respect to the Raman signal. To compare the spectra from multi-component compounds, the (resonant) CARS spectral amplitude should be compared to the Raman spectral intensity.

Theoretically Raman spectroscopy and CARS spectroscopy are equally sensitive as they use the same molecular transitions. However, given the limits on input power (damage threshold) and detector noise (integration time), the signal from a single transition can be collected much faster in practical situation (a factor of 10^5) using CARS. Imaging of known substances (known spectra) is therefore often done using CARS. Given the fact that CARS is a higher order nonlinear process, the CARS signal from a single molecule is larger than the Raman signal from a single molecule for a sufficiently high driving intensity. However at very low concentrations, the advantages of the coherent addition for CARS signal reduces and the presence of the incoherent background becomes an increasing problem.

Since CARS is such a nonlinear process there are not really any 'typical' experimental numbers. One example is given below under the explicit warning that just changing the pulse duration by one order of magnitude changes the CARS signal by three orders of magnitude. The comparison should only be used as an indication of the order of magnitude of the signals. 200 mW average power input (CW for the Raman), in a 0.9NA objective with a center wavelength around 800 nm, constitutes a power density of 26 MW/cm,^{2} (focal length = 1.5 micrometre, focal volume = 1.16 micrometre^3, photon energy = 2.31 10^{-19} J or 1.44 eV). The Raman cross section for the vibration of the aromatic ring in Toluene around 1000 cm^{-1} is on the order of 10^{-29}cm^2/molecule*steradian. Therefore the Raman signal is around 26 10^{-22} W/molecule*steradian or 3.3 10^{-21} W/molecule (over 4Pi). That is 0.014 photon/sec*molecule. The density of Toluene = 0.8668 10^3 kg/m^3, Molecular mass = 92.14 10^{-3} kg/mol. Therefore the focal volume (~1 cubic micrometre) contains 6 10^9 molecules.

Those molecules together generate a Raman signal in the order of 2 10^{-11} W (20pW) or roughly one hundred million photons/sec (over a 4Pi solid angle). A CARS experiment with similar parameters (150 mW at 1064 nm, 200 mW at 803.5 nm, 15ps pulses at 80Mhz repetition frequency, same objective lens) yields roughly 17.5 10^{-6} W (on the 3000 cm^{-1} line, which has 1/3 of the strength and roughly 3 times the width). This CARS power is roughly 10^{6} higher than the Raman but since there are 6 10^{9} molecules, the signal per molecule from CARS is only 4 10^{-25} W/molecule*sec or 1.7 10^{-6} photons/molecule*sec. If we allow for two factors of three (line strength and line width) than the spontaneous Raman signal per molecule still exceeds the CARS per molecule by a more than two orders of magnitude. The coherent addition of the CARS signal from the molecules however yields a total signal that is much higher than the Raman.

The sensitivity in many CARS experiments is not limited by the detection of CARS photons but rather by the distinction between the resonant and non-resonant part of the CARS signal.

Applications

CARS is used for species selective microscopy and combustion diagnostics. The first exploits the selectivity of vibrational spectroscopy whereas the latter is aimed at temperature measurements; the CARS signal is temperature dependent. The strength of the signal scales with the difference in the ground state population and the vibrationally excited state population. Since the population of states follows the temperature dependent Bose-Einstein Distribution, the CARS signal carries an intrinsic temperature dependence as well. This temperature dependence makes CARS a popular technique for monitoring the temperature of hot gases and flames.

See also

- Coherent Stokes Raman spectroscopy
- Raman spectroscopy
- Four-wave mixing

References

[1] A Review of the Theory and Application of Coherent Anti-Stokes Raman Spectroscopy (CARS) Applied Spectroscopy, Volume 31, Number 4, July/August 1977, pp. 253-271(19) (http://www.ingentaconnect.com/content/sas/sas/1977/00000031/00000004/art00001)

[2] Coherent anti-Stokes Raman scattering: from proof-of-the-principle experiments to femtosecond CARS and higher order wave-mixing generalizations Journal of Raman Spectroscopy, Volume 31, Issue 8-9 , pp. 653 - 667 (http://www3.interscience.wiley.com/cgi-bin/abstract/73500427/ABSTRACT?CRETRY=1&SRETRY=0)

[3] Study of Optical Effects Due to an Induced Polarization Third Order in the Electric Field Strength Physical Review, Volume 137, Issue 3A, pp. 801-818 (http://prola.aps.org/abstract/PR/v137/i3A/pA801_1)

[4] Coherent anti-Stokes Raman spectroscopy Applied Physics Letters, Volume 25, Issue 7 , pp. 387-390 (http://scitation.aip.org/getabs/servlet/GetabsServlet?prog=normal&id=APPLAB000025000007000387000001&idtype=cvips&gifs=yes)

Fluorescence microscopy

1. REDIRECT Fluorescence microscope

Fluorescence correlation spectroscopy

Fluorescence correlation spectroscopy (**FCS**) is a common technique used by physicists, chemists, and biologists to experimentally characterize the dynamics of fluorescent species (e.g. single fluorescent dye molecules in nanostructured materials, autofluorescent proteins in living cells, etc.). Although the name indicates a specific link to fluorescence, the method is used today also for exploring other forms of luminescence (like reflections, luminescence from gold-beads or quantum dots or phosphorescent species). The "spectroscopy" in the name is not readily found as in common usage a spectrum is generally understood to be a frequency spectrum. The autocorrelation is a genuine form of spectrum, however: It is the time-spectrum generated from the power spectrum (via inverse fourier transform).

Commonly, FCS is employed in the context of optical microscopy, in particular confocal or two photon microscopy. In these techniques light is focused on a sample and the measured fluorescence intensity fluctuations (due to diffusion, physical or chemical reactions, aggregation, etc.) are analyzed using the temporal autocorrelation. Because the measured property is essentially related to the magnitude and/or the amount of fluctuations, there is an optimum measurement regime at the level when individual species enter or exit the observation volume (or turn on and off in the volume). When too many entities are measured at the same time the overall fluctuations are small in comparison to the total signal and may not be resolvable - in the other direction, if the individual fluctuation-events are too sparse in time, one measurement may take prohibitively too long. FCS is in a way the fluorescent counterpart to dynamic light scattering, which uses coherent light scattering, instead of (incoherent) fluorescence.

When an appropriate model is known, FCS can be used to obtain quantitative information such as

- diffusion coefficients
- hydrodynamic radii
- average concentrations
- kinetic chemical reaction rates
- singlet-triplet dynamics

Because fluorescent markers come in a variety of colors and can be specifically bound to a particular molecule (e.g. proteins, polymers, metal-complexes, etc.), it is possible to study the behavior of individual molecules (in rapid succession in composite solutions). With the development of sensitive detectors such as avalanche photodiodes the detection of the fluorescence signal coming from individual molecules in highly dilute samples has become practical. With this emerged the possibility to conduct FCS experiments in a wide variety of specimens, ranging from materials science to biology. The advent of engineered cells with genetically tagged proteins (like green fluorescent protein) has made FCS a common tool for studying molecular dynamics in living cells.

History

Signal-correlation techniques have first been experimentally applied to fluorescence in 1972 by Magde, Elson, and Webb[1] , who are therefore commonly credited as the "inventors" of FCS. The technique was further developed in a group of papers by these and other authors soon after, establishing the theoretical foundations and types of applications.[2] [3] [4] See Thompson (1991)[5] for a review of that period.

Beginning in 1993[6] , a number of improvements in the measurement techniques--notably using confocal microscopy, and then two photon microscopy--to better define the measurement volume and reject background greatly improved the signal-to-noise and allowed single molecule sensitivity.[7] [8] Since then, there has been a renewed interest in FCS, and as of August 2007 there has been over 3,000 papers using FCS found in Web of Science. See Krichevsky and Bonnet[9] for a recent review. In addition, there has been a flurry of activity extending FCS in various ways, for instance to laser scanning and spinning disk confocal microscopy (from a stationary, single point measurement), in using cross-correlation (FCCS) between two fluorescent channels instead of autocorrelation, and in using Förster Resonance Energy Transfer (FRET) instead of fluorescence.

Typical FCS setup

The typical FCS setup consists of a laser line (wavelengths ranging typically from 405 - 633 nm (cw), and from 690 - 1100 nm (pulsed)), which is reflected into a microscope objective by a dichroic mirror. The laser beam is focused in the sample, which contains fluorescent particles (molecules) in such high dilution, that only few are within the focal spot (usually 1 - 100 molecules in one fL). When the particles cross the focal volume, they fluoresce. This light is collected by the same objective and, because it is red-shifted with respect to the excitation light it passes the dichroic reaching a detector, typically a photomultiplier tube or avalanche photodiode detector. The resulting electronic signal can be stored either directly as an intensity versus time trace to be analyzed at a later point, or, computed to generate the autocorrelation directly (which requires special acquisition cards). The FCS curve by itself only represents a time-spectrum. Conclusions on physical phenomena have to be extracted from there with appropriate models. The parameters of interest are found after fitting the autocorrelation curve to modeled functional forms. [10] The setup is shown in Figure 1.

The Measurement Volume

The measurement volume is a convolution of illumination (excitation) and detection geometries, which result from the optical elements involved. The resulting volume is described mathematically by the point spread function (or PSF), it is essentially the image of a point source. The PSF is often described as an ellipsoid (with unsharp boundaries) of few hundred nanometers in focus diameter, and almost one micrometre along the optical axis. The shape varies significantly (and has a large impact on the resulting FCS curves) depending on the quality of the optical elements (it is crucial to avoid astigmatism and to check the real shape of the PSF on the instrument). In the case of confocal microscopy, and for small pinholes (around one Airy unit), the PSF is well approximated by Gaussians:

$$PSF(r,z) = I_0 e^{-2r^2/\omega_{xy}^2} e^{-2z^2/\omega_z^2}$$

where I_0 is the peak intensity, r and z are radial and axial position, and ω_{xy} and ω_z are the radial and axial radii, and $\omega_z > \omega_{xy}$. This Gaussian form is assumed in deriving the functional form of the autocorrelation.

Typically ω_{xy} is 200-300 nm, and ω_z is **2-6** times larger.[11] One common way of calibrating the measurement volume parameters is to perform FCS on a species with known diffusion coefficient and concentration (see below). Diffusion coefficients for common fluorophores in water are given in a later section.

The Gaussian approximation works to varying degrees depending on the optical details, and corrections can sometimes be applied to offset the errors in approximation.[12]

Autocorrelation Function

The (temporal) autocorrelation function is the correlation of a time series with itself shifted by time τ, as a function of τ:

$$G(\tau) = \frac{\langle \delta I(t) \delta I(t+\tau) \rangle}{\langle I(t) \rangle^2} = \frac{\langle I(t) I(t+\tau) \rangle}{\langle I(t) \rangle^2} - 1$$

where $\delta I(t) = I(t) - \langle I(t) \rangle$ is the deviation from the mean intensity. The normalization (denominator) here is the most commonly used for FCS, because then the correlation at $\tau = 0$, *G*(0), is related to the average number of particles in the measurement volume.

Interpreting the Autocorrelation Function

To extract quantities of interest, the autocorrelation data can be fitted, typically using a nonlinear least squares algorithm. The fit's functional form depends on the type of dynamics (and the optical geometry in question).

Normal Diffusion

The fluorescent particles used in FCS are small and thus experience thermal motions in solution. The simplest FCS experiment is thus normal 3D diffusion, for which the autocorrelation is:

$$G(\tau) = G(0) \frac{1}{(1 + (\tau/\tau_D))(1 + a^{-2}(\tau/\tau_D))^{1/2}} + G(\infty)$$

where $a = \omega_z / \omega_{xy}$ is the ratio of axial to radial e^{-2} radii of the measurement volume, and τ_D is the characteristic residence time. This form was derived assuming a Gaussian measurement volume. Typically, the fit would have three free parameters--G(0), $G(\infty)$, and τ_D--from which the diffusion coefficient and fluorophore concentration can be obtained.

With the normalization used in the previous section, G(0) gives the mean number of diffusers in the volume <N>, or equivalently--with knowledge of the observation volume size--the mean concentration:

$$G(0) = \frac{1}{< N >} = \frac{1}{V_{eff} < C >},$$

where the effective volume is found from integrating the Gaussian form of the measurement volume and is given by:

$$V_{eff} = \pi^{3/2} \omega_{xy}^2 \omega_z.$$

τ_D gives the diffusion coefficient: $D = \omega_{xy}^2 / 4\tau_D$.

Anomalous diffusion

If the diffusing particles are hindered by obstacles or pushed by a force (molecular motors, flow, etc.) the dynamics is often not sufficiently well-described by the normal diffusion model, where the mean squared displacement (MSD) grows linearly with time. Instead the diffusion may be better described as anomalous diffusion, where the temporal dependenc of the MSD is non-linear as in the power-law:

$$MSD = 6D_a t^{\alpha}$$

where D_a is an anomalous diffusion coefficient. "Anomalous diffusion" commonly refers only to this very generic model, and not the many other possibilities that might be described as anomalous. Also, a power law is, in a strict sense, the expected form only for a narrow range of rigorously defined systems, for instance when the distribution of obstacles is fractal. Nonetheless a power law can be a useful approximation for a wider range of systems.

The FCS autocorrelation function for anomalous diffusion is:

$$G(\tau) = G(0)\frac{1}{(1+(\tau/\tau_D)^{\alpha})(1+a^{-2}(\tau/\tau_D)^{\alpha})^{1/2}} + G(\infty),$$

where the anomalous exponent α is the same as above, and becomes a free parameter in the fitting.

Using FCS, the anomalous exponent has been shown to be an indication of the degree of molecular crowding (it is less than one and smaller for greater degrees of crowding)[13] .

Polydisperse diffusion

If there are diffusing particles with different sizes (diffusion coefficients), it is common to fit to a function that is the sum of single component forms:

$$G(\tau) = G(0)\sum_i \frac{\alpha_i}{(1+(\tau/\tau_{D,i}))(1+a^{-2}(\tau/\tau_{D,i}))^{1/2}} + G(\infty)$$

where the sum is over the number different sizes of particle, indexed by i, and α_i gives the weighting, which is related to the quantum yield and concentration of each type. This introduces new parameters, which makes the fitting more difficult as a higher dimensional space must be searched. Nonlinear least square fitting typically becomes unstable with even a small number of $\tau_{D,i}$s. A more robust fitting scheme, especially useful for polydisperse samples, is the Maximum Entropy Method[14] .

Diffusion with flow

With diffusion together with a uniform flow with velocity v in the lateral direction, the autocorrelation is[15] :

$$G(\tau) = G(0)\frac{1}{(1+(\tau/\tau_D))(1+a^{-2}(\tau/\tau_D))^{1/2}} \times \exp[-(\tau/\tau_v)^2 \times \frac{1}{1+\tau/\tau_D}] + G(\infty)$$

where $\tau_v = \omega_{xy}/v$ is the average residence time if there is only a flow (no diffusion).

Chemical relaxation

A wide range of possible FCS experiments involve chemical reactions that continually fluctuate from equilibrium because of thermal motions (and then "relax"). In contrast to diffusion, which is also a relaxation process, the fluctuations cause changes between states of different energies. One very simple system showing chemical relaxation would be a stationary binding site in the measurement volume, where particles only produce signal when bound (e.g. by FRET, or if the diffusion time is much faster than the sampling interval). In this case the autocorrelation is:

$$G(\tau) = G(0)\exp(-\tau/\tau_B) + G(\infty)$$

where

$$\tau_B = (k_{on} + k_{off})^{-1}$$

is the relaxation time and depends on the reaction kinetics (on and off rates), and:

$$G(0) = \frac{1}{\langle N \rangle}\frac{k_{on}}{k_{off}} = \frac{1}{\langle N \rangle}K$$

is related to the equilibrium constant K.

Most systems with chemical relaxation also show measureable diffusion as well, and the autocorrelation function will depend on the details of the system. If the diffusion and chemical reaction are decoupled, the combined autocorrelation is the product of the chemical and diffusive autocorrelations.

Triplet State Correction

The autocorrelations above assume that the fluctuations are not due to changes in the fluorescent properties of the particles. However, for the majority of (bio)organic fluorophores--e.g. green fluorescent protein, rhodamine, Cy3 and Alexa Fluor dyes--some fraction of illuminated particles are excited to a triplet state (or other non-radiative decaying states) and then do not emit photons for a characteristic relaxation time τ_F. Typically τ_F is on the order of microseconds, which is usually smaller than the dynamics of interest (e.g. τ_D) but large enough to be measured. A multiplicative term is added to the autocorrelation account for the triplet state. For normal diffusion:

$$G(\tau) = G(0)\frac{1 - F + Fe^{-\tau/\tau_F}}{1 - F}\frac{1}{(1 + (\tau/\tau_{D,i}))(1 + a^{-2}(\tau/\tau_{D,i}))^{1/2}} + G(\infty)$$

where F is the fraction of particles that have entered the triplet state and τ_F is the corresponding triplet state relaxation time. If the dynamics of interest are much slower than the triplet state relaxation, the short time component of the autocorrelation can simply be truncated and the triplet term is unnecessary.

Common fluorescent probes

The fluorescent species used in FCS is typically a biomolecule of interest that has been tagged with a fluorophore (using immunohistochemistry for instance), or is a naked fluorophore that is used to probe some environment of interest (e.g. the cytoskeleton of a cell). The following table gives diffusion coefficients of some common fluorophores in water at room temperature, and their excitation wavelengths.

Fluorescent dye	D (x10^{-10} m^2 s^{-1})	Excitation wavelength (nm)	Reference

Rhodamine 6G	2.8, 3.0, 4.14 ± 0.05 @ 25.00 °C	514	[16], [17], [18]
Rhodamine 110	2.7	488	[19]
Tetramethyl rhodamine	2.6	543	
Cy3	2.8	543	
Cy5	2.5, 3.7 ± 0.15 @ 25.00 °C	633	[20], [21]
carboxyfluorescein	3.2	488	
Alexa-488	1.96	488	[22]
Atto655-maleimide	4.07 ± 0.1 @ 25.00 °C	663	[23]
Atto655-carboxylicacid	4.26 ± 0.08 @ 25.00 °C	663	[24]
2′, 7′-difluorofluorescein (Oregon Green488)	4.11 ± 0.06 @ 25.00 °C	498	[25]

Variations of FCS

FCS almost always refers to the single point, single channel, temporal autocorrelation measurement, although the term "fluorescence correlation spectroscopy" out of its historical scientific context implies no such restriction. FCS has been extended in a number of variations by different researchers, with each extension generating another name (usually an acronym).

Fluorescence Cross-Correlation Spectroscopy (FCCS)

FCS is sometimes used to study molecular interactions using differences in diffusion times (e.g. the product of an association reaction will be larger and thus have larger diffusion times than the reactants individually); however, FCS is relatively insensitive to molecular mass as can be seen from the following equation relating molecular mass to the diffusion time of globular particles (e.g. proteins):

$$\tau_D = \frac{3\pi\omega_{xy}^2\eta}{2kT}(M)^{1/3}$$

where η is the viscosity of the sample and M is the molecular mass of the fluorescent species. In practice, the diffusion times need to be sufficiently different--a factor of at least **1.6**--which means the molecular masses must differ by a factor of **4**.[26] Dual color → fluorescence cross-correlation spectroscopy (FCCS) measures interactions by cross-correlating two or more fluorescent channels (one channel for each reactant), which distinguishes interactions more sensitively than FCS, particularly when the mass change in the reaction is small.

Two-and three-photon FCS excitation

Several advantages in both spatial resolution and minimizing photodamage/photobleaching in organic and/or biological samples are obtained by two-photon or three-photon excitation FCS[27] [28] [29] [30] [31] .

FRET-FCS

Another FCS based approach to studying molecular interactions uses → fluorescence resonance energy transfer (FRET) instead of fluorescence, and is called FRET-FCS.[32] With FRET, there are two types of probes, as with FCCS; however, there is only one channel and light is only detected when the two probes are very close--close enough to ensure an interaction. The FRET signal is weaker than with fluorescence, but has the advantage that there is only signal during a reaction (aside from autofluorescence).

Image Correlation Spectroscopy (ICS)

When the motion is slow (in biology, for example, diffusion in a membrane), getting adequate statistics from a single-point FCS experiment may take a prohibitively long time. More data can be obtained by performing the experiment in multiple spatial points in parallel, using a laser scanning confocal microscope. This approach has been called Image Correlation Spectroscopy (ICS)[33] . The measurements can then be averaged together.

Another variation of ICS performs a spatial autocorrelation on images, which gives information about the concentration of particles[34] . The correlation is then averaged in time.

A natural extension of the temporal and spatial correlation versions is spatio-temporal ICS (STICS) [35] . In STICS there is no explicit averaging in space or time (only the averaging inherent in correlation). In systems with non-isotropic motion (e.g. directed flow, asymmetric diffusion), STICS can extract the directional information. A variation that is closely related to STICS (by the Fourier transform) is k-space Image Correlation Spectroscopy (kICS).[36]

There are cross-correlation versions of ICS as well.[33]

Scanning FCS variations

Some variations of FCS are only applicable to serial scanning laser microscopes. Image Correlation Spectroscopy and its variations all were implemented on a scanning confocal or scanning two photon microscope, but transfer to other microscopes, like a spinning disk confocal microscope. Raster ICS (RICS)[37] , and position sensitive FCS (PSFCS)[38] incorporate the time delay between parts of the image scan into the analysis. Also, low dimensional scans (e.g. a circular ring)[39] --only possible on a scanning system--can access time scales between single point and full image measurements. Scanning path has also been made to adaptively follow particles.[40]

Spinning disk FCS, and spatial mapping

Any of the image correlation spectroscopy methods can also be performed on a spinning disk confocal microscope, which in practice can obtain faster imaging speeds compared to a laser scanning confocal microscope. This approach has recently been applied to diffusion in a spatially varying complex environment, producing a pixel resolution map of diffusion coefficient.[41] . The spatial mapping of diffusion with FCS has subsequently been extended to TIRF system.[42] Spatial mapping of dynamics using correlation techniques had been applied before, but only at sparse points[43] or at coarse resolution[35] .

Total internal reflection FCS

Total internal reflection fluorescence (TIRF) is a microscopy approach that is only sensitive to a thin layer near the surface of a coverslip, which greatly minimizes background fluorscence. FCS has been extended to that type of microscope, and is called TIR-FCS[44] . Because the fluorescence intensity in TIRF falls off exponentially with distance from the coverslip (instead of as a Gaussian with a confocal), the autocorrelation function is different.

Other fluorescent dynamical approaches

There are two main non-correlation alternatives to FCS that are widely used to study the dynamics of fluorescent species.

Fluorescence recovery after photobleaching (FRAP)

In FRAP, a region is briefly exposed to intense light, irrecoverably photobleaching fluorophores, and the fluorescence recovery due to diffusion of nearby (non-bleached) fluorophores is imaged. A primary advantage of FRAP over FCS is the ease of interpreting qualitative experiments common in cell biology. Differences between cell lines, or regions of a cell, or before and after application of drug, can often be characterized by simple inspection of movies. FCS experiments require a level of processing and are more sensitive to potentially confounding influences like: rotational diffusion, vibrations, photobleaching, dependence on illumination and fluorescence color, inadequate statistics, etc. It is much easier to change the measurement volume in FRAP, which allows greater control. In practice, the volumes are typically larger than in FCS. While FRAP experiments are typically more qualitative, some researchers are studying FRAP quantitatively and including binding dynamics.[45] A disadvantage of FRAP in cell biology is the free radical perturbation of the cell caused by the photobleaching. It is also less versatile, as it cannot measure concentration or rotational diffusion, or co-localization. FRAP requires a significantly higher concentration of fluorophores than FCS.

Particle tracking

In particle tracking, the trajectories of a set of particles are measured, typically by applying particle tracking algorithms to movies.[46] Particle tracking has the advantage that all the dynamical information is maintained in the measurement, unlike FCS where correlation averages the dynamics to a single smooth curve. The advantage is apparent in systems showing complex diffusion, where directly computing the mean squared displacement allows straightforward comparison to normal or power law diffusion. To apply particle tracking, the particles have to be distinguishable and thus at lower concentration than

required of FCS. Also, particle tracking is more sensitive to noise, which can sometimes affect the results unpredictably.

References

[1] Magde, D., Elson, E. L., Webb, W. W. Thermodynamic fluctuations in a reacting system: Measurement by fluorescence correlation spectroscopy,(1972) *Phys Rev Lett*, **29**,705-708.

[2] Ehrenberg, M., Rigler, R. Rotational brownian motion and fluorescence intensity fluctuations,(1974) *Chem Phys*, **4**,390-401.

[3] Elson, E. L., Magde, D. Fluorescence correlation spectroscopy I. Conceptual basis and theory,(1974) *Biopolymers*, **13**,1-27.

[4] Magde, D., Elson, E. L., Webb, W. W. Fluorescence correlation spectroscopy II. An experimental realization,(1974) *Biopolymers*, **13**,29-61.

[5] Thompson N L 1991 Topics in Fluorescence Spectroscopy Techniques vol 1, ed J R Lakowicz (New York: Plenum) pp 337–78

[6] Rigler, R, Ü. Mets1, J. Widengren and P. Kask. Fluorescence correlation spectroscopy with high count rate and low background: analysis of translational diffusion. European Biophysics Journal (1993) 22(3), 159.

[7] Eigen, M., Rigler, M. Sorting single molecules: application to diagnostics and evolutionary biotechnology,(1994) *Proc. Natl. Acad. Sci. USA*, **91**,5740-5747.

[8] Rigler, M. Fluorescence correlations, single molecule detection and large number screening. Applications in biotechnology,(1995) *J. Biotechnol.*, **41**,177-186.

[9] O. Krichevsky, G. Bonnet, "Fluorescence correlation spectroscopy: the technique and its applications," Rep. Prog. Phys. 65, 251-297 (2002).

[10] Medina, M. A., Schwille, P. Fluorescence correlation spectroscopy for the detection and study of single molecules in biology, (2002)*BioEssays*, **24**,758-764.

[11] Mayboroda, O. A., van Remoortere, A., Tanke H. J., Hokke, C. H., Deelder, A. M., A new approach for fluorescence correlation spectroscopy (FCS) based immunoassays, (2003), *J. Biotechnol.*, **107**, 185-192.

[12] Hess, S.T., and W.W. Webb. 2002. Focal volume optics and experimental artifacts in confocal fluorescence correlation spectroscopy. Biophys. J. 83:2300-2317.

[13] Banks, D. S., and C. Fradin. 2005. Anomalous diffusion of proteins due to molecular crowding. Biophys. J. 89:2960–2971.

[14] Sengupta, P., K. Garai, J. Balaji, N. Periasamy, and S. Maiti. 2003. Measuring Size Distribution in Highly Heterogeneous Systems with Fluorescence Correlation Spectroscopy. Biophys. J. 84(3):1977-1984.

[15] Kohler, R.H., P. Schwille, W.W. Webb, and M.R. Hanson. 2000. Active protein transport through plastid tubules: velocity quantified by fluorescence correlation spectroscopy. J Cell Sci 113(22):3921-3930

[16] Magde, D., Elson, E. L., Webb, W. W. Fluorescence correlation spectroscopy II. An experimental realization,(1974) *Biopolymers*, **13**,29-61.

[17] Berland, K. M. Detection of specific DNA sequences using dual-color two-photon fluorescence correlation spectroscopy. (2004),*J. Biotechnol* ,**108(2)**, 127-136.

[18] Müller, C.B., Loman, A., Pacheco, V., Koberling, F., Willbold, D., Richtering, W., Enderlein, J. Precise measurement of diffusion by multi-color dual-focus fluorescence correlation spectroscopy (2008), *EPL*, **83**, 46001.

[19] Pristinski, D., Kozlovskaya, V., Sukhishvili, S. A. Fluorescence correlation spectroscopy studies of diffusion of a weak polyelectrolyte in aqueous solutions. (2005), *J. Chem. Phys.*, **122**, 014907.

[20] Widengren, J., Schwille, P., Characterization of photoinduced isomerization and back-isomerization of the cyanine dye Cy5 by fluorescence correlation spectroscopy. (2000), *J. Phys. Chem. A*, **104**, 6416-6428.

[21] Loman, A., Dertinger, T., Koberling, F., Enderlein, J. Comparison of optical saturation effects in conventional and dual-focus fluorescence correlation spectroscopy (2008), *Chem. Phys. Lett.*, **459**, 18–21.

[22] Pristinski, D., Kozlovskaya, V., Sukhishvili, S. A. Fluorescence correlation spectroscopy studies of diffusion of a weak polyelectrolyte in aqueous solutions. (2005), *J. Chem. Phys.*, **122**, 014907.

[23] Müller, C.B., Loman, A., Pacheco, V., Koberling, F., Willbold, D., Richtering, W., Enderlein, J. Precise measurement of diffusion by multi-color dual-focus fluorescence correlation spectroscopy (2008), *EPL*, **83**, 46001.

[24] Müller, C.B., Loman, A., Pacheco, V., Koberling, F., Willbold, D., Richtering, W., Enderlein, J. Precise measurement of diffusion by multi-color dual-focus fluorescence correlation spectroscopy (2008), *EPL*, **83**, 46001.

[25] Müller, C.B., Loman, A., Pacheco, V., Koberling, F., Willbold, D., Richtering, W., Enderlein, J. Precise measurement of diffusion by multi-color dual-focus fluorescence correlation spectroscopy (2008), *EPL*, **83**, 46001.

[26] Meseth, U., Wohland, T., Rigler, R., Vogel, H. Resolution of fluorescence correlation measurements. (1999) *Biophys. J.*, **76**, 1619-1631.
[27] Diaspro, A., and Robello, M. (1999). Multi-photon Excitation Microscopy to Study Biosystems. European Microscopy and Analysis., 5:5-7.
[28] Bagatolli, L.A., and Gratton, E. (2000). Two-photon fluorescence microscopy of coexisting lipid domains in giant unilamellar vesicles of binary phospholipid mixtures. Biophys J., 78:290-305.
[29] Schwille, P., Haupts, U., Maiti, S., and Webb. W.(1999). Molecular dynamics in living cells observed by fluorescence correlation spectroscopy with one- and two- photon excitation. *Biophysical Journal*, **77**(10):2251-2265.
[30] Near Infrared Microspectroscopy, Fluorescence Microspectroscopy,Infrared Chemical Imaging and High Resolution Nuclear Magnetic Resonance Analysis of Soybean Seeds, Somatic Embryos and Single Cells., Baianu, I.C. et al. 2004., In *Oil Extraction and Analysis.*, D. Luthria, Editor pp.241-273, AOCS Press., Champaign, IL.
[31] Single Cancer Cell Detection by Near Infrared Microspectroscopy, Infrared Chemical Imaging and Fluorescence Microspectroscopy.2004.I. C. Baianu, D. Costescu, N. E. Hofmann and S. S. Korban, q-bio/0407006 (July 2004) (http://arxiv.org/abs/q-bio/0407006)
[32] K. Remaut, B. Lucas, K. Braeckmans, N.N. Sanders, S.C. De Smedt and J. Demeester, FRET-FCS as a tool to evaluate the stability of oligonucleotide drugs after intracellular delivery, J Control Rel 103 (2005) (1), pp. 259–271.
[33] Wiseman, P. W., J. A. Squier, M. H. Ellisman, and K. R. Wilson. 2000. Two-photon video rate image correlation spectroscopy (ICS) and image cross-correlation spectroscopy (ICCS). J. Microsc. 200:14–25.
[34] Petersen, N. O., P. L. Ho¨ddelius, P. W. Wiseman, O. Seger, and K. E. Magnusson. 1993. Quantitation of membrane receptor distributions by image correlation spectroscopy: concept and application. Biophys. J. 65:1135–1146.
[35] Hebert, B., S. Constantino, and P. W. Wiseman. 2005. Spatio-temporal image correlation spectroscopy (STICS): theory, verification and application to protein velocity mapping in living CHO cells. Biophys. J. 88:3601–3614.
[36] Kolin, D.L., D. Ronis, and P.W. Wiseman. 2006. k-Space Image Correlation Spectroscopy: A Method for Accurate Transport Measurements Independent of Fluorophore Photophysics. Biophys. J. 91(8):3061-3075.
[37] Digman, M.A., P. Sengupta, P.W. Wiseman, C.M. Brown, A.R. Horwitz, and E. Gratton. 2005. Fluctuation Correlation Spectroscopy with a Laser-Scanning Microscope: Exploiting the Hidden Time Structure. Biophys. J. 88(5):L33-36.
[38] Skinner, J.P., Y. Chen, and J.D. Mueller. 2005. Position-Sensitive Scanning Fluorescence Correlation Spectroscopy. Biophys. J.:biophysj.105.060749.
[39] Ruan, Q., M.A. Cheng, M. Levi, E. Gratton, and W.W. Mantulin. 2004. Spatial-temporal studies of membrane dynamics: scanning fluorescence correlation spectroscopy (SFCS). Biophys. J. 87:1260–1267.
[40] A. Berglund and H. Mabuchi, "Tracking-FCS: Fluorescence correlation spectroscopy of individual particles," Opt. Express 13, 8069-8082 (2005).
[41] Sisan, D.R., R. Arevalo, C. Graves, R. McAllister, and J.S. Urbach. 2006. Spatially resolved fluorescence correlation spectroscopy using a spinning disk confocal microscope. Biophysical Journal 91(11):4241-4252.
[42] Kannan, B., L. Guo, T. Sudhaharan, S. Ahmed, I. Maruyama, and T. Wohland. 2007. Spatially resolved total internal reflection fluorescence correlation microscopy using an electron multiplying charge-coupled device camera. Analytical Chemistry 79(12):4463-4470
[43] Wachsmuth, M., W. Waldeck, and J. Langowski. 2000. Anomalous diffusion of fluorescent probes inside living cell nuclei investigated by spatially-resolved fluorescence correlation spectroscopy. J. Mol. Biol. 298(4):677-689.
[44] Lieto, A.M., and N.L. Thompson. 2004. Total Internal Reflection with Fluorescence Correlation Spectroscopy: Nonfluorescent Competitors. Biophys. J. 87(2):1268-1278.
[45] Sprague, B.L., and J.G. McNally. 2005. FRAP analysis of binding: proper and fitting. Trends in Cell Biology 15(2):84-91.
[46] http://www.physics.emory.edu/~weeks/idl/

See also

- → Confocal microscopy
- → Fluorescence cross-correlation spectroscopy
- FRET
- Dynamic light scattering
- Diffusion coefficient

External links

- Single-molecule spectroscopic methods (http://dx.doi.org/10.1016/j.sbi.2004.09.004)
- FCS Classroom (http://www.fcsxpert.com/classroom)

Fluorescence cross-correlation spectroscopy

Fluorescence cross-correlation spectroscopy (FCCS) was introduced by Eigen and Rigler in 1994 and experimentally realized by Schwille in 1997. It extends the → fluorescence correlation spectroscopy (FCS) procedure by introducing high sensitivity for distinguishing fluorescent particles which have a similar diffusion coefficient. FCCS uses two species which are independently labelled with two spectrally separated fluorescent probes. These fluorescent probes are excited and detected by two different laser light sources and detectors commonly known as green and red respectively. Both laser light beams are focused into the sample and tuned so that they overlap to form a superimposed confocal observation volume.

The normalized cross-correlation function is defined for two fluorescent species G and R which are independent green, G and red, R channels as follows:

$$G_{GR}(\tau) = 1 + \frac{< \delta I_G(t) \delta I_R(t+\tau) >}{< I_G(t) >< I_R(t) >} = \frac{< I_G(t) I_R(t+\tau) >}{< I_G(t) >< I_R(t) >}$$

where differential fluorescent signals δI_G at a specific time, t and δI_R at a delay time, τ later is correlated with each other.

Modeling

Cross-correlation curves are modeled according to a slightly more complicated mathematical function than applied in FCS. First of all, the effective superimposed observation volume in which the G and R channels form a single observation volume, $V_{eff,RG}$ in the solution:

$$V_{eff,RG} = \pi^{3/2} (\omega_{xy,G}^2 + \omega_{xy,R}^2)(\omega_{z,G}^2 + \omega_{z,R}^2)^{1/2} / 2^{3/2}$$

where $\omega_{xy,G}^2$ and $\omega_{xy,R}^2$ are radial parameters and $\omega_{z,G}$ and $\omega_{z,R}$ are the axial parameters for the G and R channels respectively.
The diffusion time, $\tau_{D,GR}$ for a doubly (G and R) fluorescent species is therefore described as follows:

$$\tau_{D,GR} = \frac{\omega_{xy,G}^2 + \omega_{xy,R}^2}{8D_{GR}}$$

where D_{GR} is the diffusion coefficient of the doubly fluorescent particle.

The cross-correlation curve generated from diffusing doubly labelled fluorescent particles can be modelled in separate channels as follows:

$$G_G(\tau) = 1 + \frac{(< C_G > Diff_k(\tau) + < C_{GR} > Diff_k(\tau))}{V_{eff,GR}(< C_G > + < C_{GR} >)^2}$$

$$G_R(\tau) = 1 + \frac{(< C_R > Diff_k(\tau) + < C_{GR} > Diff_k(\tau))}{V_{eff,GR}(< C_R > + < C_{GR} >)^2}$$

In the ideal case, the cross-correlation function is proportional to the concentration of the doubly labeled fluorescent complex:

$$G_{GR}(\tau) = 1 + \frac{< C_{GR} > Diff_{GR}(\tau)}{V_{eff}(< C_G > + < C_{GR} >)(< C_R > + < C_{GR} >)}$$

with $Diff_k(\tau) = \frac{1}{(1 + \frac{\tau}{\tau_{D,i}})(1 + a^{-2}(\frac{\tau}{\tau_{D,i}})^{1/2}}$

Contrary to FCS, the intercept of the cross-correlation curve does not yield information about the doubly labelled fluorescent particles in solution.

See also

- → Fluorescence correlation spectroscopy
- Dynamic light scattering
- Fluorescence spectroscopy
- Diffusion coefficient

External links

- FCS Classroom [1]

References

[1] http://www.fcsxpert.com/classroom

Fluorescence resonance energy transfer

Förster resonance energy transfer (abbreviated **FRET**), also known as **fluorescence resonance energy transfer**, **resonance energy transfer** (**RET**) or **electronic energy transfer** (**EET**), is a mechanism describing energy transfer between two chromophores.

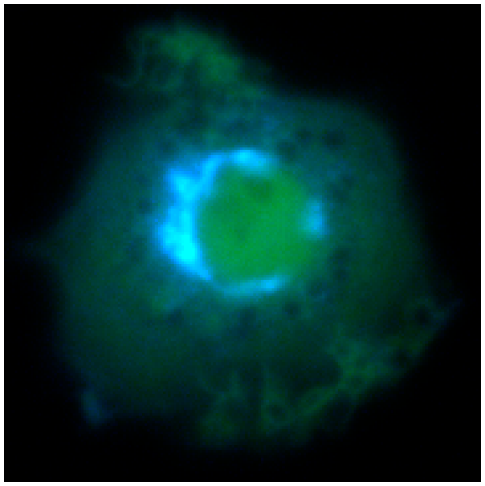

Fluorescently-labeled guanosine 5'-triphosphate hydrolase ARF reveals the protein's localization in the Golgi apparatus of a living macrophage. FRET studies revealed ARF activation in the Golgi and in the formation of phagosomes.[1]

A donor chromophore, intially in its electronic excited state, may transfer energy to an acceptor chromophore (in close proximity, typically <10nm) through nonradiative dipole-dipole coupling. This mechanism is termed "Förster resonance energy transfer" and is named after the German scientist Theodor Förster.[2] When both chromophores are fluorescent, the term "fluorescence resonance energy transfer" is often used instead, although the energy is not actually transferred by fluorescence.[3],[4] In order to avoid an erroneous interpretation of the phenomenon that (even when occurring between two fluorescent chromophores) is always a nonradiative transfer of energy, the name "Förster resonance energy transfer" is preferred to "fluorescence resonance energy transfer" - although the latter enjoys common usage in scientific literature. FRET is analogous to Near Field Communication, in that the radius of interaction is much smaller than the wavelength of light emitted. In the near field region, the excited chromophore emits a virtual photon that is instantly absorbed by a receiving chromophore. These virtual photons are undetectable, since their existence violates the conservation of energy and momentum, and hence FRET is known as a radiationless mechanism. From quantum electrodynamical calculations, it is determined that radiationless (FRET) and radiative energy transfer are the short- and long-range asymptotes of a single unified mechanism.[5],[6]

Theoretical basis

The FRET efficiency (E) is the quantum yield of the energy transfer transition, *i.e.* the fraction of energy transfer event occurring per donor excitation event:

$$E = \frac{k_{ET}}{k_f + k_{ET} + \sum k_i}$$

where k_{ET} is the rate of energy transfer, k_f the radiative decay rate and the k_i are the rate constants of any other de-excitation pathway.
The FRET efficiency depends on many parameters that can be grouped as follows:

- The distance between the donor and the acceptor
- The spectral overlap of the donor emission spectrum and the acceptor absorption spectrum.
- The relative orientation of the donor emission dipole moment and the acceptor absorption dipole moment.

E depends on the donor-to-acceptor separation distance r with an inverse 6th power law due to the dipole-dipole coupling mechanism:

$$E = \frac{1}{1 + (r/R_0)^6}$$

with R_0 being the Förster distance of this pair of donor and acceptor i.e. the distance at which the energy transfer efficiency is 50%. The Förster distance depends on the overlap integral of the donor emission spectrum with the acceptor absorption spectrum and their mutual molecular orientation as expressed by the following equation:

$${R_0}^6 = \frac{9\,Q_0\,(\ln 10)\kappa^2\,J}{128\,\pi^5\,n^4\,N_A}$$

where Q_0 is the fluorescence quantum yield of the donor in the absence of the acceptor, κ^2 is the dipole orientation factor, n is the refractive index of the medium, N_A is Avogadro's_number, and J is the spectral overlap integral calculated as

$$J = \int f_{\mathrm{D}}(\lambda)\,\epsilon_{\mathrm{A}}(\lambda)\,\lambda^4\,d\lambda$$

where f_{D} is the normalized donor emission spectrum, and ϵ_{A} is the acceptor molar extinction coefficient. κ^2 =2/3 is often assumed. This value is obtained when both dyes are freely rotating and can be considered to be isotropically oriented during the excited state lifetime. If either dye is fixed or not free to rotate, then κ^2 =2/3 will not be a valid assumption. In most cases, however, even modest reorientation of the dyes results in enough orientational averaging that κ^2 = 2/3 does not result in a large error in the estimated energy transfer distance due to the sixth power dependence of R_0 on κ^2. Even when κ^2 is quite different from 2/3 the error can be associated with a shift in R_0 and thus determinations of changes in relative distance for a particular system are still valid. Fluorescent proteins do not reorient on a timescale that is faster than their fluorescence lifetime. In this case $0 \le \kappa^2 \le 4$.
The FRET efficiency relates to the quantum yield and the fluorescence lifetime of the donor molecule as follows:

$$E = 1 - \tau'_{\mathrm{D}}/\tau_{\mathrm{D}}$$

where τ'_{D} and τ_{D} are the donor fluorescence lifetimes in the presence and absence of an acceptor, respectively, or as

$$E = 1 - F'_{\mathrm{D}}/F_{\mathrm{D}}$$

where F'_{D} and F_{D} are the donor fluorescence intensities with and without an acceptor, respectively.

Methods

In fluorescence microscopy, fluorescence confocal laser scanning microscopy, as well as in molecular biology, FRET is a useful tool to quantify molecular dynamics in biophysics and biochemistry, such as protein-protein interactions, protein-→ DNA interactions, and protein conformational changes. For monitoring the complex formation between two molecules, one of them is labeled with a donor and the other with an acceptor, and these fluorophore-labeled molecules are mixed. When they are dissociated, the donor emission is detected upon the donor excitation. On the other hand, when the donor and acceptor are in proximity (1-10 nm) due to the interaction of the two molecules, the acceptor emission is predominantly observed because of the intermolecular FRET from the donor to the acceptor. For monitoring protein conformational changes, the target protein is labeled with a donor and an acceptor at two loci. When a twist or bend of the protein brings the change in the distance or relative orientation of the donor and acceptor, FRET change is observed. If a molecular interaction or a protein conformational change is dependent on ligand binding, this FRET technique is applicable to fluorescent indicators for the ligand detection.

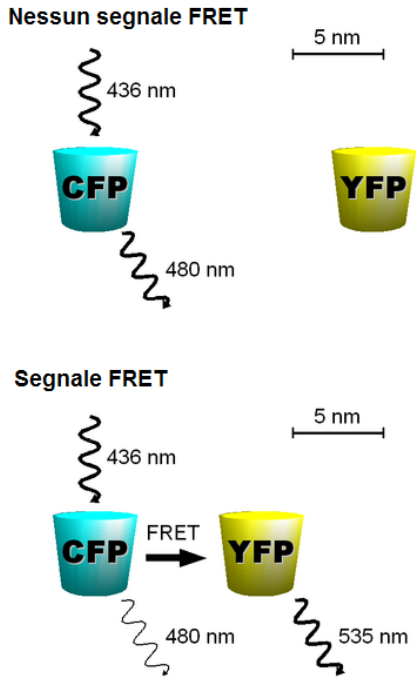

Example of FRET between CFP and YFP (Wavelength vs. Absorption): a fusion protein containing CFP and YFP excited at 440nm wavelength. The fluorescent emission peak of CFP overlaps the excitation peak of YFP. Because the two proteins are adjacent to each other, the energy transfer is significant–a large proportion of the energy from CFP is transferred to YFP and creates a much larger YFP emission peak.

FRET studies are scalable: the extent of energy transfer is often quantified from the milliliter scale of cuvette-based experiments to the femtoliter scale of microscopy-based experiments. This quantification can be based directly (sensitized emission method) on detecting two emission channels under two different excitation conditions (primarily donor and primarily acceptor). However, for robustness reasons, FRET quantification is most often based on measuring changes in fluorescence intensity or fluorescence lifetime upon changing the experimental conditions (e.g. a microscope image of donor emission is taken with the acceptor being present. The acceptor is then bleached, such that it is incapable of accepting energy transfer and another donor emission image is acquired. A pixel-based quantification using the second equation in the theory section above is then possible.) An alternative way of temporarily deactivating the acceptor is based on its fluorescence saturation. Exploiting polarisation characteristics of light, a FRET quantification is also possible with only a single camera exposure.

CFP-YFP pairs

The most popular FRET pair for biological use is a cyan fluorescent protein (**CFP**)-yellow fluorescent protein (**YFP**) pair. Both are color variants of green fluorescent protein (GFP). While labeling with organic fluorescent dyes requires troublesome processes of purification, chemical modification, and intracellular injection of a host protein, GFP variants can be easily attached to a host protein by genetic engineering. By virtue of GFP variants, the use of FRET techniques for biological research is becoming more and more popular.

BRET

A limitation of FRET is the requirement for external illumination to initiate the fluorescence transfer, which can lead to background noise in the results from direct excitation of the acceptor or to photobleaching. To avoid this drawback, Bioluminescence Resonance Energy Transfer (or **BRET**) has been developed. This technique uses a bioluminescent luciferase (typically the luciferase from *Renilla reniformis*) rather than CFP to produce an initial photon emission compatible with YFP.

FRET and BRET are also the common tools in the study of biochemical reaction kinetics and molecular motors.

Photobleaching FRET

FRET efficiencies can also be inferred from the photobleaching rates of the donor in the presence and absence of an acceptor. This method can be performed on most fluorescence microscopes; one simply shines the excitation light (of a frequency that will excite the donor but not the acceptor significantly) on specimens with and without the acceptor fluorophore and monitors the donor fluorescence (typically separated from acceptor fluorescence using a bandpass filter) over time. The timescale is that of photobleaching, which is seconds to minutes, with fluorescence in each curve being given by

$$(\text{background}) + (\text{constant}) * e^{-(\text{time})/\tau_{\text{pb}}}$$

where τ_{pb} is the photobleaching decay time constant and depends on whether the acceptor is present or not. Since photobleaching consists in the permanent inactivation of excited fluorophores, resonance energy transfer from an excited donor to an acceptor fluorophore prevents the photobleaching of that donor fluorophore, and thus high FRET efficiency leads to a longer photobleaching decay time constant:

$$E = 1 - \tau_{\text{pb}}/\tau'_{\text{pb}}$$

where τ'_{pb} and τ_{pb} are the photobleaching decay time constants of the donor in the presence and in the absence of the acceptor, respectively. (Notice that the fraction is the reciprocal of that used for lifetime measurements).

This technique was introduced by Jovin in 1989.[7] Its use of an entire curve of points to extract the time constants can give it accuracy advantages over the other methods. Also, the fact that time measurements are over seconds rather than nanoseconds makes it easier than fluorescence lifetime measurements, and because photobleaching decay rates do not generally depend on donor concentration (unless acceptor saturation is an issue), the careful control of concentrations needed for intensity measurements is not needed. It is, however, important to keep the illumination the same for the with- and without-acceptor measurements, as photobleaching increases markedly with more intense incident light.

Other methods

A different, but related, mechanism is Dexter Electron Transfer.

An alternative method to detecting protein-protein proximity is BiFC where two halves of a YFP are fused to a protein (Hu, Kerppola et al. 2002). When these two halves meet they form a fluorophore after about 60 s - 1 hr.

Applications

FRET has been applied in an experimental method for the detection of phosgene. In it, phosgene or rather triphosgene as a safe substitute serves as a linker between an acceptor and a donor coumarine (forming urea groups).[8] The presence of phosgene is detected at $5x10^{-5}$M with a typical FRET emission at 464 nm.

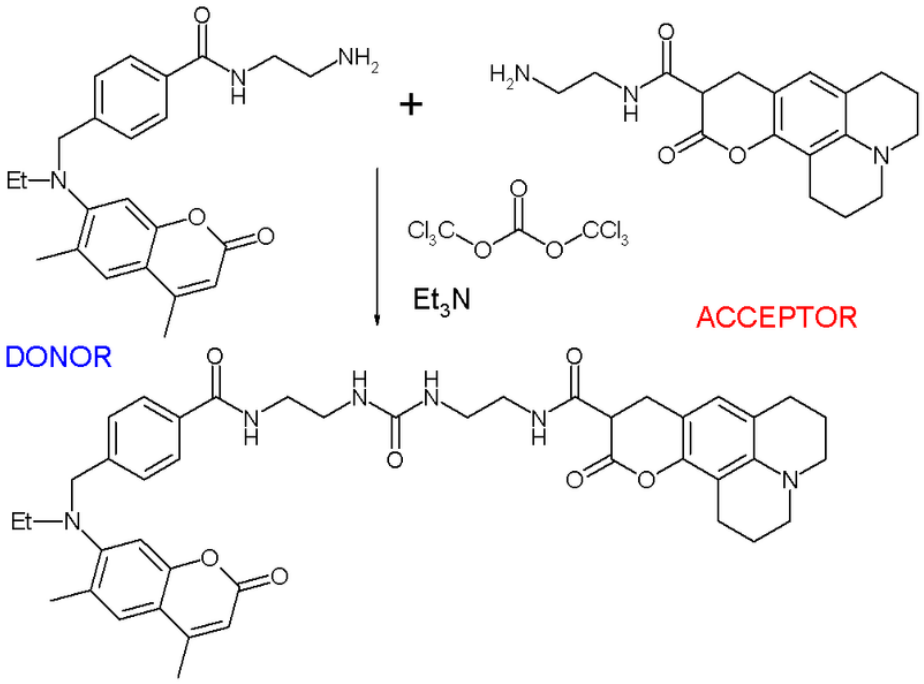

MISTAKE: The chromophore on the right must be also coumarine (double bond is missing)

FRET is also used to study lipid rafts in cell membranes.[9]

External links

- Browser-based calculator to find the critical distance and FRET efficiency with known spectral overlap [10]
- → FCS[11] [12] [13] [14] [15] .

References

[1] *Inconspicuous Consumption: Uncovering the Molecular Pathways behind Phagocytosis.* Inman M, PLoS Biology Vol. 4/6/**2006**, e190. doi: 10.1371/journal.pbio.0040190 (http://dx.doi.org/10.1371/journal.pbio.0040190)

[2] Förster T., Zwischenmolekulare Energiewanderung und Fluoreszenz, *Ann. Physik* **1948**, *437*, 55. doi: 10.1002/andp.19484370105 (http://dx.doi.org/10.1002/andp.19484370105)

[3] Joseph R. Lakowicz, "Principles of Fluorescence Spectroscopy", Plenum Publishing Corporation, 2nd edition (July 1, 1999)

[4] FRET microscopy tutorial from Olympus (http://www.olympusfluoview.com/applications/fretintro.html)

[5] D. L. Andrews, "A unified theory of radiative and radiationless molecular energy transfer", *Chem. Phys.* **1989**, 135, 195-201. doi: 10.1016/0301-0104(89)87019-3 (http://dx.doi.org/10.1016/0301-0104(89)87019-3)
[6] D. L. Andrews and D. S. Bradshaw, "Virtual photons, dipole fields and energy transfer: A quantum electrodynamical approach", *Eur. J. Phys.* **2004**, 25, 845-858. doi: 10.1088/0143-0807/25/6/017 (http://dx.doi.org/10.1088/0143-0807/25/6/017)
[7] Jovin, T.M. and Arndt-Jovin, D.J. FRET microscopy: Digital imaging of fluorescence resonance energy transfer. Application in cell biology. In Cell Structure and Function by Microspectrofluometry, E. Kohen, J. G. Hirschberg and J. S. Ploem. London: Academic Press, 1989. pp. 99-117.
[8] *A FRET approach to phosgene detection* Hexiang Zhang and Dmitry M. Rudkevich Chem. Commun., **2007**, 1238 - 1239, doi: 10.1039/b614725a (http://dx.doi.org/10.1039/b614725a)
[9] Silvius, J.R. and Nabi, I.R. Fluorescence-quenching and resonance energy transfer studies of lipid microdomains in model and biological membranes. (Review) *Molec. Membr. Bio.* **2006**, *23*, 5-16. doi: 10.1080/09687860500473002 (http://dx.doi.org/10.1080/09687860500473002)
[10] http://www.calctool.org/CALC/chem/photochemistry/fret
[11] Diaspro, A., and Robello, M. (1999). Multi-photon Excitation Microscopy to Study Biosystems. European Microscopy and Analysis., 5:5-7.
[12] Bagatolli, L.A., and Gratton, E. (2000). Two-photon fluorescence microscopy of coexisting lipid domains in giant unilamellar vesicles of binary phospholipid mixtures. Biophys J., 78:290-305.
[13] Schwille, P., Haupts, U., Maiti, S., and Webb. W.(1999). Molecular dynamics in living cells observed by fluorescence correlation spectroscopy with one- and two- photon excitation. *Biophysical Journal*, **77**(10):2251-2265.
[14] Near Infrared Microspectroscopy, Fluorescence Microspectroscopy,Infrared Chemical Imaging and High Resolution Nuclear Magnetic Resonance Analysis of Soybean Seeds, Somatic Embryos and Single Cells., Baianu, I.C. et al. 2004., In *Oil Extraction and Analysis.*, D. Luthria, Editor pp.241-273, AOCS Press., Champaign, IL.
[15] Single Cancer Cell Detection by Near Infrared Microspectroscopy, Infrared Chemical Imaging and Fluorescence Microspectroscopy.2004.I. C. Baianu, D. Costescu, N. E. Hofmann and S. S. Korban, q-bio/0407006 (July 2004) (http://arxiv.org/abs/q-bio/0407006)

Confocal microscopy

Confocal microscopy is an optical imaging technique used to increase micrograph contrast and/or to reconstruct three-dimensional images by using a spatial pinhole to eliminate out-of-focus light or flare in specimens that are thicker than the focal plane.[1] This technique has gained popularity in the scientific and industrial communities. Typical applications include life sciences and semiconductor inspection.

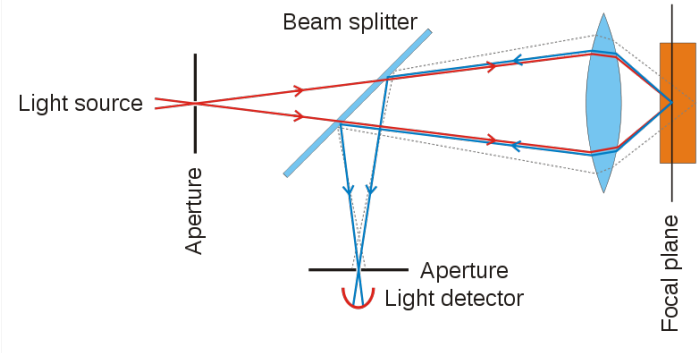

Principle of confocal microscopy

Basic concept

The principle of confocal imaging was patented by Marvin Minsky in 1957.[2] In a conventional (i.e., wide-field) fluorescence microscope, the entire specimen is flooded in light from a light source. Due to the conservation of light intensity transportation, all parts of the specimen throughout the optical path will be excited and the fluorescence detected by a photodetector or a camera. In contrast, a confocal microscope uses point illumination

and a pinhole in an optically conjugate plane in front of the detector to eliminate out-of-focus information. Only the light within the focal plane can be detected, so the image quality is much better than that of wide-field images. As only one point is illuminated at a time in confocal microscopy, 2D or 3D imaging requires scanning over a regular raster (i.e. a rectangular pattern of parallel scanning lines) in the specimen. The thickness of the focal plane is defined mostly by the inverse of the square of the numerical aperture of the objective lens, and also by the optical properties of the specimen and the ambient index of refraction. These microscopes also are able to see into the image by taking images at different depths.

Types

Three types of confocal microscopes are commercially available: Confocal laser scanning microscopes, spinning-disk (Nipkow disk) confocal microscopes and Programmable Array Microscopes (PAM). Confocal laser scanning microscopy yields better image quality than Nipkow and PAM, but the imaging frame rate was very slow (less than 3 frames/second) until recently; spinning-disk confocal microscopes can achieve video rate imaging—a desirable feature for dynamic observations such as live cell imaging. Confocal laser scanning microscopy has now been improved to provide better than video rate (60 frames/second) imaging by using MEMS based scanning mirrors.

Images

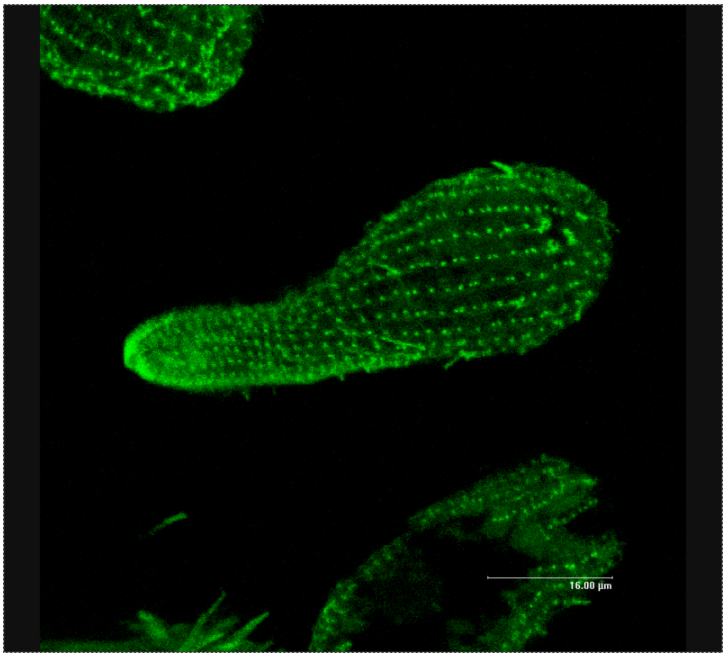

β-tubulin in Tetrahymena (a ciliated protozoan).

References

[1] Pawley JB (editor) (2006). *Handbook of Biological Confocal Microscopy* (3rd ed. ed.). Berlin: Springer. ISBN 038725921x.

[2] US patent 3013467 (http://v3.espacenet.com/textdoc?DB=EPODOC&IDX=US3013467)

External links

- *Molecular Expressions*: (http://micro.magnet.fsu.edu) Laser Scanning Confocal Microscopy (http://micro.magnet.fsu.edu/primer/techniques/confocal/index.html)
- Nikon's MicroscopyU (http://www.microscopyu.com/articles/confocal/confocalintrobasics.html). Comprehensive introduction to confocal microscopy.
- Emory’s Physics Department (http://www.physics.emory.edu/~weeks/confocal/). Introduction to confocal microscopy and fluorescence.
- The Science Creative Quarterly's overview of confocal microscopy (http://www.scq.ubc.ca/?p=278) - high res images also available.
- Programmable Array Microscope (http://spiedl.aip.org/getabs/servlet/GetabsServlet?prog=normal&id=PSISDG006441000001644 10S000001&idtype=cvips&gifs=yes) - Confocal Microscope Capabilities.

Article Sources and Contributors

Molecular models of DNA *Source*: http://en.wikipedia.org/w/index.php?oldid=291825131 *Contributors*: Bci2, Chris the speller, Oscarthecat

DNA *Source*: http://en.wikipedia.org/w/index.php?oldid=291852295 *Contributors*: (, (jarbarf), -Majestic-, 168.., 168..., 169, 17Drew, 3dscience, 4u1e, 62.253.64.xxx, 7434be, 84user, A D 13, A bit iffy, A-giau, Aaaxlp, Aatomic1, Academic Challenger, Acer, Adam Bishop, Adambiswanger1, Adamstevenson, Adashiel, Adenosine, Adrian.benko, Ahoerstemeier, Aitias, Aj123456, Alai, Alan Au, Aldaron, Aldie, Alegoo92, Alexandremas, Alkivar, Alphachimp, Alzhaid, Amboo85, Anarchy on DNA, Ancheta Wis, AndonicO, Andre Engels, Andrew wilson, Andreww, Andrij Kursetsky, Andycjp, Anita1988, Anomalocaris, Antandrus, Ante Aikio, Anthere, Anthony, Anthony Appleyard, Antilived, Antony-22, Aquaplus, Aquilla34, ArazZeynili, Arcadian, Ardyn, ArielGold, Armored Ear, Asbestos, Astrowob, Atlant, Aude, Autonova, Avala, AxelBoldt, AySz88, AzaToth, BD2412, BMF81, Banus, BaronLarf, Bbatsell, Bci2, Bcorr, Ben Webber, Ben-Zin, BenBildstein, Benjah-bmm27, Bensaccount, Bernie Sanders' DNA, Bevo, Bhadani, Bhar100101, BiH, Bijee, BikA06, Bill Nelson's DNA, Billmcgn189, Biolinker, Biriwilg, Bjwebb, Blastwizard, Blondtraillite, Bmtbomb, Bobblewik, Bobo192, Bongwarrior, Borisblue, Bornhj, Brian0918, Brighterorange, Brim, Brockett, Bryan, Bryan Derksen, CWY2190, Cacycle, Caerwine, Cainer91, Cal 1234, Calaschysm, Can't sleep, clown will eat me, Canadaduane, Carbon-16, Carcharoth, Carlo.milanesi, Carlwev, Casliber, Cathalgarvey, CatherineMunro, CattleGirl, Cburnett, Cerberus lord, Chanora, Chanting Fox, Charm, Chill Pill Bill, Chino, Chodges, Chris 73, Chris84, Chuck Grassley's DNA, Chuck02, Clivedelmonte, ClockworkSoul, CloudNine, Collins.mc, Colorajo, CommonsDelinker, Conversion script, Cool3, Coolawesome, Coredesat, Cornacchia123, Cosmotron, Cradlelover123, Crazycomputers, Crowstar, Crusadeonilliteracy, CryptoDerk, Crzrussian, Cubskrazy29, CupOBeans, Curps, Cyan, Cyclonenim, Cyrius, D6, DIREKTOR, DJAX, DJRafe, DNA EDIT WAR, DNA is shyt, DVD R W, Daniel Olsen, Daniel987600, Danielkueh, Danny, Danny B-), Danski14, Darklilac, Darth Panda, Davegrupp, David D., David Eppstein, Davidbspalding, Daycd, Db099221, Dbabbitt, Dcoetzee, DeAceShooter, DeadEyeArrow, Delldot, Delta G, Deltabeignet, DevastatorIIC, Diberri, Dicklyon, Digger3000, Digitalme, Dina, Djm1279, Dlohcierekim's sock, Dmn, Docjames, Doctor Faust, Docu, DonSiano, Donarreiskoffer, Dr d12, Dr.Kerr, Drini, Dudewheresmywallet, Dullhunk, Duncan.france, Dungodung, Dysmorodrepanis, E. Wayne, ERcheck, ESkog, Echo park00, Echuck215, Eddycrai, Editing DNA, Edwy, Efbfweborg, Egil, ElTyrant, Elb2000, Eleassar777, EliasAlucard, ElinorD, Ellmist, Eloquence, Emoticon, Epingchris, Erik Zachte, Escape Artist Swyer, Esurnir, Etanol, Ettrig, EurekaLott, Everyking, Evil Monkey, Ewawer, Execvator, FOTEMEH, Fabhcún, Factual, Fagstein, Fastfission, Fconaway, Fcrick, Fernando S. Aldado, Ffirehorse, Figma, Figure, Firefoxman, Firetrap9254, Fishingpal99, Flavaflav1005, Florentino floro, Fnielsen, Forluvoft, Freakofnurture, FreplySpang, Friendly Neighbour, Frostyservant, Fruge, Fvasconcellos, G3pro, GAThrawn22, GHe, GODhack, Gaara san, Galoubet, Gary King, Gatortpk, Gazibara, GeeJo, Gene Nygaard, GeoMor, Giftlite, Gilisa, Gilliam, Gimmetrow, Gjuggler, Glen Hunt's DNA, Glenn, Gmaxwell, GoEThe, Goatasaur, Gogo Dodo, Golnazfotohabadi, GordonWatts, Gracenotes, Graeme Bartlett, GraemeL, Grafikm fr, Graft, Graham87, GrahamColm, Grandegrandegrande, GregorB, Grover cleveland, Gurko, Gustav von Humpelschmumpel, Gutza, Gwsrinme, Hadal, Hagerman, Hairchrm, Hairwheel, Hannes Röst, Harianto, Heathhunnicutt, Hephaestos, Heron, Heyheyhack, Hockey21dude, Horatio, Hu, Hughdbrown, Hurricanehink, Hut 8.5, Hvn0413, I Seek To Help & Repair!, I hate DNA, Iapetus, Icairns, Ilia Kr., Impamiizgraa, InShaneee, Inge-Lyubov, Isilanes, Isis07, Itub, Ixfd64, Izehar, JHMM13, JWSchmidt, JWSurf, Jacek Kendysz, Jackrm, JamesMLane, JamesMt1984, Janejellyroll, Jaxl, Jeka911, Jer ome, JeremyA, Jerzy, Jetsetpainter, Jh51681, Jiddisch, Jimriz, Jimwong, Jlh29, Jls043, Jmcc150, Jo9100, JoanneB, Joconnol, Johanvs, JohnArmagh, Johntex, Jojit fb, JonMoulton, Jonrunles, Jorvik, JoshuaZ, Josq, Jossi, Jstech, Julian Diamond, Jumbo Snails, Junes, Jwrosenzweig, Kahlfin, Kapow, Karrmann, Kazkaskazkasako, Kbh3rd, Keegan, Keepweek, Keilana, Kelly Martin, Kemyou, Kendrick7, KerryO77, Kevin Breitenstein, Kevmitch, Kghose, Kholdstare99, Kierano, KimvdLinde, King of Hearts, KingTT, Kingturtle, Kitch, Knaggs, Knowledge Seeker, KnowledgeOfSelf, Koavf, KrakatoaKatie, Kums, Kungfuadam, Kuru, Kwamikagami, Kwekubo, KyNephi, LA2, La goutte de pluie, Lascorz, Latka, Lavateraguy, Lee Daniel Crocker, Lemchesvej, Lerdsuwa, Leuko, Lexor, Lhenslee, Lia Todua, LightFlare, Lightmouse, Lightspeedchick, Ligulem, Lincher, Lion Wilson, Lir, Llongland, Llull, Lockesdonkey, Logical2u, Loginbuddy, Looxix, Loren36, Loris, Luigi30, Luk, Lumos3, Luna Santin, Luuva, MER-C, MKoltnow, MONGO, Mac, Madeleine Price Ball, Madhero88, Magadan, Magnus Manske, Majorly, Malcolm rowe, Malo, Mandyj61596, Mantissa128, Marcus.aerlous, Marj Tiefert, MarvPaule, Master dingley, Mattbr, Mattbrundage, Mattjblythe, Mav, Max Baucus' DNA, Max Naylor, McDogm, Medessec, Medos2, Melaen, Melchoir, Mentalmaniac07, Mgiganteus1, Mgtoohey, Mhking, Michael Devore, MichaelHa, Michaelas10, Michigan user, MidgleyDJ, Midnightblueowl, Midoriko, Mika293, Mike Rosoft, Mikker, Mikko Paananen, Mintman16, MisfitToys, Misza13, Mithent, Mjpieters, Mleefs7, Moink, Moorice, Mortene, Mr Bungle, Mr Meow Meow, Mr Stephen, MrErku, Mstislavl, Mstroeck, Mulad, Munita Prasad, Muro de Aguas, Mwanner, Mxn, Nakon, Narayanese, Natalie Erin, Natarajanganesan, Nate1028, NatureA16, Nauseam, Nbauman, Neckro, Netkinetic, Netoholic, Neutrality, NewEnglandYankee, Nighthawk380, NighthawkJ, Nihiltres, Nirajrm, Nishkid64, Nitecrawler, Nitramrekcap, No Guru, NoIdeaNick, NochnoiDozor, Nohat, Northfox, NorwegianBlue, Nthornberry, Nunh-huh, OBloodyHell, OOODDD, Obli, Oblivious, Ocolon, Ojl, Omicronpersei8, Onco p53, Opabinia regalis, Opelio, Orrin Hatch's DNA, Orthologist, Ortolan88, Ouishoebean, Outriggr, OwenX, P99am, PDH, PFHLai, PaePae, Pakaran, Pascal666, Patrick0Moran, Patrick2480, Patstuart, Paul venter, Paulinho28, Pcb21, Pde, Peak, Pedro, Persian Poet Gal, Peter Isotalo, Peter K., Peter Winnberg, Pgan002, Philip Trueman, PhilipO, Phoenix Hacker, PierreAbbat, Pigman, Pigmietheclub, Pilotguy, Pkirlin, Poor Yorick, Portugue6927, Potatoswatter, Preston47, Priscilla 95925, Pristontale111, Pro crast in a tor, Prodego, Psora, PsyMar, Psymier, Pumpkingrower05, Pyrospirit, Quebec99, Quickbeam, Qutezuce, Qxz, R'n'B, R. S. Shaw, RDBrown, RSido, Ragesoss, Rajwiki123, RandomP, Randomblue, Raul654, Raven in Orbit, Ravidreams, Rdb, Rdsmith4, Red Director, Reddi, Rednblu, Redneckjimmy, Redquark, Retired username, Rettetast, RexNL, Rich Farmbrough, RichG, Richard Durbin's DNA, Ricky81682, Rjwilmsi, Roadnottaken, Robdurbar, RobertG, Rocastelo, RoddyYoung, Rory096, Rotem Dan, Roy Brumback, RoyBoy, RoyLaurie, Royalguard11, RunOrDie, Russ47025, RxS, Ryan Delaney, RyanGerbil10, Ryulong, S77914767, SCEhardt, STAN SWANSON, SWAdair, Sabbre, Safwan40, Sakkura, SallyForth123, Sam Burne James, Samsara, Samuel, Samuel Blanning, SandyGeorgia, Sango123, Sangwine, Savidan, Sceptre, Schutz, Sciencechick, Scienceman123, Scincesociety, Sciurinæ, Scope creep, Scotterican, Sean William, SeanMack, Seans Potato Business, SebastianHawes, Seldon1, Serephine, Shadowlynk, Shanes, ShaunL, Shekharsuman, Shizhao, Shmee47, Shoy, Silsor, SimonD, Sintaku, Sir.Loin, Sjjupadhyay, Sjollema, Sloth monkey, Slrubenstein, Sly G, SmilesALot, Smithbrenon, Snowmanradio, Snowolf, Snurks, Solipsist, Someone else, Sonett72, Sopoforic, Spaully, Spectrogram, Splette, Spondoolicks, Spongebobsqpants, SpuriousQ, Squidonius, Squirepants101, Statsone, Steel, Steinsky, Stemonitis, Stephenb, SteveHopson, Stevertigo, Stevietheman, Stewartadcock, Stuart7m, Stuhacking, SupaStarGirl, Supspirit, Susvolans, Sverdrup, Swid, Switchercat, T'Shael, Taco325i, Takometer, TakuyaMurata, Tariqabjotu, Tarret, Taulant23, Tavilis, Tazmaniacs, Ted Longstaffe, Tellyaddict, TenOfAllTrades, Terraguy, Test100000, TestPilot, The Rambling Man, The WikiWhippet, TheAlphaWolf, TheChrisD, TheGrza, TheKMan, TheRanger, Thorwald, ThreeDaysGraceFan101, Thue, Tiddly Tom, Tide rolls, TigerShark, TimVickers, Timewatcher, Timir2, Timl2k4, Timrollpickering, Timwi, Tobogganoggin, Toby Bartels, TobyWilson1992, Tom Allen, Tom Harkin's DNA, Tomgally, Toninu, Tony1, Tonyrenploki, Trd300gt, Trent Lott's DNA, Triwbe, Troels Arvin, Tstrobaugh, Tufflaw, Turnstep, Twilight Realm, Ty146Ty146, UBeR, Unint, Unukorno, Usergreatpower, Utcursch, Uthbrian, Vaernnond, Vandelizer, Vanished user, Vary, Virtualphtn, Visium, Vividonset, VladimirKorablin, Vsmith, Vyasa, WAS 4.250, WAvegetarian, WHeimbigner, WJBscribe, Wafulz, WarthogDemon, Wavelength, WelshMatt, West Brom 4ever, Where, Whosasking, Whoutz, Why My Fleece?, Wik, Wiki alf, Wiki emma johnson, Wikiborg, Wikipedia Administration, William Pietri, WillowW, Wimt, Wknight94, Wmahan, Wnt, Wobble, WolfmanSF, Wouterstomp, Wwwwolf, Xy7, YOUR DNA, Yahel Guhan, Yamamoto Ichiro, Yamla, YanWong, Yansa, Yaser al-Nabriss, Yasha, Yomama9753, Younusporteous, Yurik, ZScout370, Zahid Abdassabur, Zahiri, Zazou, Zell Miller's DNA, Zephyris, Zoicon5, Zouavman Le Zouave, Zsinj, Zven, 1329 anonymous edits

DNA nanotechnology *Source*: http://en.wikipedia.org/w/index.php?oldid=288766577 *Contributors*: 0x38I9J*, Alnokta, Amaling, Anthonydelaware, Antony-22, Cyfal, Epbr123, Giftlite, Pwkr, ShawnDouglas, Thorwald, Tolosthemagician, ZayZayEM, 30 anonymous edits

2D-FT NMRI and Spectroscopy *Source*: http://en.wikipedia.org/w/index.php?oldid=290773884 *Contributors*: Bci2, Ched Davis, Drilnoth, H Padleckas, JaGa, Reedy, Rich Farmbrough, Rjwilmsi, 2 anonymous edits

NMR spectroscopy *Source*: http://en.wikipedia.org/w/index.php?oldid=280684865 *Contributors*: Aihre, Andy M. Wang, AxelBoldt, Bci2, Beetstra, Benandjonice, Biophysik, Borisovav, Bruker, CaneryMBurns, Ceyockey, ChemistHans, Cryptophile, DMacks, Djdaedalus, Flogiston, Freestyle-69, G-W, GeeJo, Gehtnix, Gene Nygaard, Ghiles, Graeme Bartlett, Hammer1980, Headbomb, Jclerman, Jenpen, Jingxin, Jrizor8504, Julesd, Kafziel, Kaiserkarl13, Keraman, Kjaergaard, Kkmurray, La goutte de pluie, Lee-Jon, LinguisticDemographer, Linmhall, Mac Davis, Markjoseph125, Mboverload, Measure4Measure, Mike.lifeguard, Neparis, OMCV, Oxymoron83, Pekaje, Quantockgoblin, RG2, Ribol, Rifleman 82, Runningonbrains, Salsb, Santiago Dominguez, Shalom Yechiel, Shrew, Sikkema, Smokefoot, Spellmaster, Srnec, Stepa, Takometer, TenOfAllTrades, Tkircher, Troodon, V8rik, Walkerma, WhatamIdoing, Xenonice, Zosma, 55 anonymous edits

Fourier transform spectroscopy *Source*: http://en.wikipedia.org/w/index.php?oldid=288496691 *Contributors*: AJim, Asterion, Bci2, Berserkerus, BigFatBuddha, Bobby1011, Christopherlin, Damian Yerrick, Deglr6328, E104421, Epbr123, Graeme Bartlett, Guillom, Hankwang, Harold f, Haydarkustu, HelgeStenstrom, Jaraalbe, Jcwf, John.lindner, Jonathan F, Kcordina, Kingpin13, Kkmurray, Martyjmch, Michael Hardy, Nikai, Nitrogen15,

Peter, Peterlewis, Rifleman 82, Rnt20, Ronningt, Roybb95, Seidenstud, Skier Dude, Slapidus, Smeyer1, Stannered, Sverdrup, Thepretenders22, Thinkinnng, Tim Starling, Veinor, Victorsong, 69 anonymous edits

Chemical imaging *Source*: http://en.wikipedia.org/w/index.php?oldid=290927658 *Contributors*: Alansohn, Andyphil, AngelOfSadness, Annabel, Banus, Batykefer, Bci2, BierHerr, Chris the speller, Closedmouth, D6, Davewild, Editore99, GeeJo, HYPN2457, Iridescent, JIP, Jim.henderson, Kkmurray, Mdd, Mkansiz, Natalie Erin, Skysmith, Ultraexactzz, Wilson003, 38 anonymous edits

Hyperspectral imaging *Source*: http://en.wikipedia.org/w/index.php?oldid=291759304 *Contributors*: Adoniscik, Andrew c, Bci2, Cm the p, Dhaluza, Gcrisford, Geologicharka, Hankwang, Jprikkel, Lantonov, Moin95, Victorsong, 15 anonymous edits

FT-IR *Source*: http://en.wikipedia.org/w/index.php?oldid=170276231 *Contributors*: -

CARS *Source*: http://en.wikipedia.org/w/index.php?oldid=291555109 *Contributors*: Alash, Delldot, Epotma, Feezo, Gwernol, HLOfferhaus, Interiot, Kkmurray, Lightmouse, MWS, Maartend8, Nick Y., Ohnoitsjamie, PigFlu Oink, Rich Farmbrough, ShakingSpirit, Signalhead, The wub, Thehelpfulone, V8rik, Vladsinger, 28 anonymous edits

Fluorescence microscopy *Source*: http://en.wikipedia.org/w/index.php?oldid=48762017 *Contributors*: -

Fluorescence correlation spectroscopy *Source*: http://en.wikipedia.org/w/index.php?oldid=291763472 *Contributors*: Bci2, BenFrantzDale, Berky, Danrs, Dkkim, Gogowitsch, Hbayat, Jcwf, John, Karol Langner, Lightmouse, Maartend8, ST47, Skier Dude, Tizeff, Wisdom89, 32 anonymous edits

Fluorescence cross-correlation spectroscopy *Source*: http://en.wikipedia.org/w/index.php?oldid=274364772 *Contributors*: Clicketyclack, Maartend8, 4 anonymous edits

Fluorescence resonance energy transfer *Source*: http://en.wikipedia.org/w/index.php?oldid=291762957 *Contributors*: Aciel, Aclapp, Alansohn, Alessandro Esposito, Aloening, Asger.kryger, Asgerk, Banderaazul, Bci2, Chodges, Cleggrobert, Clicketyclack, Cnickelfr, Cortonin, Cpichardo, DeadEyeArrow, Edgar181, Hankwang, Haukurth, Ian Pitchford, JOK, Jaganath, Jammedshut, Kawaiyas, Kungfuadam, Lantonov, Lifeisaserenade, Looie, Mah159, Markus Poessel, Miguel Andrade, Mr d logan, Nono64, Oakwood, OldakQuill, PDH, Phi-Gastrein, RH, Rich Farmbrough, RockyRaccoon, Rushphoton, Sam Hocevar, Seans Potato Business, ShakingSpirit, Sintaku, SocratesJedi, TenOfAllTrades, Theron110, Tomgally, Trevva, V8rik, Wisdom89, Yiddy55, 101 anonymous edits

Confocal microscopy *Source*: http://en.wikipedia.org/w/index.php?oldid=284160852 *Contributors*: 9eyedeel, Axelv, Blechnic, Butterfly reflections, Carrasmith, Celephicus, Chewie, Ciphers, ColinEberhardt, Donarreiskoffer, Drdaveng, EpiVictor, EronMain, Femto, Ff5166, Flameviper, H2g2bob, Jaeger5432, Joechao, Jumboman, LegitimateAndEvenCompelling, MarcoTolo, Martious, MetrologyMan, MicroBio Hawk, Ncross35, Nikevich, OlavN, OttoTheFish, Plantsurfer, Pyo, Skookumdad, Smith609, Srleffler, Tabascoj, Umangagarwal, Utbg2008, Vanillacreem, Whosasking, 59 anonymous edits

Image Sources, Licenses and Contributors

Image:Sarfus.DNABiochip.jpg *Source*: http://en.wikipedia.org/w/index.php?title=File:Sarfus.DNABiochip.jpg *License*: unknown *Contributors*: Nanolane

Image:Spinning DNA.gif *Source*: http://en.wikipedia.org/w/index.php?title=File:Spinning_DNA.gif *License*: Public Domain *Contributors*: USDA

File:Methanol.pdb.png *Source*: http://en.wikipedia.org/w/index.php?title=File:Methanol.pdb.png *License*: Creative Commons Attribution-Sharealike 2.5 *Contributors*: ALoopingIcon, Benjah-bmm27

File:DNA-fragment-3D-vdW.png *Source*: http://en.wikipedia.org/w/index.php?title=File:DNA-fragment-3D-vdW.png *License*: Public Domain *Contributors*: Benjah-bmm27

File:Simple harmonic oscillator.gif *Source*: http://en.wikipedia.org/w/index.php?title=File:Simple_harmonic_oscillator.gif *License*: Public Domain *Contributors*: User:Oleg Alexandrov

File:DNA chemical structure.svg *Source*: http://en.wikipedia.org/w/index.php?title=File:DNA_chemical_structure.svg *License*: unknown *Contributors*: Madprime, Wickey, 1 anonymous edits

File:ADN animation.gif *Source*: http://en.wikipedia.org/w/index.php?title=File:ADN_animation.gif *License*: Public Domain *Contributors*: Aushulz, Bawolff, Brian0918, Kersti Nebelsiek, Magadan, Mattes, Origamiemensch, Stevenfruitsmaak, 3 anonymous edits

File:Parallel telomere quadruple.png *Source*: http://en.wikipedia.org/w/index.php?title=File:Parallel_telomere_quadruple.png *License*: unknown *Contributors*: User:Splette

File:Four-way DNA junction.gif *Source*: http://en.wikipedia.org/w/index.php?title=File:Four-way_DNA_junction.gif *License*: Public Domain *Contributors*: Aushulz, Molatwork, Origamiemensch, TimVickers, 1 anonymous edits

File:DNA replication.svg *Source*: http://en.wikipedia.org/w/index.php?title=File:DNA_replication.svg *License*: Public Domain *Contributors*: user:LadyofHats

File:ABDNAxrgpj.jpg *Source*: http://en.wikipedia.org/w/index.php?title=File:ABDNAxrgpj.jpg *License*: GNU Free Documentation License *Contributors*: I.C. Baianu et al.

File:Plos VHL.jpg *Source*: http://en.wikipedia.org/w/index.php?title=File:Plos_VHL.jpg *License*: Creative Commons Attribution 2.5 *Contributors*: Akinom, Anniolek, Filip em, Thommiddleton

File:3D model hydrogen bonds in water.jpg *Source*: http://en.wikipedia.org/w/index.php?title=File:3D_model_hydrogen_bonds_in_water.jpg *License*: GNU Free Documentation License *Contributors*: User:snek01

Image:Methanol.pdb.png *Source*: http://en.wikipedia.org/w/index.php?title=File:Methanol.pdb.png *License*: Creative Commons Attribution-Sharealike 2.5 *Contributors*: ALoopingIcon, Benjah-bmm27

File:Bragg diffraction.png *Source*: http://en.wikipedia.org/w/index.php?title=File:Bragg_diffraction.png *License*: GNU General Public License *Contributors*: user:hadmack

File:DNA in water.jpg *Source*: http://en.wikipedia.org/w/index.php?title=File:DNA_in_water.jpg *License*: unknown *Contributors*: User:Bbkkk

File:X ray diffraction.png *Source*: http://en.wikipedia.org/w/index.php?title=File:X_ray_diffraction.png *License*: unknown *Contributors*: Thomas Splettstoesser

File:X Ray Diffractometer.JPG *Source*: http://en.wikipedia.org/w/index.php?title=File:X_Ray_Diffractometer.JPG *License*: GNU Free Documentation License *Contributors*: Ff02::3, Pieter Kuiper

File:SLAC detector edit1.jpg *Source*: http://en.wikipedia.org/w/index.php?title=File:SLAC_detector_edit1.jpg *License*: unknown *Contributors*: User:Mfield, User:Starwiz

File:ISIS exptal hall.jpg *Source*: http://en.wikipedia.org/w/index.php?title=File:ISIS_exptal_hall.jpg *License*: unknown *Contributors*: User:wurzeller

File:Dna-SNP.svg *Source*: http://en.wikipedia.org/w/index.php?title=File:Dna-SNP.svg *License*: unknown *Contributors*: User:Gringer

File:DNA Under electron microscope Image 3576B-PH.jpg *Source*: http://en.wikipedia.org/w/index.php?title=File:DNA_Under_electron_microscope_Image_3576B-PH.jpg *License*: unknown *Contributors*: Original uploader was SeanMack at en.wikipedia

File:DNA Model Crick-Watson.jpg *Source*: http://en.wikipedia.org/w/index.php?title=File:DNA_Model_Crick-Watson.jpg *License*: Public Domain *Contributors*: User:Alkivar

File:DNA labels.jpg *Source*: http://en.wikipedia.org/w/index.php?title=File:DNA_labels.jpg *License*: GNU Free Documentation License *Contributors*: User:Raul654

File:AT DNA base pair pt.svg *Source*: http://en.wikipedia.org/w/index.php?title=File:AT_DNA_base_pair_pt.svg *License*: Public Domain *Contributors*: User:Lijealso

File:A-B-Z-DNA Side View.png *Source*: http://en.wikipedia.org/w/index.php?title=File:A-B-Z-DNA_Side_View.png *License*: Public Domain *Contributors*: Original uploader was Thorwald at en.wikipedia

File:Museo Príncipe Felipe. ADN.jpg *Source*: http://en.wikipedia.org/w/index.php?title=File:Museo_Príncipe_Felipe._ADN.jpg *License*: Creative Commons Attribution-Sharealike 2.0 *Contributors*: Fernando

File:AGCT DNA mini.png *Source*: http://en.wikipedia.org/w/index.php?title=File:AGCT_DNA_mini.png *License*: unknown *Contributors*: Iquo

File:BU Bio5.jpg *Source*: http://en.wikipedia.org/w/index.php?title=File:BU_Bio5.jpg *License*: Creative Commons Attribution-Sharealike 2.0 *Contributors*: Original uploader was Elapied at fr.wikipedia

File:Circular DNA Supercoiling.png *Source*: http://en.wikipedia.org/w/index.php?title=File:Circular_DNA_Supercoiling.png *License*: GNU Free Documentation License *Contributors*: Richard Wheeler (Zephyris)

File:Rosalindfranklinsjokecard.jpg *Source*: http://en.wikipedia.org/w/index.php?title=File:Rosalindfranklinsjokecard.jpg *License*: unknown *Contributors*: Bci2, Martyman, Nitramrekcap, Rjm at sleepers, 2 anonymous edits

Image:Rosalindfranklinsjokecard.jpg *Source*: http://en.wikipedia.org/w/index.php?title=File:Rosalindfranklinsjokecard.jpg *License*: unknown *Contributors*: Bci2, Martyman, Nitramrekcap, Rjm at sleepers, 2 anonymous edits

File:Genomics GTL Pictorial Program.jpg *Source*: http://en.wikipedia.org/w/index.php?title=File:Genomics_GTL_Pictorial_Program.jpg *License*: Public Domain *Contributors*: Mdd

File:RNA pol.jpg *Source*: http://en.wikipedia.org/w/index.php?title=File:RNA_pol.jpg *License*: Public Domain *Contributors*: InfoCan

File:Primase 3B39.png *Source*: http://en.wikipedia.org/w/index.php?title=File:Primase_3B39.png *License*: Public Domain *Contributors*: own work

File:DNA Repair.jpg *Source*: http://en.wikipedia.org/w/index.php?title=File:DNA_Repair.jpg *License*: Public Domain *Contributors*: Courtesy of Tom Ellenberger, Washington University School of Medicine in St. Louis.

File:MGMT+DNA 1T38.png *Source*: http://en.wikipedia.org/w/index.php?title=File:MGMT+DNA_1T38.png *License*: Public Domain *Contributors*: own work

File:DNA damaged by carcinogenic 2-aminofluorene AF .jpg *Source*: http://en.wikipedia.org/w/index.php?title=File:DNA_damaged_by_carcinogenic_2-aminofluorene_AF_.jpg *License*: Public Domain *Contributors*: Brian E. Hingerty, Oak Ridge National Laboratory Suse Broyde, New York University Dinshaw J. Patel, Memorial Sloan Kettering Cancer Center

File:A-DNA orbit animated small.gif *Source*: http://en.wikipedia.org/w/index.php?title=File:A-DNA_orbit_animated_small.gif *License*: GNU Free Documentation License *Contributors*: User:Bstlee, User:Zephyris

File:Plasmid emNL.jpg *Source*: http://en.wikipedia.org/w/index.php?title=File:Plasmid_emNL.jpg *License*: GNU Free Documentation License *Contributors*: Denniss, Glenn, Rasbak

File:Chromatin chromosom.png *Source*: http://en.wikipedia.org/w/index.php?title=File:Chromatin_chromosom.png *License*: Public Domain *Contributors*: User:Magnus Manske

File:Chromosome.svg *Source*: http://en.wikipedia.org/w/index.php?title=File:Chromosome.svg *License*: unknown *Contributors*: User:Dietzel65, User:Magnus Manske, User:Tryphon

File:Chr2 orang human.jpg *Source*: http://en.wikipedia.org/w/index.php?title=File:Chr2_orang_human.jpg *License*: Creative Commons Attribution-Sharealike 2.5 *Contributors*: Verena Schubel, Stefan Müller, Department Biologie der Ludwig-Maximilians-Universität München.

File:3D-SIM-3 Prophase 3 color.jpg *Source*: http://en.wikipedia.org/w/index.php?title=File:3D-SIM-3_Prophase_3_color.jpg *License*: Creative Commons Attribution-Sharealike 3.0 *Contributors*: Lothar Schermelleh

File:Chromosome2 merge.png *Source*: http://en.wikipedia.org/w/index.php?title=File:Chromosome2_merge.png *License*: Public Domain *Contributors*: Original uploader was Evercat at en.wikipedia

File:Transkription Translation 01.jpg *Source*: http://en.wikipedia.org/w/index.php?title=File:Transkription_Translation_01.jpg *License*: Public Domain *Contributors*: User:Kuebi

File:RibosomaleTranskriptionsEinheit.jpg *Source*: http://en.wikipedia.org/w/index.php?title=File:RibosomaleTranskriptionsEinheit.jpg *License*: GNU Free Documentation License *Contributors*: User:Merops

File:Chromosome Conformation Capture Technology.jpg *Source*: http://en.wikipedia.org/w/index.php?title=File:Chromosome_Conformation_Capture_Technology.jpg *License*: Public Domain *Contributors*: User:Kangyun1985

File:Mitochondrial DNA and diseases.png *Source*: http://en.wikipedia.org/w/index.php?title=File:Mitochondrial_DNA_and_diseases.png *License*: unknown *Contributors*: User:XXXL1986

File:PCR.svg *Source*: http://en.wikipedia.org/w/index.php?title=File:PCR.svg *License*: unknown *Contributors*: User:Madprime

File:Pcr gel.png *Source*: http://en.wikipedia.org/w/index.php?title=File:Pcr_gel.png *License*: GNU Free Documentation License *Contributors*: Habj, Ies, PatríciaR, Retama, Saperaud

File:DNA nanostructures.png *Source*: http://en.wikipedia.org/w/index.php?title=File:DNA_nanostructures.png *License*: unknown *Contributors*: (Images were kindly provided by Thomas H. LaBean and Hao Yan.)

File:SFP discovery principle.jpg *Source*: http://en.wikipedia.org/w/index.php?title=File:SFP_discovery_principle.jpg *License*: unknown *Contributors*: User:Agbiotec

File:Cdnaarray.jpg *Source*: http://en.wikipedia.org/w/index.php?title=File:Cdnaarray.jpg *License*: unknown *Contributors*: Mangapoco

File:Expression of Human Wild-Type and P239S Mutant Palladin.png *Source*: http://en.wikipedia.org/w/index.php?title=File:Expression_of_Human_Wild-Type_and_P239S_Mutant_Palladin.png *License*: unknown *Contributors*: see above

File:Random genetic drift chart.png *Source*: http://en.wikipedia.org/w/index.php?title=File:Random_genetic_drift_chart.png *License*: unknown *Contributors*: User:Professor marginalia

File:Co-dominance Rhododendron.jpg *Source*: http://en.wikipedia.org/w/index.php?title=File:Co-dominance_Rhododendron.jpg *License*: Creative Commons Attribution 2.0 *Contributors*: Ayacop, Cillas, FlickrLickr, FlickreviewR, Horcha, Kanonkas, Kevmin, MPF, Para

File:DNA_nanostructures.png *Source*: http://en.wikipedia.org/w/index.php?title=File:DNA_nanostructures.png *License*: unknown *Contributors*: (Images were kindly provided by Thomas H. LaBean and Hao Yan.)

File:Holliday junction coloured.png *Source*: http://en.wikipedia.org/w/index.php?title=File:Holliday_junction_coloured.png *License*: GNU Free Documentation License *Contributors*: Original uploader was Zephyris at en.wikipedia

File:Holliday Junction cropped.png *Source*: http://en.wikipedia.org/w/index.php?title=File:Holliday_Junction_cropped.png *License*: GNU Free Documentation License *Contributors*: Original uploader was TimVickers at en.wikipedia

File:Atomic force microscope by Zureks.jpg *Source*: http://en.wikipedia.org/w/index.php?title=File:Atomic_force_microscope_by_Zureks.jpg *License*: unknown *Contributors*: User:Zureks

File:Atomic force microscope block diagram.png *Source*: http://en.wikipedia.org/w/index.php?title=File:Atomic_force_microscope_block_diagram.png *License*: Public Domain *Contributors*: Original uploader was Askewmind at en.wikipedia

File:AFM view of sodium chloride.gif *Source*: http://en.wikipedia.org/w/index.php?title=File:AFM_view_of_sodium_chloride.gif *License*: Public Domain *Contributors*: Courtesy of prof. Ernst Meyer, university of Basel

File:Single-Molecule-Under-Water-AFM-Tapping-Mode.jpg *Source*: http://en.wikipedia.org/w/index.php?title=File:Single-Molecule-Under-Water-AFM-Tapping-Mode.jpg *License*: unknown *Contributors*: User:Yurko

File:AFMimageRoughGlass20x20.png *Source*: http://en.wikipedia.org/w/index.php?title=File:AFMimageRoughGlass20x20.png *License*: Public Domain *Contributors*: Chych

File:Maldi informatics figure 6.JPG *Source*: http://en.wikipedia.org/w/index.php?title=File:Maldi_informatics_figure_6.JPG *License*: Public Domain *Contributors*: Rbeavis

File:Stokes shift.png *Source*: http://en.wikipedia.org/w/index.php?title=File:Stokes_shift.png *License*: unknown *Contributors*: User:Mykhal

File:CARS Scheme.svg *Source*: http://en.wikipedia.org/w/index.php?title=File:CARS_Scheme.svg *License*: unknown *Contributors*: Onno Gabriel

File:HyperspectralCube.jpg *Source*: http://en.wikipedia.org/w/index.php?title=File:HyperspectralCube.jpg *License*: Public Domain *Contributors*: Dr. Nicholas M. Short, Sr.

File:MultispectralComparedToHyperspectral.jpg *Source*: http://en.wikipedia.org/w/index.php?title=File:MultispectralComparedToHyperspectral.jpg *License*: Public Domain *Contributors*: Dr. Nicholas M. Short, Sr.

File:Confocalprinciple.svg *Source*: http://en.wikipedia.org/w/index.php?title=File:Confocalprinciple.svg *License*: GNU Free Documentation License *Contributors*: Danh

File:3D-SIM-1 NPC Confocal vs 3D-SIM detail.jpg *Source*: http://en.wikipedia.org/w/index.php?title=File:3D-SIM-1_NPC_Confocal_vs_3D-SIM_detail.jpg *License*: Creative Commons Attribution-Sharealike 3.0 *Contributors*: Changes in layout by the uploader. Only the creator of the original (Lothar Schermelleh) should be credited.

File:Tirfm.svg *Source*: http://en.wikipedia.org/w/index.php?title=File:Tirfm.svg *License*: Public Domain *Contributors*: Dawid Kulik

File:Inverted microscope.jpg *Source*: http://en.wikipedia.org/w/index.php?title=File:Inverted_microscope.jpg *License*: unknown *Contributors*: Nuno Nogueira (Nmnogueira) Original uploader was Nmnogueira at en.wikipedia

File:Fluorescence microscop.jpg *Source*: http://en.wikipedia.org/w/index.php?title=File:Fluorescence_microscop.jpg *License*: unknown *Contributors*: Masur

File:Microscope And Digital Camera.JPG *Source*: http://en.wikipedia.org/w/index.php?title=File:Microscope_And_Digital_Camera.JPG *License*: GNU Free Documentation License *Contributors*: User:Zephyris

File:FluorescenceFilters 2008-09-28.svg *Source*: http://en.wikipedia.org/w/index.php?title=File:FluorescenceFilters_2008-09-28.svg *License*: unknown *Contributors*: User:Mastermolch

File:FluorescentCells.jpg *Source*: http://en.wikipedia.org/w/index.php?title=File:FluorescentCells.jpg *License*: Public Domain *Contributors*: DO11.10, Emijrp, NEON ja, Origamiemensch, Splette, Tolanor, 5 anonymous edits

File:Yeast membrane proteins.jpg *Source*: http://en.wikipedia.org/w/index.php?title=File:Yeast_membrane_proteins.jpg *License*: unknown *Contributors*: User:Masur

File:S cerevisiae septins.jpg *Source*: http://en.wikipedia.org/w/index.php?title=File:S_cerevisiae_septins.jpg *License*: Public Domain *Contributors*: Spitfire ch, Philippsen Lab, Biozentrum Basel

File:Dividing Cell Fluorescence.jpg *Source*: http://en.wikipedia.org/w/index.php?title=File:Dividing_Cell_Fluorescence.jpg *License*: unknown *Contributors*: Will-moore-dundee

File:HeLa Hoechst 33258.jpg *Source*: http://en.wikipedia.org/w/index.php?title=File:HeLa_Hoechst_33258.jpg *License*: Public Domain *Contributors*: TenOfAllTrades

File:FISH 13 21.jpg *Source*: http://en.wikipedia.org/w/index.php?title=File:FISH_13_21.jpg *License*: Public Domain *Contributors*: Gregor1976

File:300px-Anaphase-fluorescent.jpg *Source*: http://en.wikipedia.org/w/index.php?title=File:300px-Anaphase-fluorescent.jpg *License*: GNU Free Documentation License *Contributors*: New York State Department of Health

File:Bloodcell sun flares pathology.jpeg *Source*: http://en.wikipedia.org/w/index.php?title=File:Bloodcell_sun_flares_pathology.jpeg *License*: Public Domain *Contributors*: Birindand, Karelj, NEON ja, 1 anonymous edits

File:Carboxysome 3 images.png *Source*: http://en.wikipedia.org/w/index.php?title=File:Carboxysome_3_images.png *License*: Creative Commons Attribution 3.0 *Contributors*: Prof. Todd O. Yeates, UCLA Dept. of Chem. and Biochem.

Image:DNA chemical structure.svg *Source*: http://en.wikipedia.org/w/index.php?title=File:DNA_chemical_structure.svg *License*: unknown *Contributors*: Madprime, Wickey, 1 anonymous edits

File:DNA orbit animated static thumb.png *Source*: http://en.wikipedia.org/w/index.php?title=File:DNA_orbit_animated_static_thumb.png *License*: GNU Free Documentation License *Contributors*: 84user adapting file originally uploaded by Richard Wheeler (Zephyris) at en.wikipedia

Image:GC DNA base pair.svg *Source*: http://en.wikipedia.org/w/index.php?title=File:GC_DNA_base_pair.svg *License*: Public Domain *Contributors*: User:Isilanes

Image:AT DNA base pair.svg *Source*: http://en.wikipedia.org/w/index.php?title=File:AT_DNA_base_pair.svg *License*: Public Domain *Contributors*: User:Isilanes

Image:A-DNA, B-DNA and Z-DNA.png *Source*: http://en.wikipedia.org/w/index.php?title=File:A-DNA,_B-DNA_and_Z-DNA.png *License*: GNU Free Documentation License *Contributors*: Original uploader was Richard Wheeler (Zephyris) at en.wikipedia

Image:Parallel telomere quadruple.png *Source*: http://en.wikipedia.org/w/index.php?title=File:Parallel_telomere_quadruple.png *License*: unknown *Contributors*: User:Splette

Image:Branch-dna.png *Source*: http://en.wikipedia.org/w/index.php?title=File:Branch-dna.png *License*: unknown *Contributors*: Peter K.

Image:Multi-branch-dna.png *Source*: http://en.wikipedia.org/w/index.php?title=File:Multi-branch-dna.png *License*: unknown *Contributors*: User:Peter K.

Image:Cytosine chemical structure.png *Source*: http://en.wikipedia.org/w/index.php?title=File:Cytosine_chemical_structure.png *License*: GNU Free Documentation License *Contributors*: BorisTM, Bryan Derksen, Cacycle, Edgar181, Engineer gena

Image:5-methylcytosine.png *Source*: http://en.wikipedia.org/w/index.php?title=File:5-methylcytosine.png *License*: unknown *Contributors*: EDUCA33E, Luigi Chiesa, Mysid

Image:Thymine chemical structure.png *Source*: http://en.wikipedia.org/w/index.php?title=File:Thymine_chemical_structure.png *License*: GNU Free Documentation License *Contributors*: Arrowsmaster, BorisTM, Bryan Derksen, Cacycle, Edgar181, Leyo

Image:Benzopyrene DNA adduct 1JDG.png *Source*: http://en.wikipedia.org/w/index.php?title=File:Benzopyrene_DNA_adduct_1JDG.png *License*: GNU Free Documentation License *Contributors*: Benjah-bmm27, Bstlee, 1 anonymous edits

Image:T7 RNA polymerase at work.png *Source*: http://en.wikipedia.org/w/index.php?title=File:T7_RNA_polymerase_at_work.png *License*: unknown *Contributors*: User:Splette

Image:DNA replication.svg *Source*: http://en.wikipedia.org/w/index.php?title=File:DNA_replication.svg *License*: Public Domain *Contributors*: user:LadyofHats

Image:Nucleosome 2.jpg *Source*: http://en.wikipedia.org/w/index.php?title=File:Nucleosome_2.jpg *License*: Public Domain *Contributors*: Original uploader was TimVickers at en.wikipedia

Image:Nucleosome (opposites attracts).JPG *Source*: http://en.wikipedia.org/w/index.php?title=File:Nucleosome_(opposites_attracts).JPG *License*: Public Domain *Contributors*: Illustration by David S. Goodsell of The Scripps Research Institute (see this site)

Image:Lambda repressor 1LMB.png *Source*: http://en.wikipedia.org/w/index.php?title=File:Lambda_repressor_1LMB.png *License*: GNU Free Documentation License *Contributors*: Original uploader was Zephyris at en.wikipedia

Image:EcoRV 1RVA.png *Source*: http://en.wikipedia.org/w/index.php?title=File:EcoRV_1RVA.png *License*: GNU Free Documentation License *Contributors*: Original uploader was Zephyris at en.wikipedia

Image:Holliday Junction cropped.png *Source*: http://en.wikipedia.org/w/index.php?title=File:Holliday_Junction_cropped.png *License*: GNU Free Documentation License *Contributors*: Original uploader was TimVickers at en.wikipedia

Image:Holliday junction coloured.png *Source*: http://en.wikipedia.org/w/index.php?title=File:Holliday_junction_coloured.png *License*: GNU Free Documentation License *Contributors*: Original uploader was Zephyris at en.wikipedia

Image:Chromosomal Recombination.svg *Source*: http://en.wikipedia.org/w/index.php?title=File:Chromosomal_Recombination.svg *License*: Creative Commons Attribution 2.5 *Contributors*: User:Gringer

Image:DNA nanostructures.png *Source*: http://en.wikipedia.org/w/index.php?title=File:DNA_nanostructures.png *License*: unknown *Contributors*: (Images were kindly provided by Thomas H. LaBean and Hao Yan.)

Image:JamesDWatson.jpg *Source*: http://en.wikipedia.org/w/index.php?title=File:JamesDWatson.jpg *License*: Public Domain *Contributors*: Edward, RP88, Shizhao, Stellatomailing, Vonvon, 3 anonymous edits

Image:Francis Crick.png *Source*: http://en.wikipedia.org/w/index.php?title=File:Francis_Crick.png *License*: unknown *Contributors*: Photo: Marc Lieberman

Image:FrancisHarryComptonCrick.jpg *Source*: http://en.wikipedia.org/w/index.php?title=File:FrancisHarryComptonCrick.jpg *License*: unknown *Contributors*: Bunzil, Million Moments, PDH

Image:Rosalind Franklin.jpg *Source*: http://en.wikipedia.org/w/index.php?title=File:Rosalind_Franklin.jpg *License*: Public Domain *Contributors*: unknown

Image:Raymond Gosling.jpg *Source*: http://en.wikipedia.org/w/index.php?title=File:Raymond_Gosling.jpg *License*: GNU Free Documentation License *Contributors*: User:Davidruben

Image:maurice_wilkins.jpg *Source*: http://en.wikipedia.org/w/index.php?title=File:Maurice_wilkins.jpg *License*: unknown *Contributors*: Anetode, PDH, Rvilbig

Image:Erwin Chargaff.jpg *Source*: http://en.wikipedia.org/w/index.php?title=File:Erwin_Chargaff.jpg *License*: Public Domain *Contributors*: unknown

Image:Holliday Junction.png *Source*: http://en.wikipedia.org/w/index.php?title=File:Holliday_Junction.png *License*: Public Domain *Contributors*: Ahruman, Crux, Infrogmation, TimVickers, Wickey

Image:Mao-DX-schematic.jpg *Source*: http://en.wikipedia.org/w/index.php?title=File:Mao-DX-schematic.jpg *License*: Creative Commons Attribution 2.5 *Contributors*: Antony-22

Image:Mao-DXarray-schematic.gif *Source*: http://en.wikipedia.org/w/index.php?title=File:Mao-DXarray-schematic.gif *License*: Creative Commons Attribution 2.5 *Contributors*: Antony-22

Image:SierpinskiTriangle.svg *Source*: http://en.wikipedia.org/w/index.php?title=File:SierpinskiTriangle.svg *License*: Public Domain *Contributors*: User:PiAndWhippedCream

Image:Rothemund-DNA-SierpinskiGasket.jpg *Source*: http://en.wikipedia.org/w/index.php?title=File:Rothemund-DNA-SierpinskiGasket.jpg *License*: Creative Commons Attribution 2.5 *Contributors*: Antony-22

Image:Modern 3T MRI.JPG *Source*: http://en.wikipedia.org/w/index.php?title=File:Modern_3T_MRI.JPG *License*: unknown *Contributors*: User:KasugaHuang

License

Version 1.2, November 2002

0.PREAMBLE

The purpose of this License is to make a manual, textbook, or other functional and useful document "free" in the sense of freedom: to assure everyone the effective freedom to copy and redistribute it, with or without modifying it, either commercially or noncommercially. Secondarily, this License preserves for the author and publisher a way to get credit for their work, while not being considered responsible for modifications made by others.
This License is a kind of "copyleft", which means that derivative works of the document must themselves be free in the same sense. It complements the GNU General Public License, which is a copyleft license designed for free software.
We have designed this License in order to use it for manuals for free software, because free software needs free documentation: a free program should come with manuals providing the same freedoms that the software does. But this License is not limited to software manuals; it can be used for any textual work, regardless of subject matter or whether it is published as a printed book. We recommend this License principally for works whose purpose is instruction or reference.

1.APPLICABILITY AND DEFINITIONS

This License applies to any manual or other work, in any medium, that contains a notice placed by the copyright holder saying it can be distributed under the terms of this License. Such a notice grants a world-wide, royalty-free license, unlimited in duration, to use that work under the conditions stated herein. The "Document", below, refers to any such manual or work. Any member of the public is a licensee, and is addressed as "you". You accept the license if you copy, modify or distribute the work in a way requiring permission under copyright law.
A "Modified Version" of the Document means any work containing the Document or a portion of it, either copied verbatim, or with modifications and/or translated into another language.
A "Secondary Section" is a named appendix or a front-matter section of the Document that deals exclusively with the relationship of the publishers or authors of the Document to the Document's overall subject (or to related matters) and contains nothing that could fall directly within that overall subject. (Thus, if the Document is in part a textbook of mathematics, a Secondary Section may not explain any mathematics.) The relationship could be a matter of historical connection with the subject or with related matters, or of legal, commercial, philosophical, ethical or political position regarding them.
The "Invariant Sections" are certain Secondary Sections whose titles are designated, as being those of Invariant Sections, in the notice that says that the Document is released under this License. If a section does not fit the above definition of Secondary then it is not allowed to be designated as Invariant. The Document may contain zero Invariant Sections. If the Document does not identify any Invariant Sections then there are none.
The "Cover Texts" are certain short passages of text that are listed, as Front-Cover Texts or Back-Cover Texts, in the notice that says that the Document is released under this License. A Front-Cover Text may be at most 5 words, and a Back-Cover Text may be at most 25 words.
A "Transparent" copy of the Document means a machine-readable copy, represented in a format whose specification is available to the general public, that is suitable for revising the document straightforwardly with generic text editors or (for images composed of pixels) generic paint programs or (for drawings) some widely available drawing editor, and that is suitable for input to text formatters or for automatic translation to a variety of formats suitable for input to text formatters. A copy made in an otherwise Transparent file format whose markup, or absence of markup, has been arranged to thwart or discourage subsequent modification by readers is not Transparent. An image format is not Transparent if used for any substantial amount of text. A copy that is not "Transparent" is called "Opaque".
Examples of suitable formats for Transparent copies include plain ASCII without markup, Texinfo input format, LaTeX input format, SGML or XML using a publicly available DTD, and standard-conforming simple HTML, PostScript or PDF designed for human modification. Examples of transparent image formats include PNG, XCF and JPG. Opaque formats include proprietary formats that can be read and edited only by proprietary word processors, SGML or XML for which the DTD and/or processing tools are not generally available, and the machine-generated HTML, PostScript or PDF produced by some word processors for output purposes only.
The "Title Page" means, for a printed book, the title page itself, plus such following pages as are needed to hold, legibly, the material this License requires to appear in the title page. For works in formats which do not have any title page as such, "Title Page" means the text near the most prominent appearance of the work's title, preceding the beginning of the body of the text.
A section "Entitled XYZ" means a named subunit of the Document whose title either is precisely XYZ or contains XYZ in parentheses following text that translates XYZ in another language. (Here XYZ stands for a specific section name mentioned below, such as "Acknowledgements", "Dedications", "Endorsements", or "History".) To "Preserve the Title" of such a section when you modify the Document means that it remains a section "Entitled XYZ" according to this definition.
The Document may include Warranty Disclaimers next to the notice which states that this License applies to the Document. These Warranty Disclaimers are considered to be included by reference in this License, but only as regards disclaiming warranties: any other implication that these Warranty Disclaimers may have is void and has no effect on the meaning of this License.

2.VERBATIM COPYING

You may copy and distribute the Document in any medium, either commercially or noncommercially, provided that this License, the copyright notices, and the license notice saying this License applies to the Document are reproduced in all copies, and that you add no other conditions whatsoever to those of this License. You may not use technical measures to obstruct or control the reading or further copying of the copies you make or distribute. However, you may accept compensation in exchange for copies. If you distribute a large enough number of copies you must also follow the conditions in section 3.
You may also lend copies, under the same conditions stated above, and you may publicly display copies.

3.COPYING IN QUANTITY

If you publish printed copies (or copies in media that commonly have printed covers) of the Document, numbering more than 100, and the Document's license notice requires Cover Texts, you must enclose the copies in covers that carry, clearly and legibly, all these Cover Texts: Front-Cover Texts on the front cover, and Back-Cover Texts on the back cover. Both covers must also clearly and legibly identify you as the publisher of these copies. The front cover must present the full title with all words of the title equally prominent and visible. You may add other material on the covers in addition. Copying with changes limited to the covers, as long as they preserve the title of the Document and satisfy these conditions, can be treated as verbatim copying in other respects.
If the required texts for either cover are too voluminous to fit legibly, you should put the first ones listed (as many as fit reasonably) on the actual cover, and continue the rest onto adjacent pages.
If you publish or distribute Opaque copies of the Document numbering more than 100, you must either include a machine-readable Transparent copy along with each Opaque copy, or state in or with each Opaque copy a computer-network location from which the general network-using public has access to download using public-standard network protocols a complete Transparent copy of the Document, free of added material. If you use the latter option, you must take reasonably prudent steps, when you begin distribution of Opaque copies in quantity, to ensure that this Transparent copy will remain thus accessible at the stated location until at least one year after the last time you distribute an Opaque copy (directly or through your agents or retailers) of that edition to the public.
It is requested, but not required, that you contact the authors of the Document well before redistributing any large number of copies, to give them a chance to provide you with an updated version of the Document.

4.MODIFICATIONS

You may copy and distribute a Modified Version of the Document under the conditions of sections 2 and 3 above, provided that you release the Modified Version under precisely this License, with the Modified Version filling the role of the Document, thus licensing distribution and modification of the Modified Version to whoever possesses a copy of it. In addition, you must do these things in the Modified Version:

1. Use in the Title Page (and on the covers, if any) a title distinct from that of the Document, and from those of previous versions (which should, if there were any, be listed in the History section of the Document). You may use the same title as a previous version if the original publisher of that version gives permission.
2. List on the Title Page, as authors, one or more persons or entities responsible for authorship of the modifications in the Modified Version, together with at least five of the principal authors of the Document (all of its principal authors, if it has fewer than five), unless they release you from this requirement.
3. State on the Title page the name of the publisher of the Modified Version, as the publisher.
4. Preserve all the copyright notices of the Document.
5. Add an appropriate copyright notice for your modifications adjacent to the other copyright notices.

6. Include, immediately after the copyright notices, a license notice giving the public permission to use the Modified Version under the terms of this License, in the form shown in the Addendum below.
7. Preserve in that license notice the full lists of Invariant Sections and required Cover Texts given in the Document's license notice.
8. Include an unaltered copy of this License.
9. Preserve the section Entitled "History", Preserve its Title, and add to it an item stating at least the title, year, new authors, and publisher of the Modified Version as given on the Title Page. If there is no section Entitled "History" in the Document, create one stating the title, year, authors, and publisher of the Document as given on its Title Page, then add an item describing the Modified Version as stated in the previous sentence.
10. Preserve the network location, if any, given in the Document for public access to a Transparent copy of the Document, and likewise the network locations given in the Document for previous versions it was based on. These may be placed in the "History" section. You may omit a network location for a work that was published at least four years before the Document itself, or if the original publisher of the version it refers to gives permission.
11. For any section Entitled "Acknowledgements" or "Dedications", Preserve the Title of the section, and preserve in the section all the substance and tone of each of the contributor acknowledgements and/or dedications given therein.
12. Preserve all the Invariant Sections of the Document, unaltered in their text and in their titles. Section numbers or the equivalent are not considered part of the section titles.
13. Delete any section Entitled "Endorsements". Such a section may not be included in the Modified Version.
14. Do not retitle any existing section to be Entitled "Endorsements" or to conflict in title with any Invariant Section.
15. Preserve any Warranty Disclaimers.

If the Modified Version includes new front-matter sections or appendices that qualify as Secondary Sections and contain no material copied from the Document, you may at your option designate some or all of these sections as invariant. To do this, add their titles to the list of Invariant Sections in the Modified Version's license notice. These titles must be distinct from any other section titles.

You may add a section Entitled "Endorsements", provided it contains nothing but endorsements of your Modified Version by various parties--for example, statements of peer review or that the text has been approved by an organization as the authoritative definition of a standard.

You may add a passage of up to five words as a Front-Cover Text, and a passage of up to 25 words as a Back-Cover Text, to the end of the list of Cover Texts in the Modified Version. Only one passage of Front-Cover Text and one of Back-Cover Text may be added by (or through arrangements made by) any one entity. If the Document already includes a cover text for the same cover, previously added by you or by arrangement made by the same entity you are acting on behalf of, you may not add another; but you may replace the old one, on explicit permission from the previous publisher that added the old one.

The author(s) and publisher(s) of the Document do not by this License give permission to use their names for publicity for or to assert or imply endorsement of any Modified Version.

5.COMBINING DOCUMENTS

You may combine the Document with other documents released under this License, under the terms defined in section 4 above for modified versions, provided that you include in the combination all of the Invariant Sections of all of the original documents, unmodified, and list them all as Invariant Sections of your combined work in its license notice, and that you preserve all their Warranty Disclaimers.

The combined work need only contain one copy of this License, and multiple identical Invariant Sections may be replaced with a single copy. If there are multiple Invariant Sections with the same name but different contents, make the title of each such section unique by adding at the end of it, in parentheses, the name of the original author or publisher of that section if known, or else a unique number. Make the same adjustment to the section titles in the list of Invariant Sections in the license notice of the combined work.

In the combination, you must combine any sections Entitled "History" in the various original documents, forming one section Entitled "History"; likewise combine any sections Entitled "Acknowledgements", and any sections Entitled "Dedications". You must delete all sections Entitled "Endorsements."

6.COLLECTIONS OF DOCUMENTS

You may make a collection consisting of the Document and other documents released under this License, and replace the individual copies of this License in the various documents with a single copy that is included in the collection, provided that you follow the rules of this License for verbatim copying of each of the documents in all other respects.

You may extract a single document from such a collection, and distribute it individually under this License, provided you insert a copy of this License into the extracted document, and follow this License in all other respects regarding verbatim copying of that document.

7.AGGREGATION WITH INDEPENDENT WORKS

A compilation of the Document or its derivatives with other separate and independent documents or works, in or on a volume of a storage or distribution medium, is called an "aggregate" if the copyright resulting from the compilation is not used to limit the legal rights of the compilation's users beyond what the individual works permit. When the Document is included in an aggregate, this License does not apply to the other works in the aggregate which are not themselves derivative works of the Document.

If the Cover Text requirement of section 3 is applicable to these copies of the Document, then if the Document is less than one half of the entire aggregate, the Document's Cover Texts may be placed on covers that bracket the Document within the aggregate, or the electronic equivalent of covers if the Document is in electronic form. Otherwise they must appear on printed covers that bracket the whole aggregate.

8.TRANSLATION

Translation is considered a kind of modification, so you may distribute translations of the Document under the terms of section 4. Replacing Invariant Sections with translations requires special permission from their copyright holders, but you may include translations of some or all Invariant Sections in addition to the original versions of these Invariant Sections. You may include a translation of this License, and all the license notices in the Document, and any Warranty Disclaimers, provided that you also include the original English version of this License and the original versions of those notices and disclaimers. In case of a disagreement between the translation and the original version of this License or a notice or disclaimer, the original version will prevail.

If a section in the Document is Entitled "Acknowledgements", "Dedications", or "History", the requirement (section 4) to Preserve its Title (section 1) will typically require changing the actual title.

9.TERMINATION

You may not copy, modify, sublicense, or distribute the Document except as expressly provided for under this License. Any other attempt to copy, modify, sublicense or distribute the Document is void, and will automatically terminate your rights under this License. However, parties who have received copies, or rights, from you under this License will not have their licenses terminated so long as such parties remain in full compliance.

10.FUTURE REVISIONS OF THIS LICENSE

The Free Software Foundation may publish new, revised versions of the GNU Free Documentation License from time to time. Such new versions will be similar in spirit to the present version, but may differ in detail to address new problems or concerns. See http://www.gnu.org/copyleft/.

Each version of the License is given a distinguishing version number. If the Document specifies that a particular numbered version of this License "or any later version" applies to it, you have the option of following the terms and conditions either of that specified version or of any later version that has been published (not as a draft) by the Free Software Foundation. If the Document does not specify a version number of this License, you may choose any version ever published (not as a draft) by the Free Software Foundation.

How to use this License for your documents

To use this License in a document you have written, include a copy of the License in the document and put the following copyright and license notices just after the title page:

> Copyright (c) YEAR YOUR NAME.
>
> Permission is granted to copy, distribute and/or modify this document
>
> under the terms of the GNU Free Documentation License, Version 1.2
>
> or any later version published by the Free Software Foundation;
>
> with no Invariant Sections, no Front-Cover Texts, and no Back-Cover Texts.
>
> A copy of the license is included in the section entitled "GNU
>
> Free Documentation License".

If you have Invariant Sections, Front-Cover Texts and Back-Cover Texts, replace the "with...Texts." line with this:

> with the Invariant Sections being LIST THEIR TITLES, with the
>
> Front-Cover Texts being LIST, and with the Back-Cover Texts being LIST.

If you have Invariant Sections without Cover Texts, or some other combination of the three, merge those two alternatives to suit the situation.

If your document contains nontrivial examples of program code, we recommend releasing these examples in parallel under your choice of free software license, such as the GNU General Public License, to permit their use in free software.